TP 8781E

TANK-CAR INTERNAL SHELL EXPLOSION SUPPRESSION SYSTEM: PRELIMINARY THERMAL FEASIBILITY STUDY

Prepared For:

TRANSPORTATION DEVELOPMENT CENTRE
TRANSPORT CANADA
Ottawa, Canada

Prepared By:

W.R. DAVIS ENGINEERING LIMITED
Ottawa, Canada

In Cooperation With:

A.M. BIRK ENGINEERING
Kingston, Canada

DAVIS File No.: 85-159

NOVEMBER 1987

89-06054/

The Contents of this report reflect the views of the Contractor and not necessarily the official view or policies of the Transportation Development Centre.

Un sommaire en francais de ce document est inclus avant la table des matieres.

PROJECT TEAM

The project team was composed of:

W.R. DAVIS ENGINEERING LIMITED

Mr. A.J. Bosik
Mr. R.G. Wilkinson
Mr. D. VanDam

A.M. BIRK ENGINEERING

Dr. A.M. Birk

UNIVERSITY OF NEW BRUNSWICK

Dr. J.E.S. Venart
Mr. K. Sumathipala

Transport Canada / Transports Canada

Development / Développement

REPORT DOCUMENTATION FORM

1. Transport Canada Report No.	2. TDC Project No.	3. Recipient's Catalogue No.
TP 8781E	6475/76/77	

4. Title and Subtitle	5. Report Date
TANK-CAR INTERNAL SHELL EXPLOSION SUPPRESSION SYSTEM: Preliminary Thermal Feasibility Study	March 1987
	6. Performing Organization Report No. 85-159

7. Author(s)	8. Transport Canada File No.
R.G. Wilkinson / Dr. A.M. Birk	D1465-302-9

9. Performing Organization Name and Address	10. DSS File No.
W.R. Davis Engineering Ltd. 1260 Old Innes Road Ottawa, Ontario K1B 3V3	11SD.T8200-5-5524
	11. DSS or Transport Canada Contract No. 1SD85-00231

12. Sponsoring Agency Name and Address	13. Type of Report and Period Covered
Transportation Development Centre (TDC) 200 Dorchester West Suite 601, West Tower Montreal, Quebec H2Z 1X4	Technical
	14. Sponsoring Agency Code Funded under the Energy R&D Program.

15. Supplementary Notes	16. TDC Project Officer
	D.W. Dibble

17. Abstract

This interim report contains a preliminary thermal feasibility study of the internal shell thermal protection device for railroad tank cars. The study was carried out in two parts, small-scale experimental tests and computer modelling.

The experimental program was carried out using the UNB Tank Car Test Facility. Baseline tests of an unrolled tank without an internal shell were conducted. The thermal performance of a tank fitted with an internal shell was then determined at various roll angles, heat flux, and pressure relief valve orifice diameters. Results showed that for a vertical tank the internal shell device does significantly reduce wall temperatures in the upper regions of the tank. For a rolled tank condition insufficient cooling took place at the top of the tank which was not liquid wetted.

Based on observations from the small-scale tests, a computer model of an internal shell equipped tank was formulated and written in FORTRAN. Full-scale simulations indicated that an upright or rolled tank could survive and engulfing fire accident situation. However, a torch fire impinging on the top of the tank resulted in thermal rupture of the internal shell equipped tank.

18. Key Words	19. Distribution Statement
Railroad tank car, fire, thermal protection, explosion suppression, internal shell	Limited number of copies available from the Transportation Development Centre

20. Security Classification (of this report)	21. Security Classification (of this page)	22. No. of Pages	23. Price
unclassified	unclassified	157	---

TDC/CDT 79-005
Rev 86

Canada

Transports Canada / Transport Canada
Développement / Development

FORMULE DOCUMENTAIRE DU RAPPORT

1. N° du rapport Transports Canada	2. N° de l'étude — CDT	3. N° de catalogue du destinataire
TP 8781E	6475/76/77	

4. Titre et sous-titre	5. Date du rapport
TANK-CAR INTERNAL SHELL EXPLOSION SUPPRESSION SYSTEM: Preliminary Thermal Feasibility Study	Mars 1987
	6. N° du rapport de l'organisme exécutant: 85-159

7. Auteur(s)	8. N° de dossier Transports Canada
R.G. Wilkinson / Dr. A.M. Birk	D1465-302-9

9. Nom et adresse de l'organisme exécutant	10. N° de dossier — ASC
W.R. Davis Engineering Ltd. 1260 Old Innes Road Ottawa (Ontario) K1B 3V3	11SD.T8200-5-5524
	11. N° de contrat — ASC ou Transports Canada: 1SD85-00231

12. Nom et adresse de l'organisme parrain	13. Genre de rapport et période visée
Centre de développement des transports (CDT) 200 ouest, boul. Dorchester Suite 601, tour ouest Montréal (Québec) H2Z 1X4	Technique
	14. Code de l'organisme parrain: Financé par le programme énergétique.

15. Remarques additionnelles	16. Agent de projet — CDT
	D.W. Dibble

17. Résumé

Ce rapport intérimaire donne les résultats d'une étude de faisabilité préliminaire sur un dispositif de protection thermique à garniture interne pour les wagons-citernes. L'étude comportait deux parties, la première étant constituée de tests expérimentaux sur un réservoir à échelle réduite et la seconde, de modélisations sur ordinateur.

Les tests expérimentaux ont été effectués à l'installation de test de wagons-citernes de l'Université du Nouveau-Brunswick (UNB). Tout d'abord, des tests ont été effectués sur un wagon-citerne en position normale sans coquille de protection interne. Puis, le comportement thermique d'un wagon-citerne muni d'une coquille interne a été observé à diverses valeurs de l'angle d'inclinaison latérale, du flux thermique et du diamètre d'orifice de la soupape de sûreté. Les résultats ont démontré que, lorsque le wagon-citerne est en position normale, la coquille interne réduit sensiblement la température de la paroi dans la partie supérieure du réservoir et que, lorsqu'il est incliné latéralement le refroidissement est insuffisant à la partie supérieure du réservoir non mouillée par le liquide.

A partir des résultats obtenus dans les tests sur un réservoir à échelle réduite, les chercheurs ont élaboré un modèle informatique (écrit en FORTRAN) d'un wagon-citerne muni d'une coquille de protection interne. Des simulations sur un modèle grandeur nature indiquent qu'un réservoir en position normale ou incliné latéralement pourrait résister à un incendie avec flammes enveloppantes. Toutefois, d'après les simulations, il y aurait rupture du réservoir en cas de flammes à effet de chalumeau appliquées à sa partie supérieure, même si le réservoir est muni d'une coquille de protection.

18. Mots-clés	19. Diffusion
Wagon-citerne, flamme, protection thermique, protection contre les explosions, coquille interne.	Le Centre de développement des transports dispose d'un nombre limité d'exemplaires.

20. Classification de sécurité (de ce rapport)	21. Classification de sécurité (de cette page)	22. Nombre de pages	23. Prix
non classifié	non classifiée	157	---

Canada

ACKNOWLEDGEMENTS

Davis Engineering wishes to acknowledge the significant contributions of Dr. J.E.S. Venart and his associates at the University of New Brunswick. Dr. Venart supervised the tests that were carried out using the UNB test tank involving the internal shell explosion suppression device. All of the test results discussed in this report were generated using the UNB test facility.

Funding by the Energy R&D Program for this portion of the project is acknowledged.

SUMMARY

The primary objective of this study was to assess the feasibility of using an internal shell for thermal protection in tank-cars from a thermal standpoint. Since a full-scope thermal feasibility study would involve various types of testing and analysis, it was considered appropriate to conduct a preliminary thermal feasibility study to establish whether the device is appropriate for use in the rail tank-car environment. Certain critical questions needed to be answered before a full-scope thermal feasibility is conducted. These critical questions included the following:

(1) Does the internal shell concept actually work to cool the wall of an upright tank exposed to high heat fluxes?

(2) Does the internal shell concept work to cause vapour flow through the relief valve in a rolled tank, and, what effect does the internal shell have on the wall temperatures in the rolled tank?

(3) Will the internal shell device work in a full size tank car containing propane when exposed to an engulfing or torch type fire environment?

Once these questions have been answered, it will be possible to make a decision whether it is appropriate to carry on to a full-scope thermal feasibility and design study. To answer the above questions, the scope of the preliminary thermal feasibility study included the following:

(1) Limited scope testing of the internal shell device in the UNB testing tank. The tests were to consider the effects of shell gap and relief valve sizing, heat flux and tank roll.

(2) Limited scope computer modelling was to be done using the tank car thermal model to study the effects of an internal shell device in a full size rail tank car. The limited scope computer modelling was to use the results of the UNB testing where possible for purposes of computer model formulation and validation.

The experimental portion of the study was carried out at the University of New Brunswick using their small scale test tank. The tests were conducted under the supervision of Dr. J.E.S. Venart.

The test results for the upright tank fitted with an internal shell device showed that the device does significantly reduce wall temperatures in the upper regions of the tank. In an unprotected tank, the wall in the upper regions of the tank is exposed to vapour and therefore extremely high wall temperatures can result. With the internal shell in place, the wall temperatures were significantly reduced because during venting the internal shell device directed frothing liquid onto the upper surface of the tank, thereby reducing its temperature.

The tests also showed that when the internal shell device is in place, a larger pressure relief valve may be required. It is believed that because the internal shell device results in a higher heat transfer rate to the lading, a larger pressure relief valve is needed.

Tests conducted with a rolled tank showed that the internal shell device did not significantly effect wall temperatures in the upper region of the tank. When the tank is rolled, the pressure relief valve is submerged under liquid at least initially. When the relief valve is submerged, it vents liquid and, as a result, vapour is not generated within the tank and, therefore, frothing and boiling do not occur to any significant degree. The internal shell device works by directing frothing liquid onto the upper surface of the tank wall, thereby cooling it. In the rolled tank, this cooling effect was not observed. In addition, forced convective cooling of the tank wall was not evident. However, the presence of the internal shell did eventually result in the annulus being drained of liquid, thereby causing vapour flow through the pressure relief valve.

Based on observations from the small-scale experimental tests, a computer model of an internal shell equipped tank was formulated and written in the FORTRAN programming language. This computer model was incorporated as part of the Tank-Car Thermal Model for the purposes of establishing the performance of an internal shell device in a full-scale rail car filled with propane. A number of full-scale simulations were performed to study the effectiveness of the internal shell concept.

The simulations showed that the internal shell device could significantly reduce wall temperatures in a full-scale upright tank car. These reductions in the wall temperatures result in the tank surviving an engulfing fire accident situation. This is in agreement with the results obtained from the small-scale testing.

Simulations of a tank exposed to torch fire impingement show that the tank will fail very quickly if the torch impinges the wall above the liquid level. This is because of the very high wall temperatures that can result during torch fire impingement. Note, however, that the torch simulation is considered to be very severe since it is based on the U.S. DOT torch fire test facility.

As a result of the small-scale experimentation and computer modelling of a full-scale tank car, it was concluded that the internal shell device can significantly reduce the risk of thermally induced rupture in an upright tank exposed to an engulfing fire. However, the internal shell device does not appear to be very effective in a rolled tank or in an upright tank exposed to torch fire impingement above the liquid level. As a result of this, it is not recommended that the internal shell device be used by itself to protect rail tank cars from thermally induced ruptures. Further testing is required to improve the performance of the device in a rolled tank.

SOMMAIRE

Le premier objectif de cette étude est d'évaluer l'efficacité d'une coquille interne comme dispositif de protection thermique contre les explosions pour les wagons-citernes. Etant donné qu'une étude de faisabilité complète comporterait divers types de tests et d'analyses, il a été jugé opportun d'effectuer une étude de faisabilité préliminaire afin d'établir si le dispositif pouvait être utile dans un wagon-citerne. Avant de procéder à cette étude complète, il fallait connaître la réponse aux questions fondamentales suivantes:

(1) Une coquille interne peut-elle refroidir la paroi d'un wagon-citerne en position normale exposé à un flux thermique élevé?

(2) Dans le cas d'un wagon-citerne incliné latéralement, la présence d'une coquille interne permet-elle à la vapeur de s'échapper par la soupape de sûreté? Quel est l'effet produit sur la température de la parroi?

(3) La coquille de protection interne est-elle efficace dans un wagon-citerne grandeur nature contenant du propane liquéfié lorsque le wagon-citerne est soumis à des flammes enveloppantes ou à une flamme à effet de chalumeau?

Il fallait connaître la réponse à ces questions afin de décider s'il valait la peine d'effectuer une étude de faisabilité et de conception complète. Pour y répondre, l'étude de faisabilité préliminaire comprenait:

(1) des tests à portée limité sur une coquille de protection interne installée dans le réservoir de test de l'Université du Nouveau-Brunswick (UNB); ces tests devaient déterminer les effets de l'espacement réservoir-coquille, du diamètre de l'ouverture de la soupape de sûreté, du flux thermique et de l'angle d'inclinaison latérale du réservoir; et

(2) une modélisation informatique à portée limitée utilisant le modèle thermique d'un wagon-citerne pour étudier les effets d'une coquille de protection interne dans un wagon-citerne grandeur nature; cette modélisation devait utiliser dans la mesure du possible les résultats obtenus dans les tests effectués à l'UNB pour formuler et vérifier le modèle informatique.

La partie expérimentale de l'étude a été effectuée avec le réservoir expérimental à échelle réduite de l'UNB sous la surveillance du Dr. J.E.S. Venart.

Les résultats des essais effectués sur un réservoir en position normale muni d'une coquille de protection interne ont montré que la présence de la coquille réduit sensiblement la température de la paroi à la partie supérieure du réservoir. Dans un réservoir sans dispositif de protection, la paroi de la partie supérieure est exposée à la vapeur et la température de la paroi peut par conséquent atteindre des valeurs très élevées. Avec la coquille de protection interne, la température de la paroi est sensiblement abaissée car durant l'évacuation, la coquille dirige le liquide en bouillonnement sur la surface supérieure du réservoir, ce qui abaisse la température de ce dernier. Les tests ont également montré qu'il peut s'avérer nécessaire d'utiliser une soupape de sûreté à grand débit avec une coquille interne car celle-ci accroît le transfert de chaleur vers le chargement.

D'après les résultats des tests, lorsque le réservoir est incliné latéralement, la coquille interne a peu d'effet sur la température de la paroi de la partie supérieure du réservoir. Dans ce cas, la soupape de sûreté est recouverte par le liquide, du moins initialement; elle évacue alors celui-ci et il n'y a pas de production de vapeur dans le réservoir, par conséquent, peu de bouillonnement dans le liquide et une ébullition minimale. La coquille interne sert à diriger le liquide en bouillonnement sur la partie supérieure de la surface du réservoir afin de la refroidir. Lorsque le réservoir était incliné latéralement cet effet de refroidissement n'a pu être observé, pas plus que le refroidissement de la paroi par convexion forcée. Toutefois, on a constaté que la présence de la coquille interne entraînait le drainage de l'espace intermédiaire, de sorte que la vapeur pouvait s'échapper par la soupape de sûreté.

A partir d'observations effectuées lors des tests expérimentaux sur le réservoir à échelle réduite, les chercheurs ont élaboré un modèle informatique (écrit en FORTRAN) d'un réservoir muni d'une coquille interne, puis l'ont incorporé au modèle thermique d'un wagon-citerne afin de déterminer l'efficacité d'une coquille de protection interne dans un wagon-citerne grandeur nature rempli de propane liquéfié. Un certain nombre de simulations d'un wagon-citerne grandeur nature ont été effectuées à cette fin.

Les simulations ont montré que la coquille interne pouvait réduire sensiblement la température de la paroi d'un wagon-citerne grandeur nature en position normale. Cette réduction de température est suffisante pour permettre au réservoir de résister à des flammes enveloppantes. Ceci concorde avec les résultats obtenus dans les tests sur le réservoir à échelle réduite.

Les simulations sur un réservoir incliné latéralement semblent indiquer que celui-ci peut résister à des flammes enveloppantes. Ce résultat découle de deux facteurs: d'abord, le refroidissement par convexion provoqué par la circulation rapide de la vapeur dans l'espace intermédiaire abaisse légèrement la température de la paroi, comparativement à un réservoir non protègé; ensuite, lorsque le liquide emprisonné dans le réservoir-interne et dans l'espace intermédiaire est drainé, la chaleur ne peut atteindre le chargement, ce qui réduit la pression dans le réservoir. Notons toutefois que la marge de sécurité pour un réservoir incliné latéralement est faible et qu'il faudra effectuer d'autres études avant de pouvoir tirer des conclusions définitives.

Les simulations sur un réservoir soumis à une flamme à effet de chalumeau indiquent qu'il y aura une rupture très rapide du réservoir si la falmme est appliquée au-dessus du niveau du liquide, une flamme à effet de chalumeau provoquent une forte élévation de la température de la paroi. Les simulations de flammes à effet de chalumeau sont considérées comme très rigoureuses car elles sont basées sur les résultats expérimentaux obtenus par le ministère des transports des Etats-Unis.

D'après les résultats de nos expériences sur le réservoir à échelle réduite et de nos modélisations informatiques d'un wagon-citerne grandeur nature, la coquille de protection interne peut réduire sensiblement le risque de rupture provoquée par la chaleur dans un wagon-citerne en position normale soumis à des flammes enveloppantes. Toutefois, cette coquille ne semble pas très efficace pour protéger un wagon-citerne incliné latéralement, ou un wagon-citerne en position normale soumis à une flamme à effet de chalumeau au-dessus du niveau du liquide. Par conséquent, la coquille de protection interne n'est pas recommandée pour protéger les wagons-citernes contre les ruptures provoquées par la chaleur. Il faudra effectuer d'autres tests en vue d'améliorer l'efficacité de ce dispositif de protection dans le cas d'un wagon-citerne incliné latéralement.

TABLE OF CONTENTS

		PAGE
1.0	INTRODUCTION	1
1.1	Background	1
1.2	Objectives and Scope	6
2.0	EXPERIMENTAL	9
2.1	Objectives and Scope	9
2.2	Description of Test Apparatus	9
2.3	Test Matrix	13
2.4	Results and Discussion	14
3.0	COMPUTER MODELLING	47
3.1	Modelled System	47
3.2	Modes of Operation	49
3.3	Modelling Approach	52
3.4	Tank-Car Thermal Model TANKCAR	53
3.5	Internal Shell Thermal Model	55
3.6	Model Validation and Testing	57
3.7	Run Cases	58
3.8	Results and Discussion	59
4.0	CONCLUSIONS AND RECOMMENDATIONS	124
REFERENCES		126

APPENDICES

Appendix A Computer Language Listing of Internal Shell Related Models

LIST OF FIGURES

FIGURE		PAGE
1.1-1	Tank with Device when Relief Valve is Closed	3
1.1-2	Tank with Device when Relief Valve is Open	4
1.1-3	Tank with Device when Relief Valve is Open (Tank Almost Empty)	5
1.1-4	Overturned Tank with Device when Relief Valve is Open	7
2.2-1	Shell Assembly	11
2.2-2	Check Vent Shape and Location	12
2.4-1	Thermocouple Arrangement along the Wall and Center	15
2.4-2	Baseline Test #1 Tank Pressure vs Time	16
2.4-3	Baseline Test #1 Lading Temperature Profile vs Time	17
2.4-4	Baseline Test #1 Wall Temperature vs Time	19
2.4-5	Baseline Test #2 Tank Pressure vs Time	21
2.4-6	Baseline Test #2 Wall Temperatures vs Time	22
2.4-7	Baseline Test #2 Lading Temperatures vs Time	23
2.4-8	Test #1 Tank Pressure vs Time	25
2.4-9	Test #1 Wall Temperatures (Upper-LHS) vs Time	26
2.4-10	Test #1 Lading Temperatures (Vertical Profile) vs Time	27
2.4-11	Test #2 Tank Pressure vs Time	30
2.4-12	Test #2 Wall Temperatures (Upper-LHS) vs Time	31
2.4-13	Test #2 Lading Temperatures (Vertical Profile) vs Time	32
2.4-14	Tank Pressure vs Time	34
2.4-15	Test #3 (Upper-RHS) vs Time	35
2.4-16	Test #3 Lading Temperature vs Time	36
2.4-17	Test #4 Tank Pressure vs Time	39
2.4-18	Test #4 Wall Temperatures (Upper-Bias) vs Time	40
2.4-19	Test #4 Lading Temperature vs Time	41
2.4-20	Test #5 Tank Pressure vs Time	43
2.4-21	Test #5 Wall Temperatures vs Time	44
3.1-1	Cross Section of Tank with Internal Shell	48

LIST OF FIGURES (cont'd)

FIGURE		PAGE
3.2-2	Modes of Operation	50
3.8-1	Baseline A Case - Predicted Tank Pressure vs Time	62
3.8-2	Baseline A Case - Predicted Wall Temperature vs Time.....	63
3.8-3	Baseline A Case - Predicted Liquid Level vs Time	64
3.8-4	Baseline A Case - Predicted Tank Wall Stresses vs Time	65
3.8-5	Baseline B Case - Predicted Tank Pressures vs Time	68
3.8-6	Baseline B Case - Predicted Wall Temperature vs Time	69
3.8-7	Baseline B Case - Predicted Liquid Level vs Time	70
3.8-8	Baseline B Case - Predicted Tank Wall Stresses vs Time	71
3.8-9	Run Case #1 - Predicted Tank Pressure vs Time	73
3.8-10	Run Case #1 - Predicted Wall Temperature vs Time	74
3.8-11	Run Case #1 - Predicted Liquid Level vs Time	76
3.8-12	Run Case #1 - Predicted Annulus and Core Levels vs Time	77
3.8-13	Run Case #1 - Wall Stresses vs Time	79
3.8-14	Run Case #2 - Predicted Tank Pressure vs Time	83
3.8-15	Run Case #2 - Predicted Wall Temperature vs Time	84
3.8-16	Run Case #2 - Predicted Liquid Level vs Time	85
3.8-17	Run Case #2 - Predicted Annulus and Core Levels vs Time	86
3.8-18	Run Case #2 - Wall Stresses vs Time	87
3.8-19	Run Case #3 - Predicted Tank Pressure vs Time	90
3.8-20	Run Case #3 - Predicted Wall Temperature vs Time	91
3.8-21	Run Case #3 - Predicted Liquid Level vs Time	92
3.8-22	Run Case #3 - Predicted Annulus and Core Levels vs Time	93
3.8-23	Run Case #3 - Wall Stresses vs Time	94

LIST OF FIGURES (Cont.)

PAGE		PAGE
3.8-24	Run Case #4 - Predicted Tank Pressure vs Time	97
3.8-25	Run Case #4 - Predicted Wall Temperature vs Time	98
3.8-26	Run Case #4 - Predicted Liquid Level vs Time	99
3.8-27	Run Case #4 - Predicted Annulus and Core Levels vs Time	100
3.8-28	Run Case #4 - Wall Stresses vs Time	101
3.8-29	Run Case #5 - Predicted Tank Pressure vs Time	105
3.8-30	Run Case #5 - Predicted Wall Temperature vs Time	106
3.8-31	Run Case #5 - Predicted Liquid Level vs Time	107
3.8-32	Run Case #5 - Predicted Annulus and Core Levels vs Time	108
3.8-33	Run Case #5 - Wall Stresses vs Time	109
3.8-34	Run Case #6 - Predicted Tank Pressure vs Time	112
3.8-35	Run Case #6 - Predicted Wall Temperature vs Time	113
3.8-36	Run Case #6 - Predicted Liquid Level vs Time	114
3.8-37	Run Case #6 - Predicted Annulus and Core Levels vs Time	115
3.8-38	Run Case #6 - Wall Stresses vs Time	116
3.8-39	Run Case #7 - Predicted Tank Pressure vs Time	119
3.8-40	Run Case #7 - Predicted Wall Temperature vs Time	120
3.8-41	Run Case #7 - Predicted Liquid Level vs Time	121
3.8-42	Run Case #7 - Predicted Annulus and Core Levels vs Time	122
3.8-43	Run Case #7 - Wall Stresses vs Time	123

LIST OF TABLES

TABLE		
2.3-1	Summary of Test Matrix	13
3.7-1	Summary of Model Run Case	58

1.0 INTRODUCTION

This document is the Milestone Report describing Task Two, the Preliminary Thermal Feasibility Study of Phase I, of the Tank-Car Explosion Suppression Project. The work was performed under DSS Contract 11SD.T8200-5-55524 for the Transportation Development Centre of Transport Canada. The contract was a result of an unsolicited proposal submitted by Dr. A.M. Birk of Davis Engineering Limited.

The submission of this report marks a go/no go decision point in the Tank-Car Explosion Suppression Project. A go decision would mean the continuation onto Task 3, the Thermal Design Study.

The work contained herein was performed by Davis Engineering Limited and its subcontractors, A.M. Birk Engineering and the University of New Brunswick.

1.1 BACKGROUND

When a Tank-Car (or any other container holding a pressurized liquid) is exposed to external fire impingement, there is a risk of thermally induced rupture. Such a rupture is usually caused by reductions in the strength of the tank primary shell due to the development of high wall temperatures. These high wall temperatures occur where the wall is wetted on the inside by vapor. In all other wall areas wetted by liquid, the temperatures remain relatively low due to the effective cooling by the liquid.

Presently, tank cars are protected against thermally induced ruptures by the use of pressure relief valves and thermal insulation. The thermal insulation acts as a barrier to the flow of heat into the tank from fires and the relief valves act to maintain tank pressures below dangerous levels in the event of accidental heating. These devices have proven to be extremely effective provided that they have been properly maintained and protected from any damage (i.e. because insulation is applied externally it can be damaged during an accident, and its effectiveness can be significantly reduced).

Even with these methods of protection, accidents happen and no system is completely safe. Therefore, research must continue to ensure that tank cars or other containers for transporting or storing hazardous commodities are

protected using the best available means. This study involves a preliminary thermal feasibility study of a new protection concept that could potentially further reduce the risk of thermally induced ruptures.

The device consists of an internal shell which is supported within a tank in such a way that an annular space exists between it and the tank wall. An opening along the bottom allows communication between the annulus and the inner cavity. Figure 1.1-1 shows a cross sectional view through a tank car with the device installed. The figure shows the situation with a relief valve closed and the device has no effect on the tank or its lading. It is when the relief valve is open, that the device has its beneficial effects.

The device has two modes of operation. The first mode has the effect of maintaining low wall temperatures when the relief valve is open, the second mode results in vapour flow through the relief valve when the tank is rolled over on its side.

The first mode is in action when the tank is upright or rolled slightly. Figures 1.1-2 and 1.1-3 show the case where the relief valve is open and the device is acting in the first mode. When the relief valve is open and the device is present, the flow out of the relief valve causes a pressure drop between the inner cavity and the annular space. This pressure difference draws the liquid up to a higher level in the annular space. This immediately reduces the vapour wetted area. During venting, large amounts of vapour are generated and the resulting frothing and boiling at the wall has no place to go except up along the wall. In addition, the restricted flow area in the annulus results in high flow velocities which entrain liquid droplets. This high velocity wet two-phase flow in the annulus results in relatively high heat transfer coefficients with the net effect of reducing the wall temperatures at the top of the tank.

The second mode of device operation comes into play when the tank roll is large. Under normal conditions (tank without device) a tank that is rolled will have its relief valve submerged in liquid. If the relief valve is properly sized for vapour flow it may not be adequate for liquid flow. Therefore it is desirable that the valve always pass vapour or dry two-phase flows.

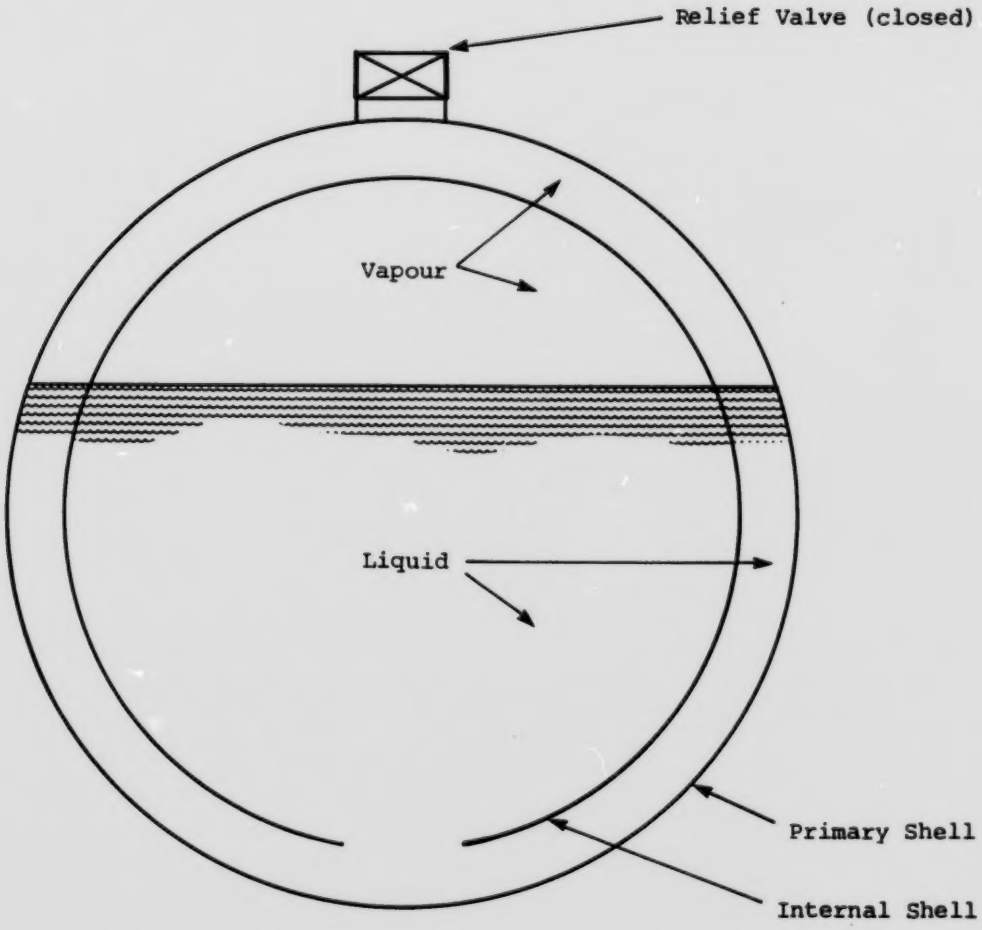

FIGURE 1.1-1 TANK WITH DEVICE WHEN RELIEF VALVE IS CLOSED

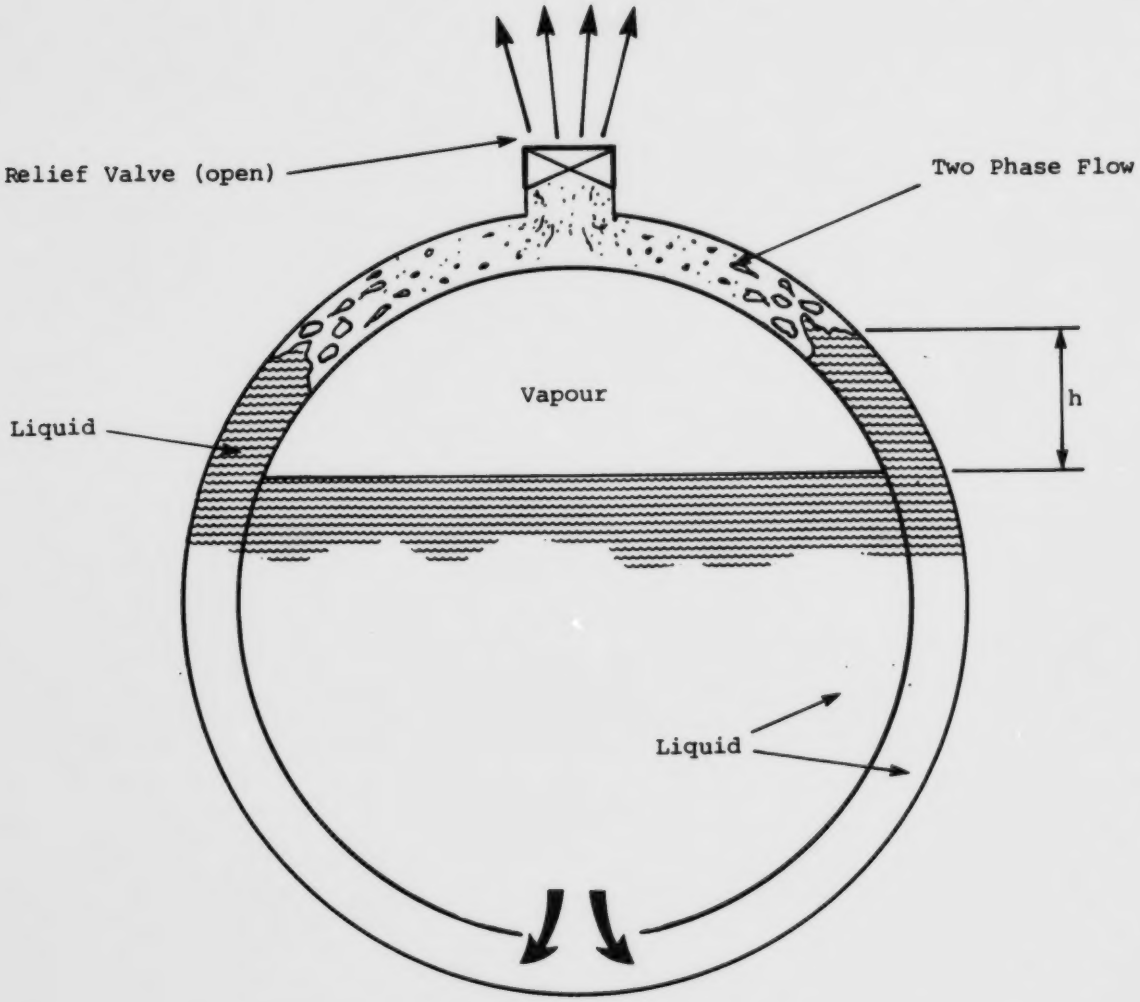

FIGURE 1.1-2 TANK WITH DEVICE WHEN RELIEF VALVE IS OPEN

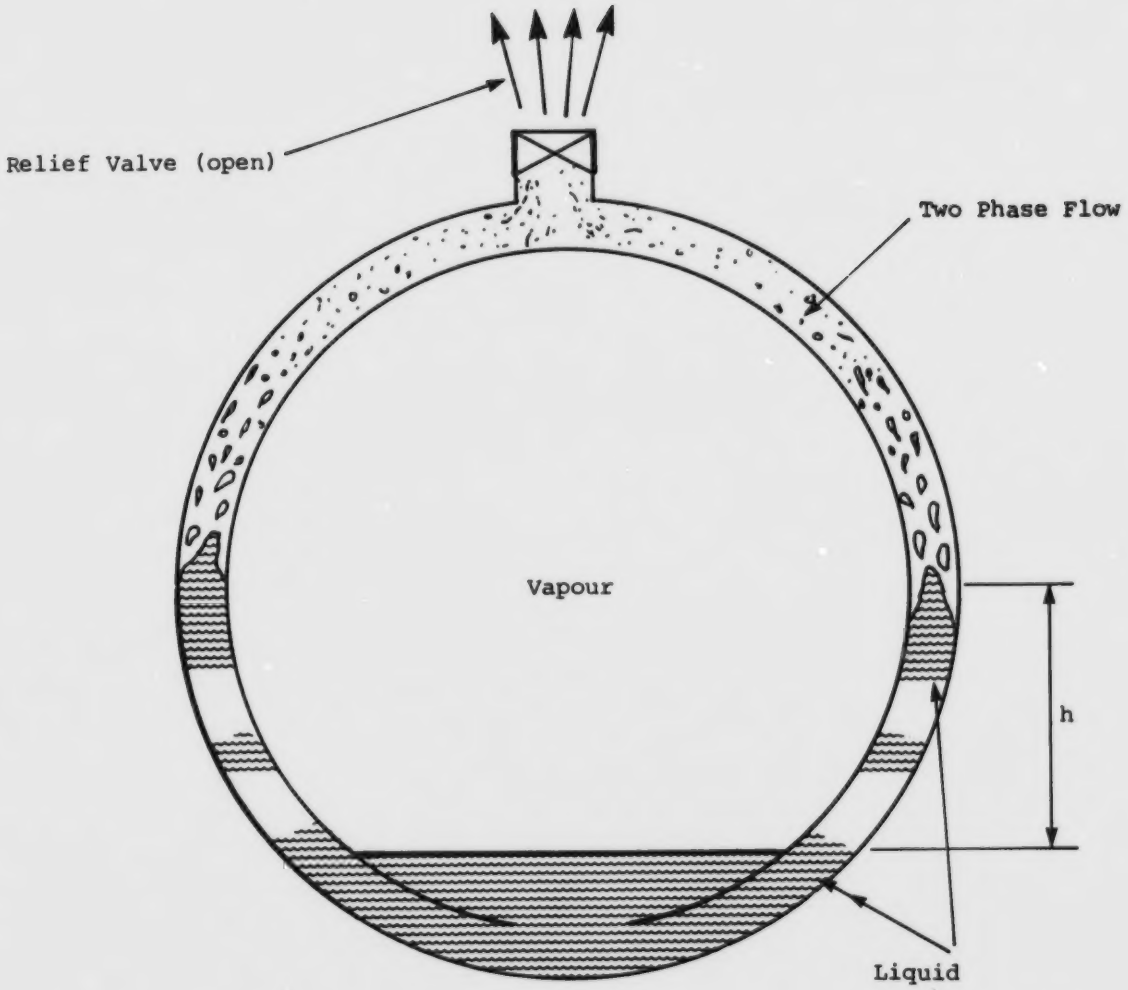

FIGURE 1.1-3 TANK WITH DEVICE WHEN RELIEF VALVE IS OPEN (TANK ALMOST EMPTY)

The second mode of device operation ensures vapour flow when a horizontal or near horizontal tank has a large roll angle. Figure 1.1-4 shows a tank rolled to the probable maximum (120 degrees) angle. When the valve first opens, it will vent liquid until the liquid level in the inner cavity is below the opening in the inner shell. From that time on, liquid will be drained from the annulus. When the annulus is clear of liquid, then the valve will pass vapour or two-phase fluids only, thus ensuring efficient pressure relief. However, during this mode of operation, the internal shell does not direct liquid or 2-phase flow along the wall and therefore it is questionable whether or not the tank will fail. It is possible the high flow velocities in the annulus will result in convective heat transfer that will maintain the wall temperatures at acceptable levels.

1.2 OBJECTIVES AND SCOPE

The primary objective of this study was to assess the feasibility of using an internal shell for thermal protection in tank-cars from a thermal standpoint. Since a full scope thermal feasibility study would involve various types of testing and analysis, it was considered appropriate to conduct a preliminary thermal feasibility study initially to establish whether or not the device is appropriate for use in the rail tank-car environment. Certain critical questions needed to be answered before a full scope thermal feasibility was to be conducted. These critical questions included the following:

(1) Does the internal shell concept actually work to cool the wall of an upright tank exposed to high heat fluxes?

(2) Does the internal shell concept work to cause vapour flow through the relief valve in a rolled tank, and, what effect does the internal shell have on the wall temperatures in the rolled tank?

(3) Will the internal shell device work in a full size tank car containing propane when exposed to an engulfing or torch type fire environment?

Once these questions have been answered, it will be possible to make a decision whether or not it is appropriate to carry on to a full scope thermal feasibility and design study. To answer the above questions, the scope of the preliminary thermal feasibility study was to include the following:

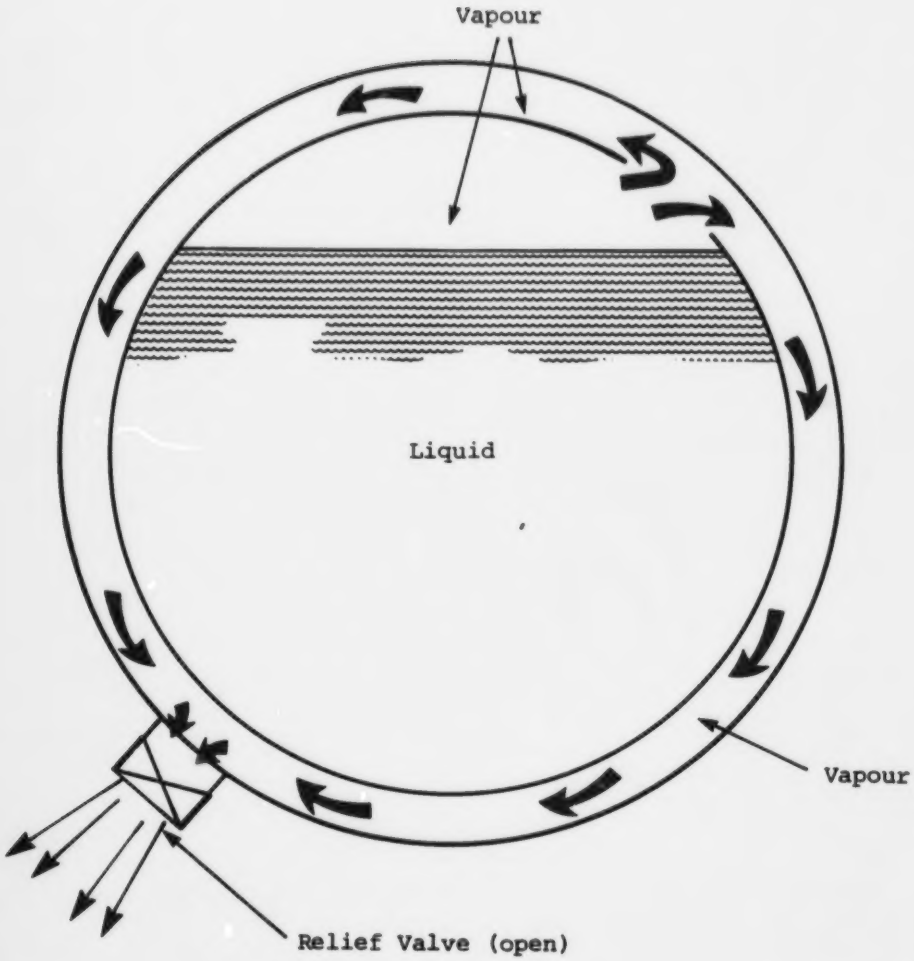

FIGURE 1.1-4 OVERTURNED TANK WITH DEVICE WHEN RELIEF VALVE IS OPEN

(1) Limited scope testing of the internal shell device in the UNB testing tank. The tests were to consider the effects of shell gap and relief valve sizing, heat flux and tank roll.

(2) Limited scope computer modelling was to be done using the tank car thermal model to study the effects of an internal shell device in a full size rail tank car. The limited scope computer modelling was to use the results of the UNB testing where possible for purposes of computer model formulation and validation.

The scope of the testing and the scope of the computer modelling was to be such that the results could be used to answer the above questions for the purpose of making the go/no go decision.

The tank vehicle considered in this study is the pressurized rail tank car designated type CTC-112J 340 W carrying propane. The full scale tank car is 18.3 meters (60 feet) in length and 3.05 meters (10 feet) in diameter with elliptical heads. The tanks considered here have a capacity of 127 cubic metres (33,600 US gallons).

2.0 EXPERIMENTAL

The preliminary thermal feasibility study included some limited scope experimentation involving a small scale test tank. The tests were conducted to provide some performance data to assist in the formulation and development of a computer model of the thermal behaviour of a tank with the internal shell in place. The tests were also to provide important data on the performance of the internal shell in a rolled tank. Since any effective thermal protection device must operate with the tank in any orientation, it is important that the internal shell performance be understood for all tank roll angles and pitch angles.

Details of the tests and of the results obtained are presented in the following pages.

2.1 OBJECTIVES AND SCOPE

As stated above, the main objectives of the experiments were as follows:

- to provide data that quantitatively describes the performance of the internal shell device for the purposes of computer model formulation and development.

- to provide data on the performance of the internal shell device in a rolled tank for the purposes of evaluating the feasibility of using the device in mobile applications (such as rail tank-cars where a rolled orientation is possible during an accident).

The scope of the tests was limited in that only a few variables were to be manipulated. The tests were limited in this way because certain critical questions were to be answered before a full test program was to be initiated. The variables manipulated in the tests included the external heat flux, the valve orifice size, and the tank roll.

2.2 DESCRIPTION OF TEST APPARATUS

The tests were carried out at the University of New Brunswick under the supervision of Dr. J.E.S. Venart.

The tests were conducted in an existing test tank which is instrumented to measure critical variables such as pressure, wall and lading temperatures, lading mass, etc. The tank measures 38.1 cm in diameter by 33 cm long and has clear plexiglass ends for the purposes of viewing the response of the lading. The tank wall is electrically heated and is equipped with a pressure activated relief valve. The tank can be rolled to any angle up to 180 degrees. The entire system is computer controlled. For further details of the test tank and the supporting data acquisition system, the reader is directed to Reference 1.

The tank was fitted with an internal shell as shown in Figure 2.2-1. The internal shell consisted of a rolled piece of stainless steel (304SS) sheet 1.5mm thick. The shell was placed in the tank and held from the wall of the tank using screw adjustable spacers as shown in the figure. The ends of the shell butted up against the plexiglass end walls of the test tank and were sealed with a rubber gasket.

The shell was designed so that the gap could be adjusted within a range of 0.63 - 1.9cm using the same shell. The bottom slot would vary slightly depending on the gap setting but was in the order of 3 - 11cm. The dimensions of the internal shell are shown in the figure.

In initial tests, the internal shell was fitted with check valve devices that would allow flow from the annulus into the inner core but not the other way. Details of these devices and their location are shown in Figure 2.2-2. The purpose of these check valves was to eliminate the possibility of the annulus pressurizing faster than the core, thereby forcing the liquid level in the annulus to go down. This would be highly undesirable. However, initial tests seemed to indicate that the check valves were not needed at least for the conditions existing in the test tank and, therefore, a new internal shell was constructed without the check vents present. A new shell was made because of difficulties encountered when an attempt was made to seal off the existing check vents. It should be noted that the tests do not necessarily prove that the check vents are not needed, for they may be needed under different scale conditions.

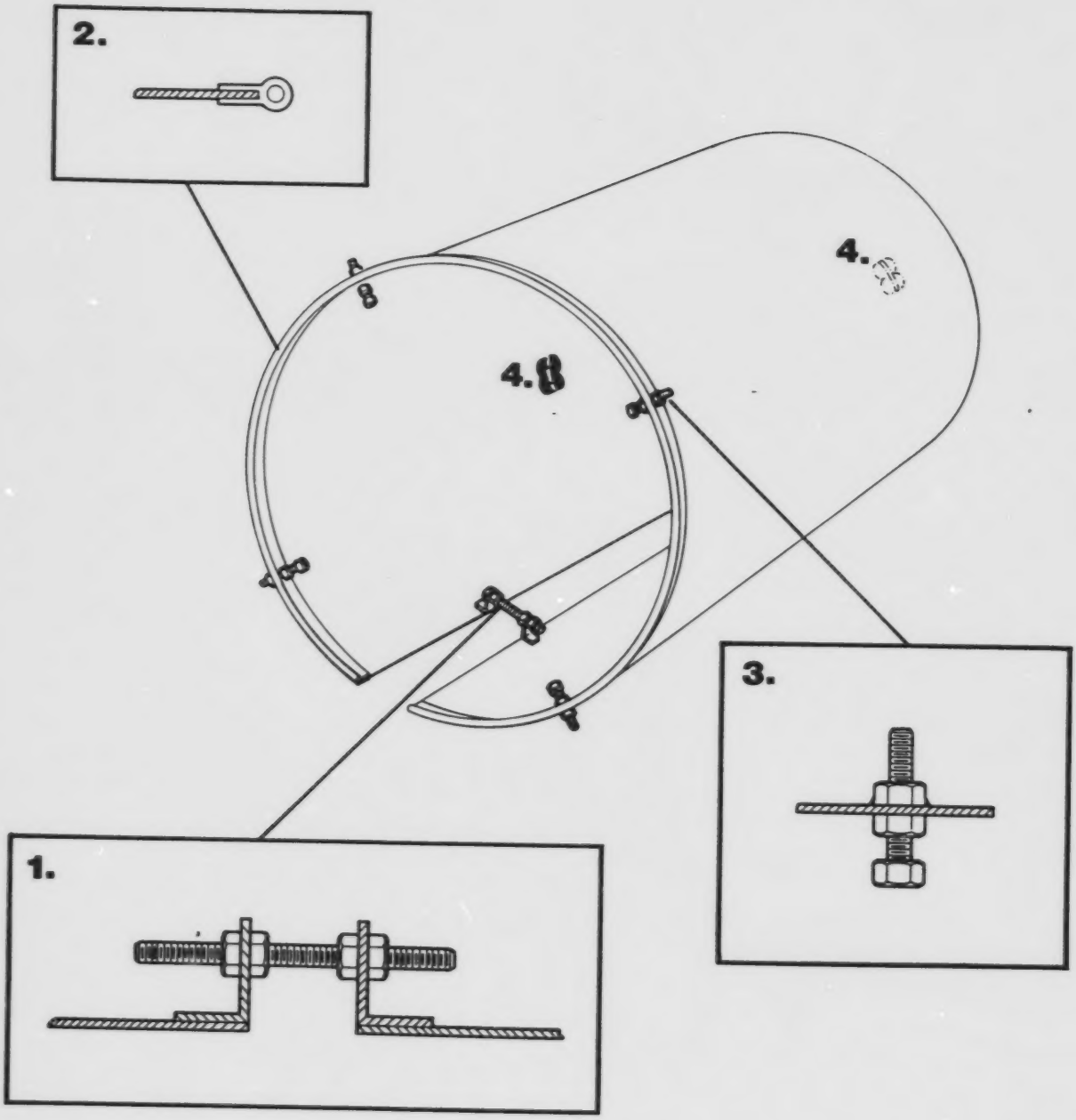

FIGURE 2.2-1 SHELL ASSEMBLY

4.

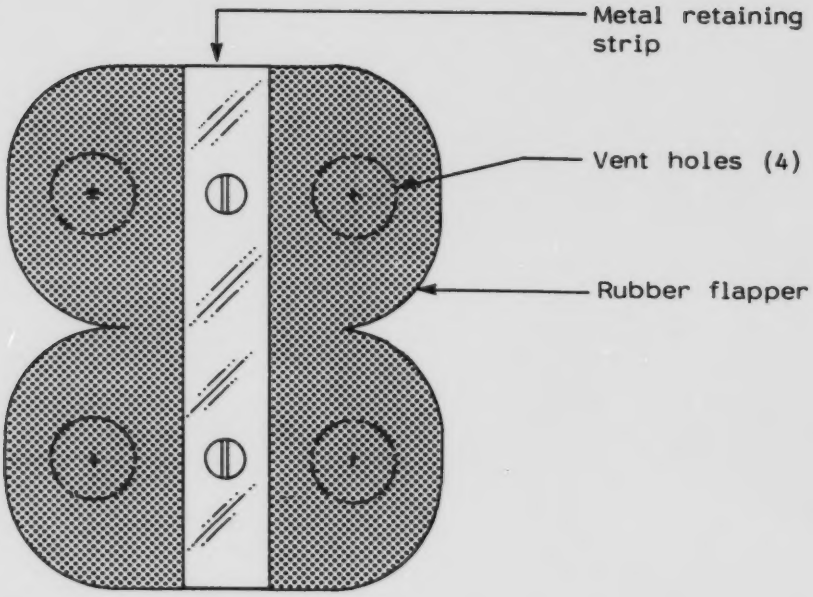

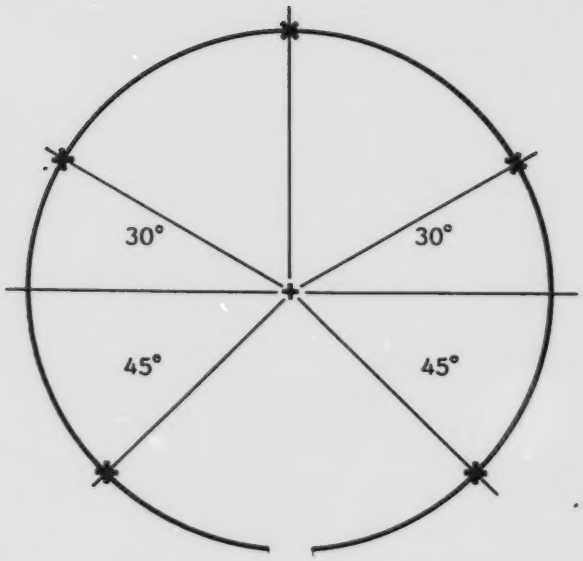

X - CHECK VENT LOCATION

FIGURE 2.2-2 CHECK VENT SHAPE AND LOCATION

2.3 TEST MATRIX

The test matrix included five tests as summarized in Table 2.3-1. All the tests involved the same test fluid (Freon 11) and the same pressure setting on the pressure relief valve (241 kPa). The internal shell was always mounted so that the bottom slot was diagonally opposite to the relief valve.

In all tests except Test #5 the check vents leaked thereby reducing the effectiveness of the internal shell. In the last test, the check vents were eliminated completely.

The gap was not varied because of clearance problems with instrumentation. Instead of reducing the gap size, the relief valve orifice area was increased in the last test in an attempt to increase flow velocities in the annulus. It was believed that this would increase the effect of lifting the liquid level in the annulus.

Test No.	Initial Fill (%)	Heat Flux (kW/sq m)	Relief Valve Orifice Diameter (mm)	Gap (mm)	Roll (degrees)	Comments
1	80	40	6.4	13	0	CVs leaked
2	80	80	6.4	13	0	CVs leaked
3	80	60	6.4	13	60/120	instrument-ation partial failure
4	80	80	6.4	13	0	CVs sealed, but leaking
5	80	80	9.5	13	120	no CVs

CV - Check Vents

Table 2.3-1 Summary of Test Matrix

2.4 RESULTS AND DISCUSSION

The results of the tests are presented in the form of graphs showing the following data:

- tank pressure vs time
- tank wall temperatures vs time (upper region)
- lading temperatures vs time

The key to the thermocouple locations for the wall and lading is shown in Figure 2.4-1.

The results of the five tests will be presented and discussed separately. Before the test results are shown for the internal shell equipped tank, baseline tests will be presented which show the results for tanks not equipped with the internal shell. These tests were not conducted as part of this project but were supplied by UNB. The results of these baseline tests are considered by UNB to be representative of the unprotected test tank performance.

Baseline 1: (80 kW/sq m, no roll)

This test involved the UNB test tank filled to 85% capacity with Freon 11. The tank surface heat flux was 80 kW/sq m. The relief valve orifice diameter was 6.4mm. The tank was vertical (i.e. no roll).

Figure 2.4-2 presents the measured tank pressure vs time for the test. As can be seen from the figure, the pressure increases due to the heating until at time 250 seconds the pressure relief valve comes into action. The relief valve cycles until approximately 350 seconds when the vapour generation within the tank is sufficient to keep the pressure relief valve open. With the relief valve open, the pressure continued to rise slowly until the test was ended at approximately 500 seconds.

The pressure plot of Figure 2.4-2 is typical for an unprotected tank. Important items to note are the slope of the pressure curve during initial pressurization, the time to first relief valve action, duration of valve cycling period and peak tank pressure.

Figure 2.4-3 presents measured lading temperatures along the vertical centreline of the tank. Measured temperatures include those for the liquid lading as well as the vapour. In the vapour region, the temperatures

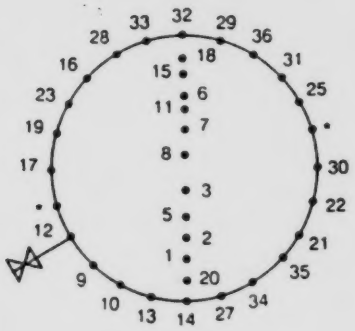

BASE LINE 2

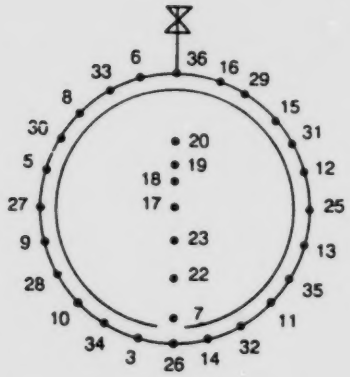

TESTS #1 & 2

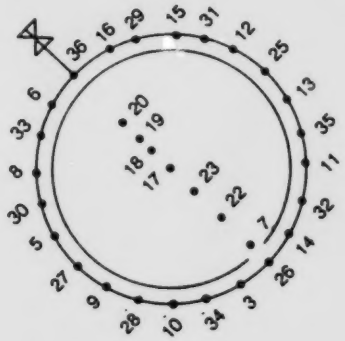

TEST #3

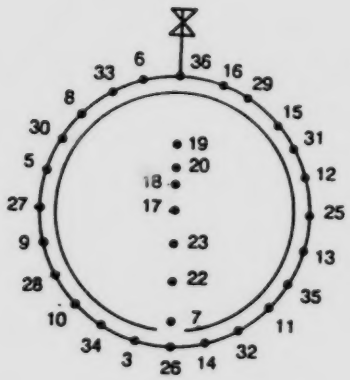

TEST #4

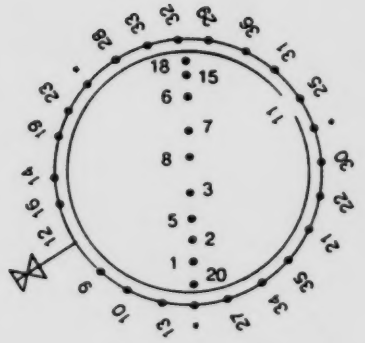

TEST #5

FIGURE 2.4-1 THERMOCOUPLE ARRANGEMENT ALONG THE WALL AND CENTER

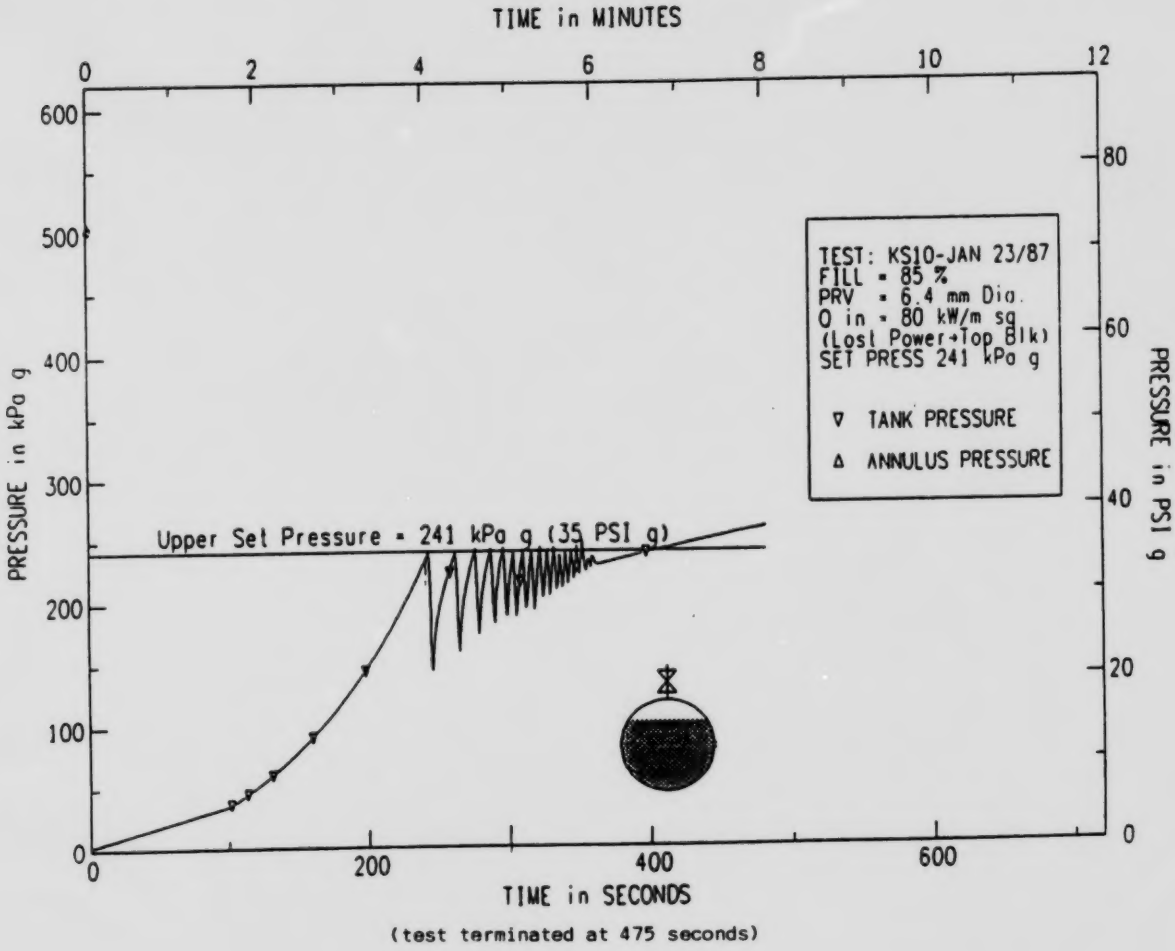

FIGURE 2.4-2 BASELINE TEST #1 TANK PRESSURE VS TIME

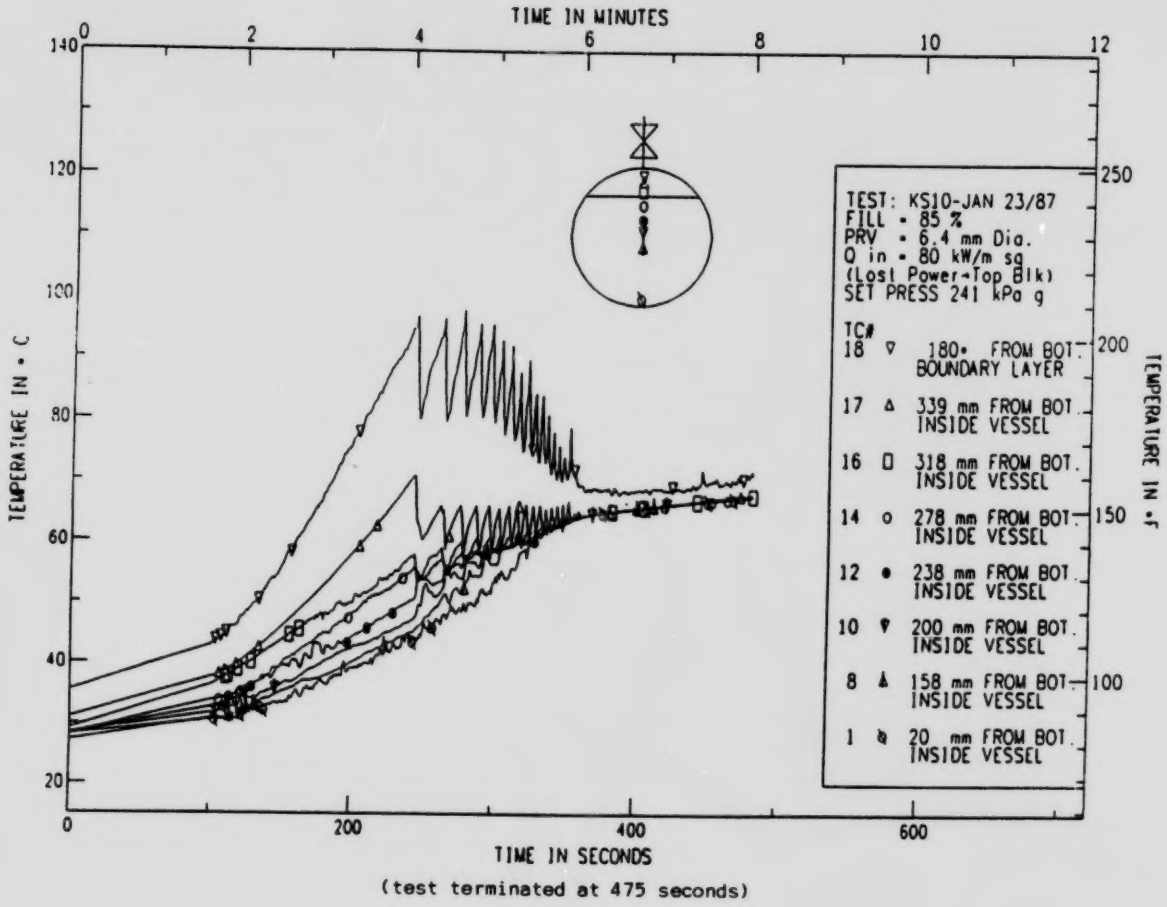

(test terminated at 475 seconds)

FIGURE 2.4-3 BASELINE TEST #1 LADING TEMPERATURE PROFILE VS TIME

rise more rapidly and are higher than in the liquid. Also, it is clear from the figure that the vapour temperatures are significantly effected by the relief valve action. When the relief valve opens during valve cycling the vapour temperatures drop. In the liquid regions lower down in the tank the temperatures are more uniform. This is because of the violent mixing that takes place during the venting process. The venting process results in boiling and churning of the lading which tends to equalize the temperature.

Figure 2.4-3 presents a typical lading response to external heating. Important items to note are the peak temperatures, the level of stratification, and the time at which the lading temperature becomes near uniform.

Figure 2.4-4 presents the measured tank wall temperatures near the top of the tank. The temperatures as shown are near the top of the tank and therefore are the peak wall temperatures. These are the temperatures of interest because the internal shell device is intended to reduce the peak wall temperatures to eliminate the risk of thermally induced ruptures.

It is assumed that the loss of power on the top block has effected thermocouple #33. The data should therefore be disregarded for time greater than 300 seconds.

As can be seen, the wall temperatures near the top of the tank rise very rapidly because of the ineffective cooling by the vapour in contact with the inside of the tank wall. Lower down in the tank the wall temperatures are lower because the wall is cooled by the liquid lading. The temperatures can vary widely depending on the location of the liquid level. If because of thermal expansion or frothing, the liquid level rises this can result in a dramatic drop in wall temperature as indicated in the figure for the thermocouple identified with the upward pointing triangle. Note that during the rapid temperature drop the recorded temperature fluctuates with the action of the relief valve. This is because the frothing that engulfs this thermocouple is most significant when the relief valve is open. Eventually as the lading is vented the liquid level drops thereby exposing more of the wall to vapour, and therefore the wall temperatures increase rapidly. This effect is not seen in the present figure because the test was terminated at 500 seconds.

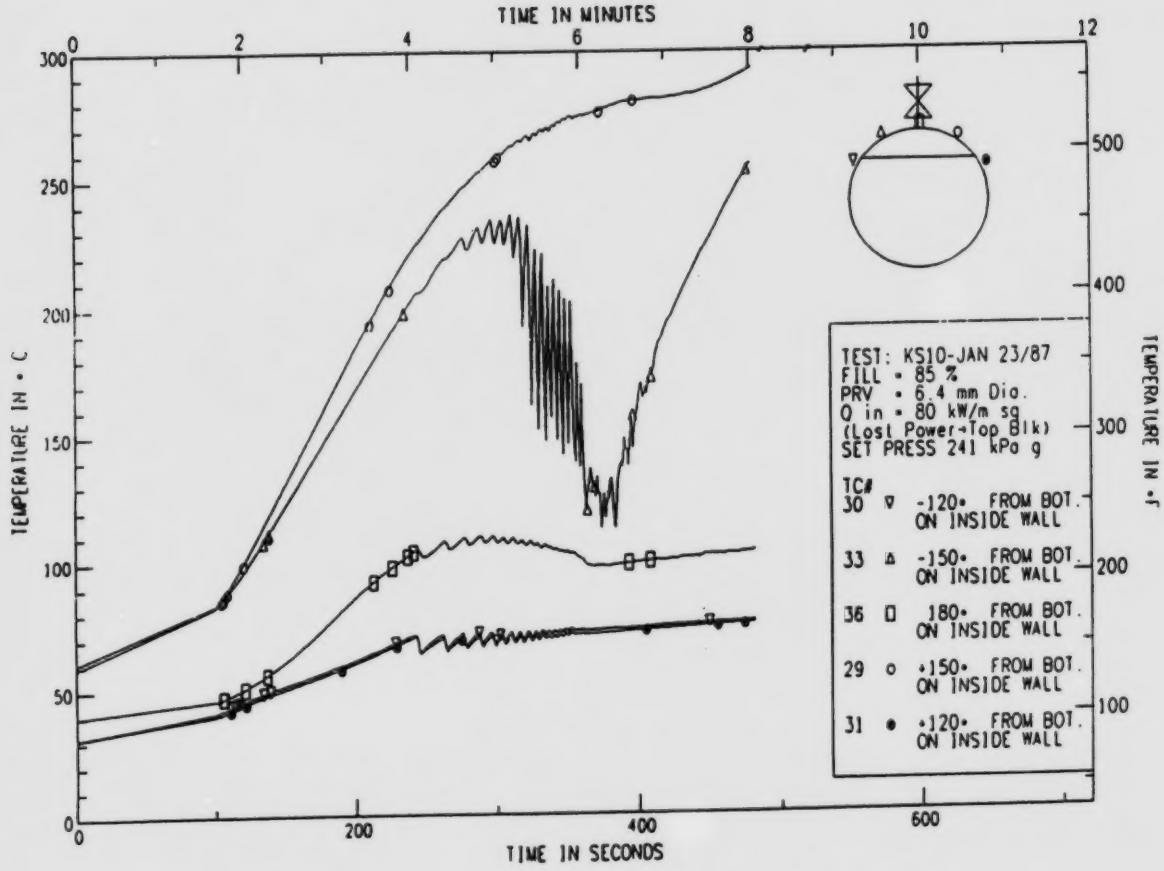

(test terminated at 475 seconds)

FIGURE 2.4-4 BASELINE TEST #1
WALL TEMPERATURE VS TIME

Figure 2.4-4 presents data that is typical for an unprotected tank exposed to high heat fluxes. Important items to note are the peak wall temperatures and their locations and any sudden changes in wall temperatures due to liquid frothing effects and valve action. The internal shell is intended to increase the effect of frothing so that all or most of the upper regions of the tank wall will be cooled by the frothing liquid during venting.

Baseline 2: (80 kW/sq m, 120 degree roll)

This test involved a tank filled to 85% capacity with Freon 11 as per Baseline #1. The relief valve orifice diameter was 6.4mm. The tank was rolled 120 degrees to one side off vertical. The tank heat flux was 80 kW/m^2.

Figure 2.4-5 presents the measured tank pressure vs time. As can be seen from the plot the pressure rises rapidly until the pressure relief valve comes into play. Note that because the tank is rolled that liquid enters the relief valve for most if not all of the test.

During most of the test that lasted 600 seconds, the relief valve cycled. However, at times 360-440 seconds and from 520-560 seconds the pressure measurements go off scale. This may be an instrument failure or it may be an indication that the valve is passing a 2-phase mixture and therefore pressure relieving ability of the valve is reduce thus causing the pressure to rise rapidly. This, however, has not been confirmed.

The time to first relief valve action is later than in Baseline 1. In fact, the times to first valve action should be identical but it is believed that non-uniform heat flux around the circumference causes the rolled tank to pressurize slower. This different heat flux rate may also be the reason that the relief valve does not enter a continuous venting mode. Liquid flow through the relief valve may also be a reason why the valve does not enter the continuous venting mode.

Figure 2.4-6 presents wall temperatures for the test. As can be seen from the figure, the wall temperatures near the top of the tank reach very high levels very rapidly. The effects of frothing are not evident. Frothing does not take place to the same degree because the valve is passing liquid not vapour and therefore large amounts of vapour generation is not required to maintain the tank pressure. As a result of the lack of frothing and wetting of the tank upper surface, the tank wall temperatures in the upper part of the tank are higher than they were in the Baseline 1 test.

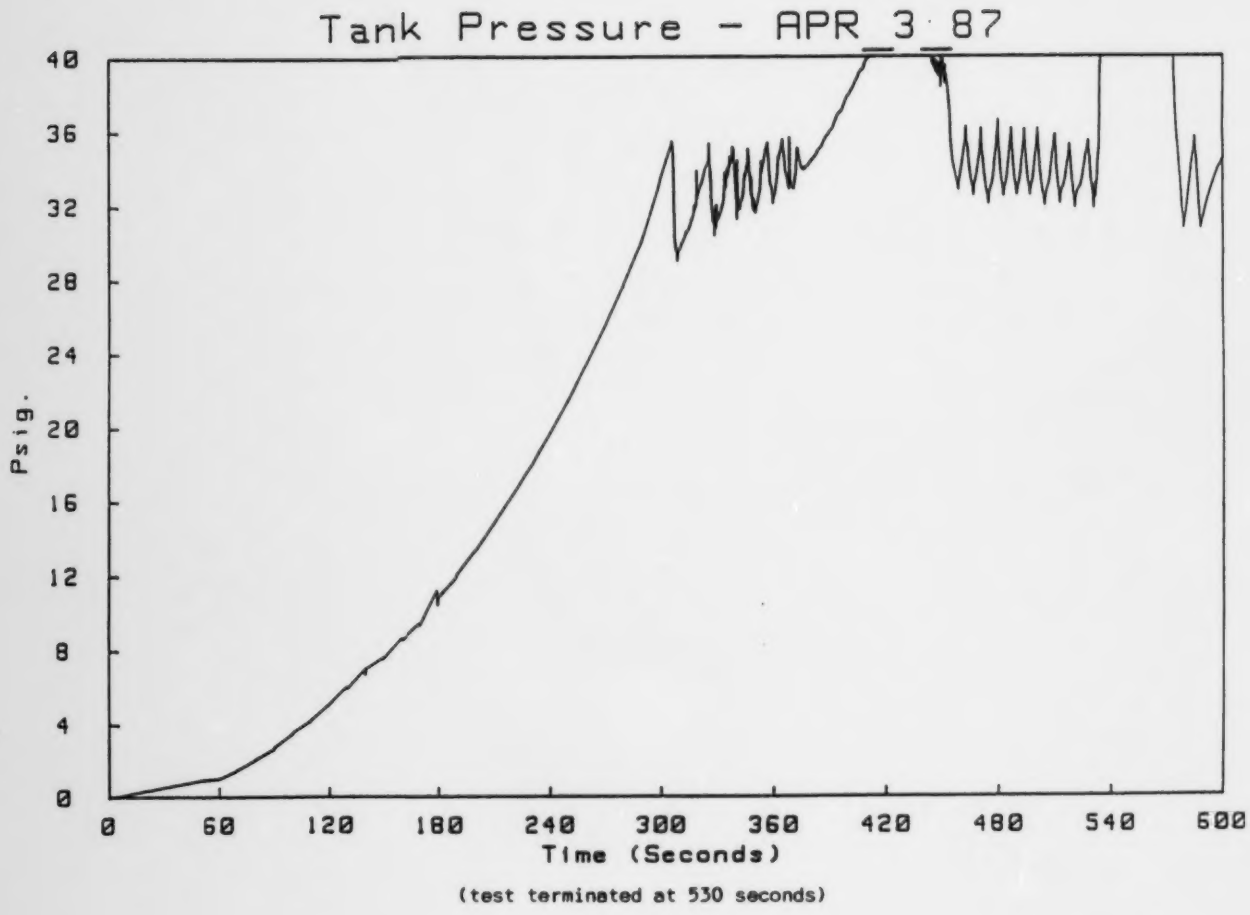

FIGURE 2.4-5 BASELINE TEST #2 TANK PRESSURE VS TIME

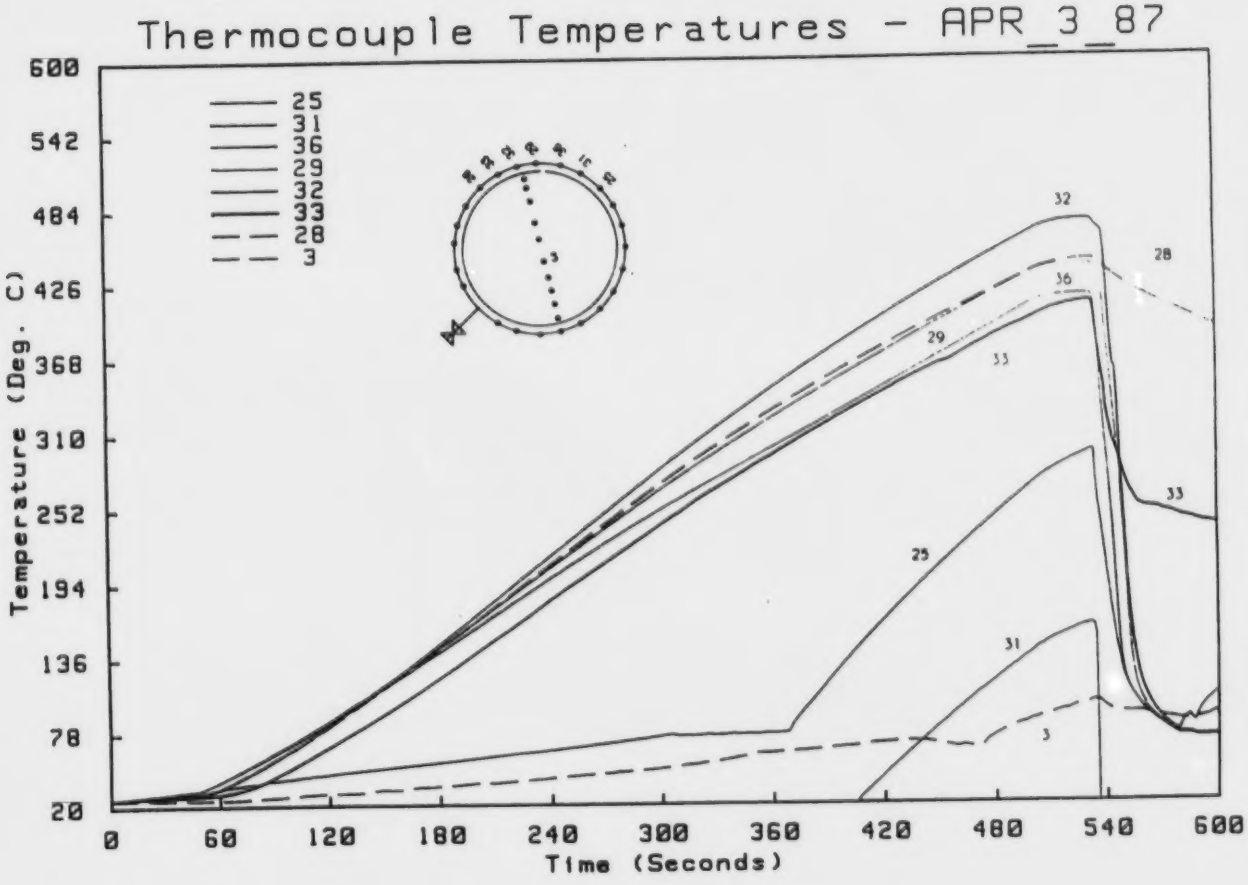

(test terminated at 530 seconds)

FIGURE 2.4-6 BASELINE TEST #2
WALL TEMPERATURES VS TIME

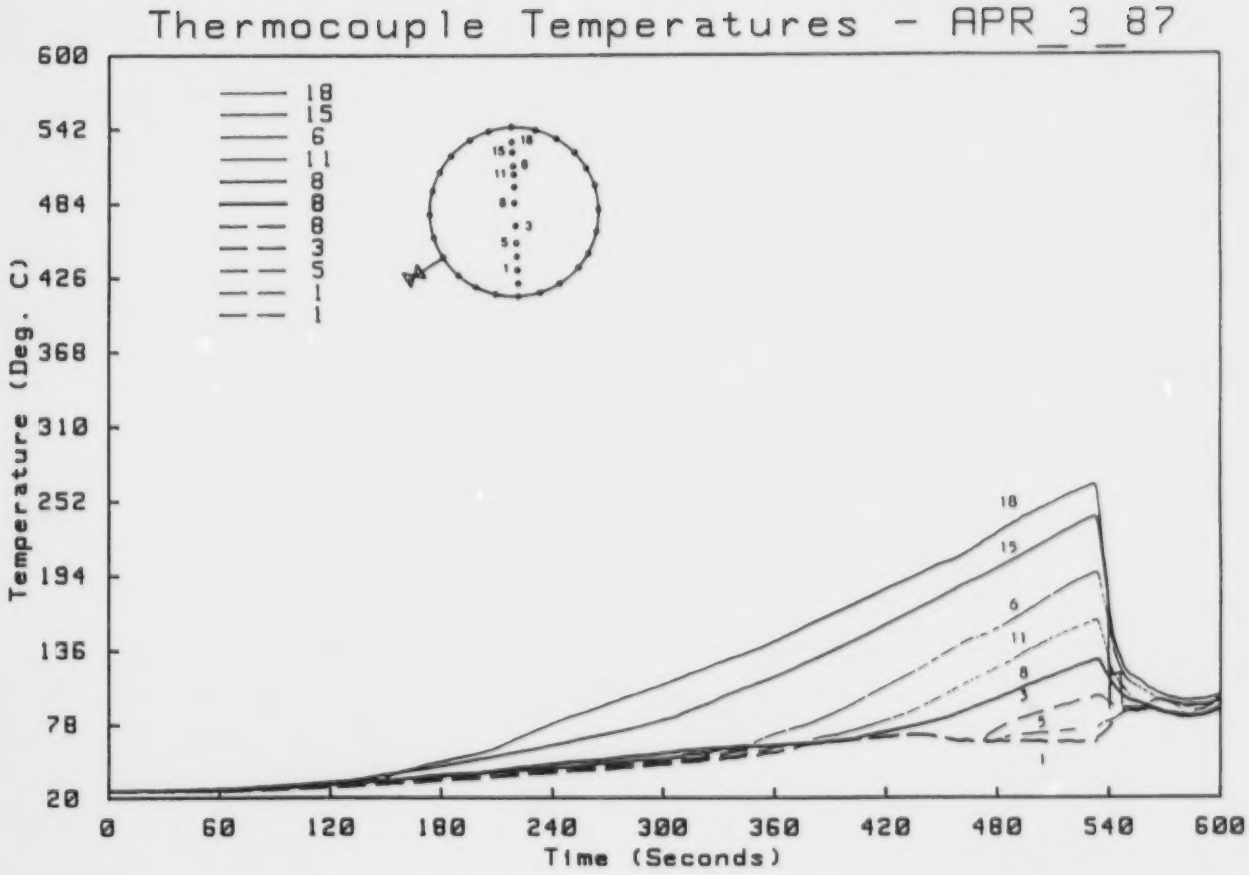

(test terminated at 530 seconds)

FIGURE 2.4-7 BASELINE TEST #2 LADING TEMPERATURE VS TIME

Figure 2.4-7 presents the lading temperatures vs time for the Baseline 2 test. As can be seen from the figure, there is significant temperature stratification. These temperature stratifications grow until approximately 540 seconds when suddenly the lading mixes and the temperature gradients die out. It is believed that at this point in time, the liquid level drops below the relief valve opening and the valve begins to pass vapour. The resultant frothing and boiling mixes the lading and renders a near uniform temperature.

Test # 1

This test involved a tank filled to 80% capacity with Freon 11 exposed to an external heat flux of 40 kW/sq m. The relief valve orifice diameter was 6.4mm. The tank was not rolled and was equipped with an internal shell device as described in Section 2.3. The annular gap was 13mm.

This test was basically a low power test run to ensure that the internal shell device did not result in any unanticipated undesirable effects. Figure 2.4-8 presents the measured tank pressure vs time. The pressure response of the tank was typical with an initial rapid pressurization until valve action and then valve cycling for the remainder of the test.

Figure 2.4-9 presents the measured tank wall temperatures near the top of the tank. In this test, the internal shell resulted in the frothing effecting more of the wall than in a tank not equipped with the internal shell. In the upper regions of the tank wall the frothing brings the wall temperatures down and holds them down for long periods. The frothing in the annulus was above the liquid level in the core by as much as one third of the tank diameter. Note that it was the froth that was above the liquid level in the core, the liquid level in the annulus was not significantly higher than the liquid in the core.

During the test it was clear that the check vent resulted in a short circuit between the annulus and the core, thereby eliminating any suction in the annulus to lift the annulus liquid levels above that in the core.

Figure 2.4-10 presents the measured lading temperatures for the test. As can be seen from the figure, there are significant temperature gradients established in the lading. These gradients die down at approximately 780 seconds into the test. As in all the tests, the gradients died down as a result of effective mixing caused by boiling and frothing actions.

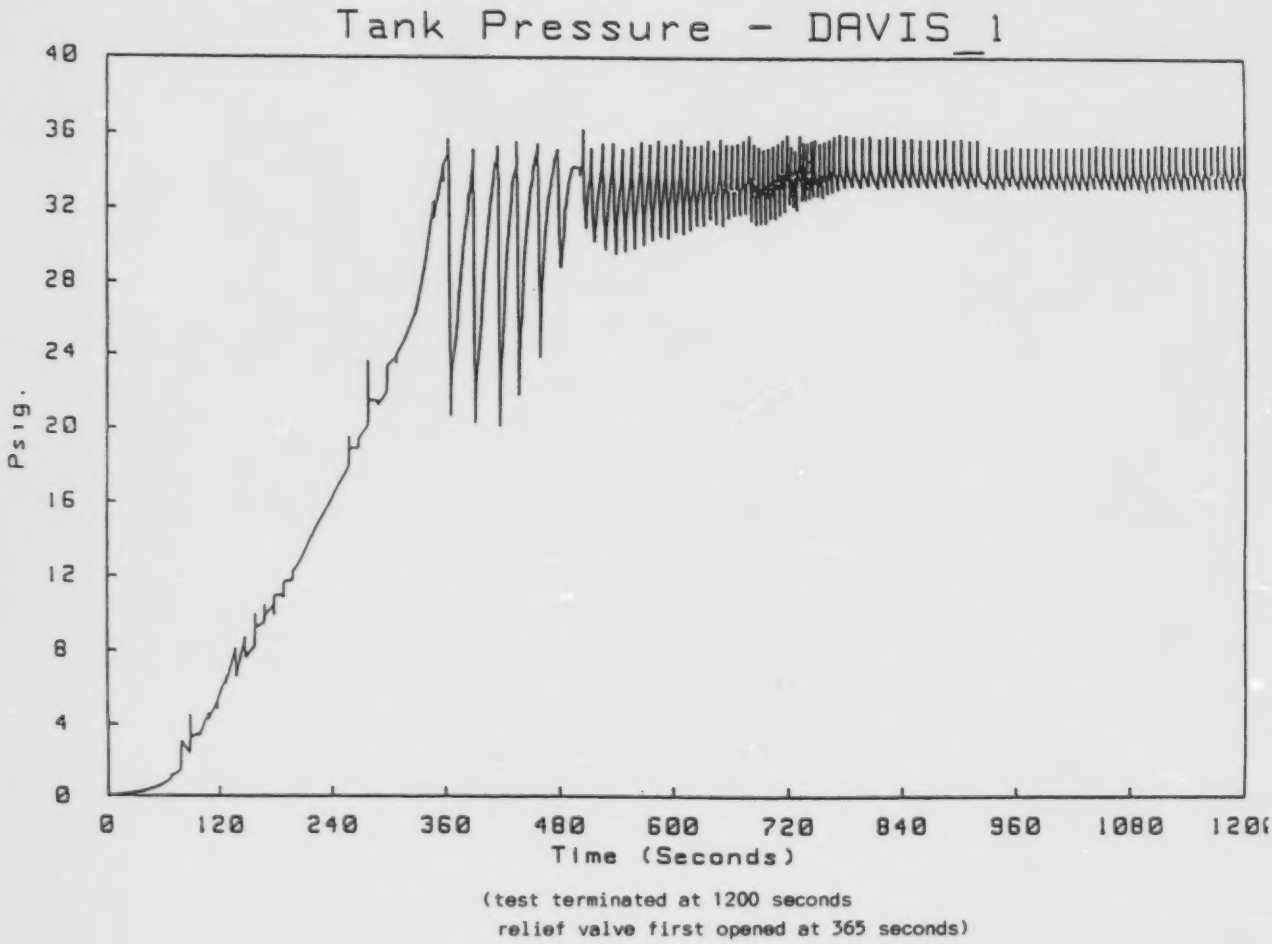

(test terminated at 1200 seconds
relief valve first opened at 365 seconds)

FIGURE 2.4-8 TEST #1 TANK PRESSURE VS TIME

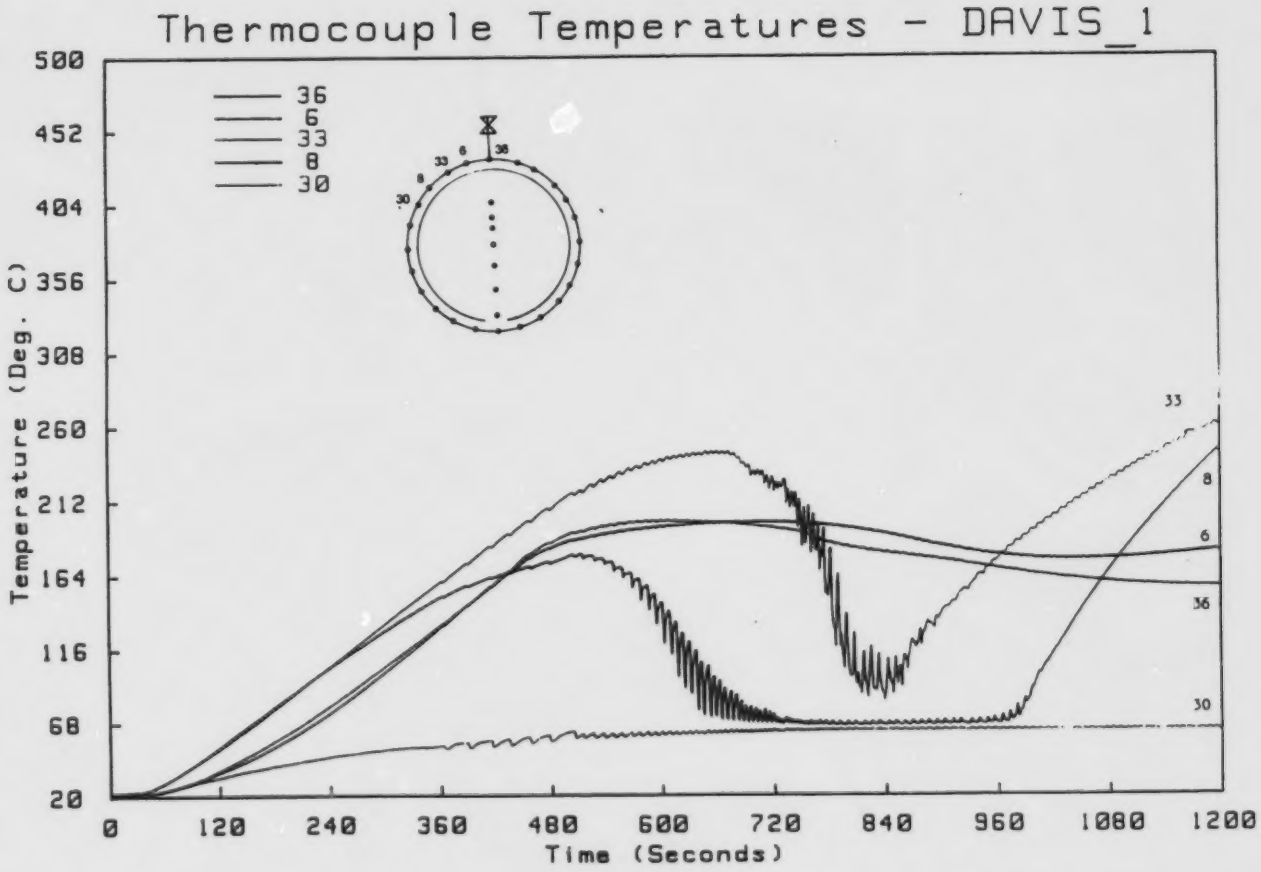

(test terminated at 1200 seconds
relief valve first opened at 365 seconds)

FIGURE 2.4-9 **TEST #1**
WALL TEMPERATURES
(UPPER-LHS) VS TIME

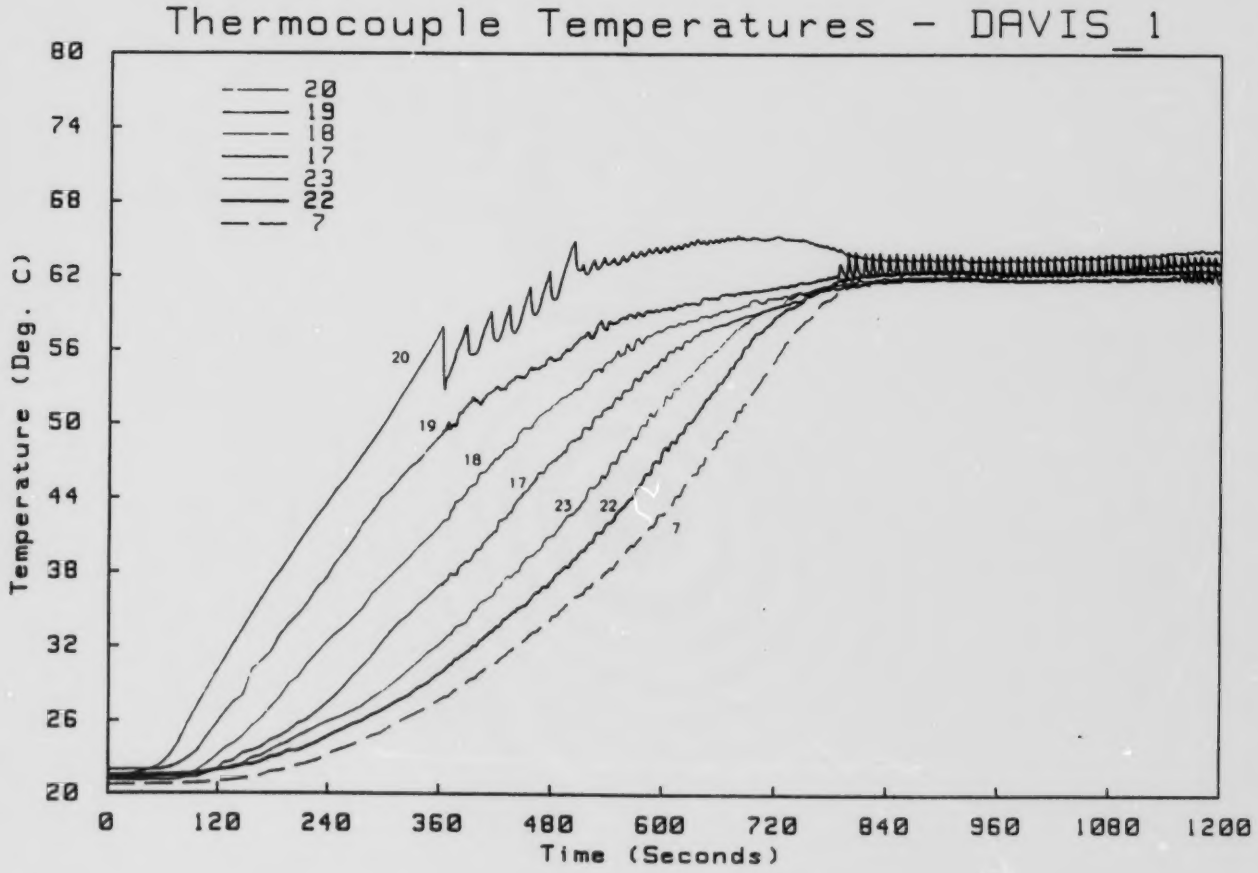

(test terminated at 1200 seconds)

FIGURE 2.4-10 **TEST #1**
LADING TEMPERATURES
(VERTICAL PROFILE)
VS TIME

Test #2

This test involved a tank filled to 80% capacity with Freon 11 exposed to an external heat flux of 80 kW/m². The relief valve orifice diameter was 6.4 mm. The tank was not rolled and was equipped with an internal shell as described in Section 2.3. The annular gap was 13mm.

Figure 2.4-11 presents the measured tank pressure versus time. As can be seen from the figure, the pressure rises rapidly until the relief valve comes into play at approximately 190 seconds. The relief valve cycled from that time until approximately 420 seconds. Beyond 420 seconds, the relief valve remained opened and the tank pressure rose steadily until approximately 720 seconds when the test was terminated. The test was terminated because the tank internal pressure continued to rise. It appears that for this condition (80 kW/sq. m heat flux with the internal shell in place) the standard size relief valve was not adequate. In other words, when an internal shell is installed it may be necessary to increase the size of the pressure relief valve because the internal shell results in more heat being transferred to the lading.

Figure 2.4-12 presents measured wall temperatures versus time. As can be seen from the figure wall temperatures near the top of the tank rise rapidly initially until the pressure relief valve comes in action and then the wall temperatures begin to drop. As mentioned earlier, the drop in wall temperatures during venting is a result of frothing and boiling that rises in the annulus and cools the wall.

The intention of the internal shell device is to direct the frothing higher into the tank, thereby cooling higher areas of the tank wall. In this test, the wall temperatures at the top of the tank at approximately 400 seconds into the test are similar to those measured in the Baseline 1 test. However, in the Baseline test, the wall temperatures continue to rise beyond 400 seconds because the frothing in the tank in that test did not lift high enough to effect the present test; however, beyond 400 seconds the internal shell causes the froth to continue to rise into the upper regions of the tank and cool the wall in that area. As can be seen from the figure in some areas of the wall (thermocouple #8) the frothing holds the temperature down until approximately 600 seconds into the test at which point the temperature rises rapidly because the frothing no longer has effect in that area.

When observing the test, it could be seen that the frothing in the annulus was up to one-third the tank diameter above the liquid level in the core. This is similar to what was observed in DAVIS Test #1. As with Figure 2.4-11 Test #2 Tank Pressure vs Time

On DAVIS test #1, the check vents resulted in a short-circuit between the annulus and the core and this had a detrimental effect on the ability of the internal shell to direct the froth into upper regions in the tank. The short-circuits also results in a lack of suction generated in the annulus by the relief valve action thereby eliminating the ability of the internal shell to draw the liquid level up in the annulus. However, even with the short circuiting effect of the check vents, there was a small height differential between the annulus liquid and the core liquid of approximately 2 cm. This height differential existed even with the relief valve closed and therefore is believed to be due to density differences between the hot liquid in the annulus and the cool liquid in the core.

Figure 2.4-13 presents the measured lading temperatures versus time. Once again, temperature stratification in the liquid and vapour is evident from the figure. The temperature gradients die down approximately 480 seconds into the test. As before, these gradients die down as a result of mixing in the lading caused by the venting action. The temperature of the lading for the remaining period of time is approximately the saturation temperature at the current tank internal pressure. The time at which the temperature gradients die down coincides closely to the point in time when continuous venting begins.

Test #3

This test involved the tank filled to 80% capacity with Freon 11 exposed to a heat flux of 60 kW/sq. m. The relief valve orifice diameter was 6.4 mm. During the test, the tank was rolled to 60 degrees from vertical at the beginning of the test, then to 120 degree roll at 650 seconds into the test. When the tank was rolled from 60 to 120 degrees at 650 seconds into the test instrumentation failure occurred. Therefore, beyond this point the measured data should be scrutinized for instrumentation errors. In the test, the tank was equipped with an internal shell as described in Section 2.3. The annular gap was 13mm.

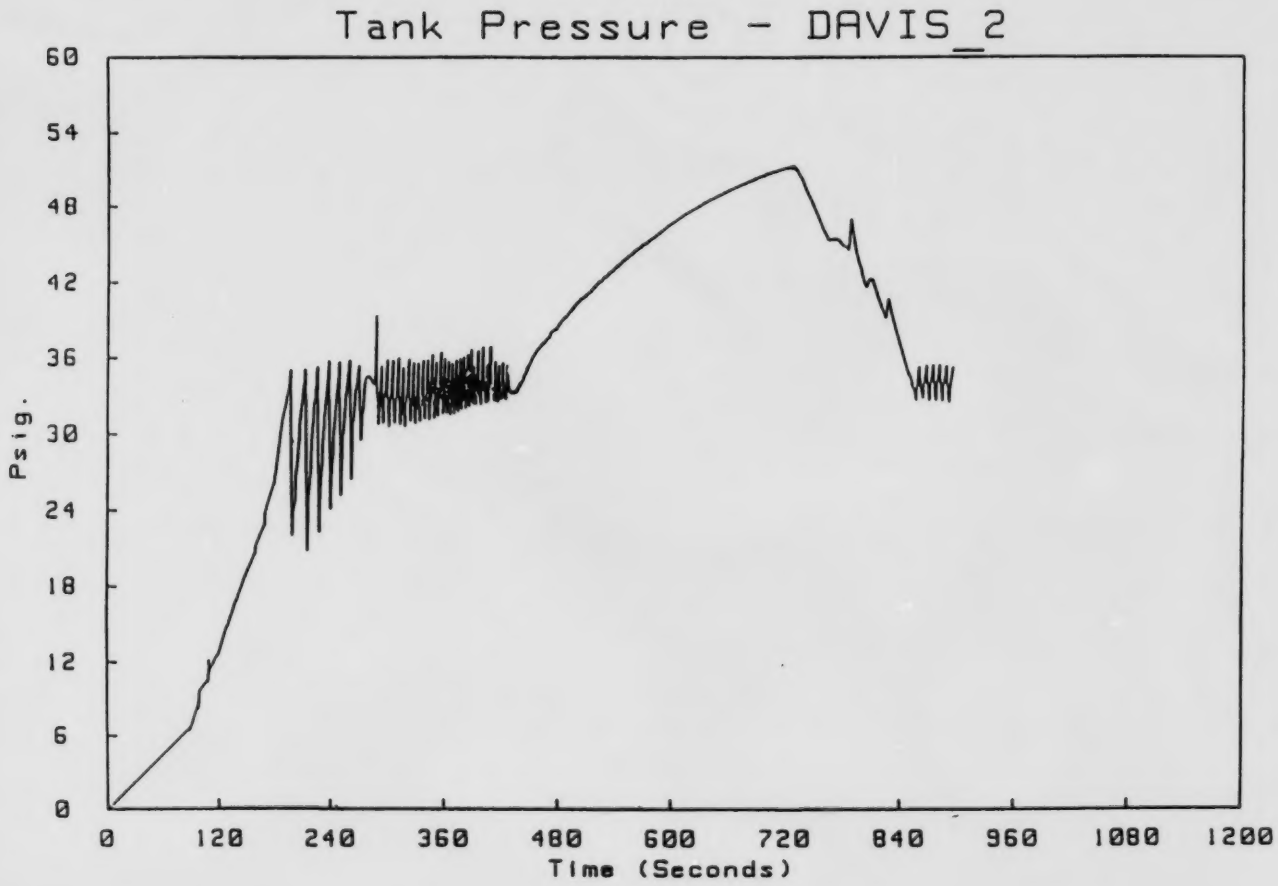

(test terminated at 720 seconds)

FIGURE 2.4-11 TEST #2 TANK PRESSURE VS TIME

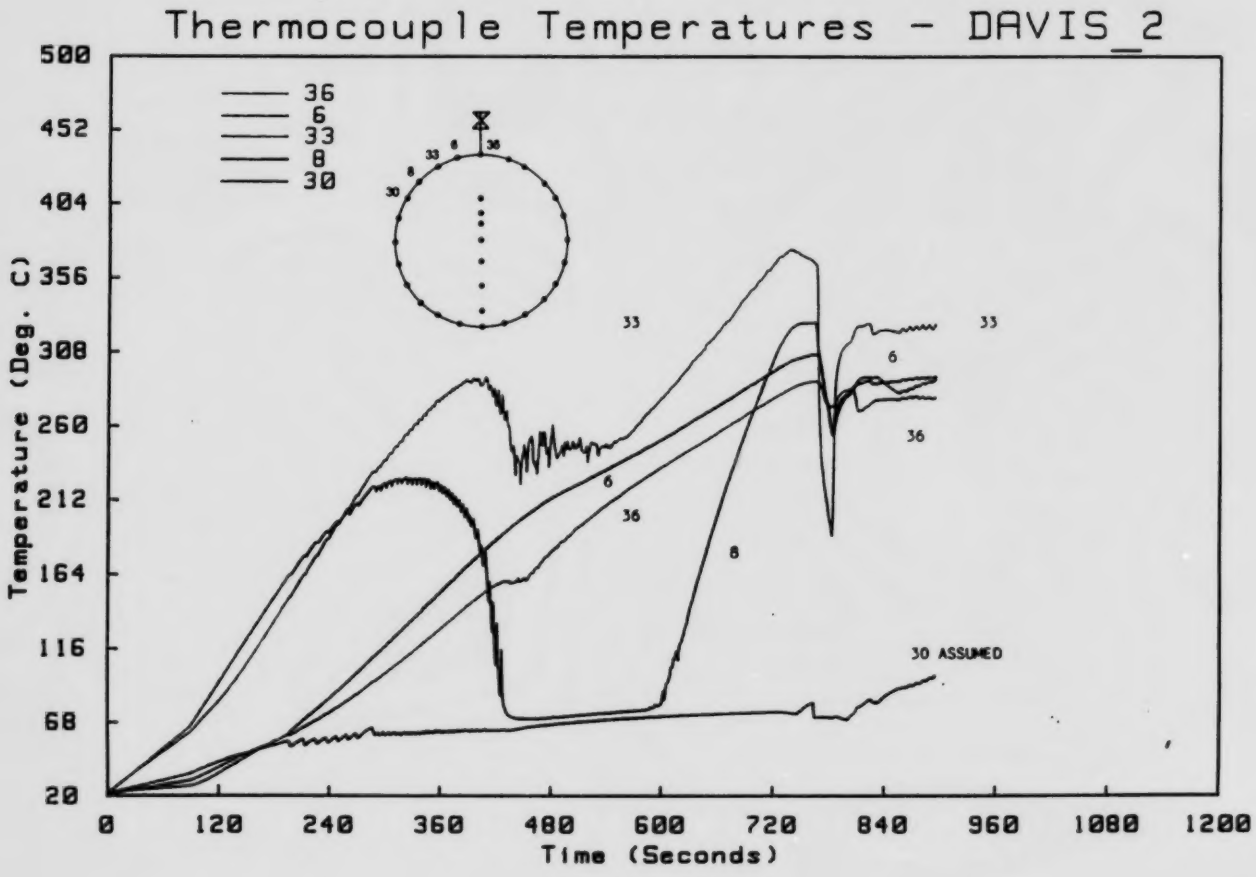

(test terminated 720 seconds)

. FIGURE 2.4-12 TEST #2 WALL TEMPERATURES (UPPER-LHS) VS TIME

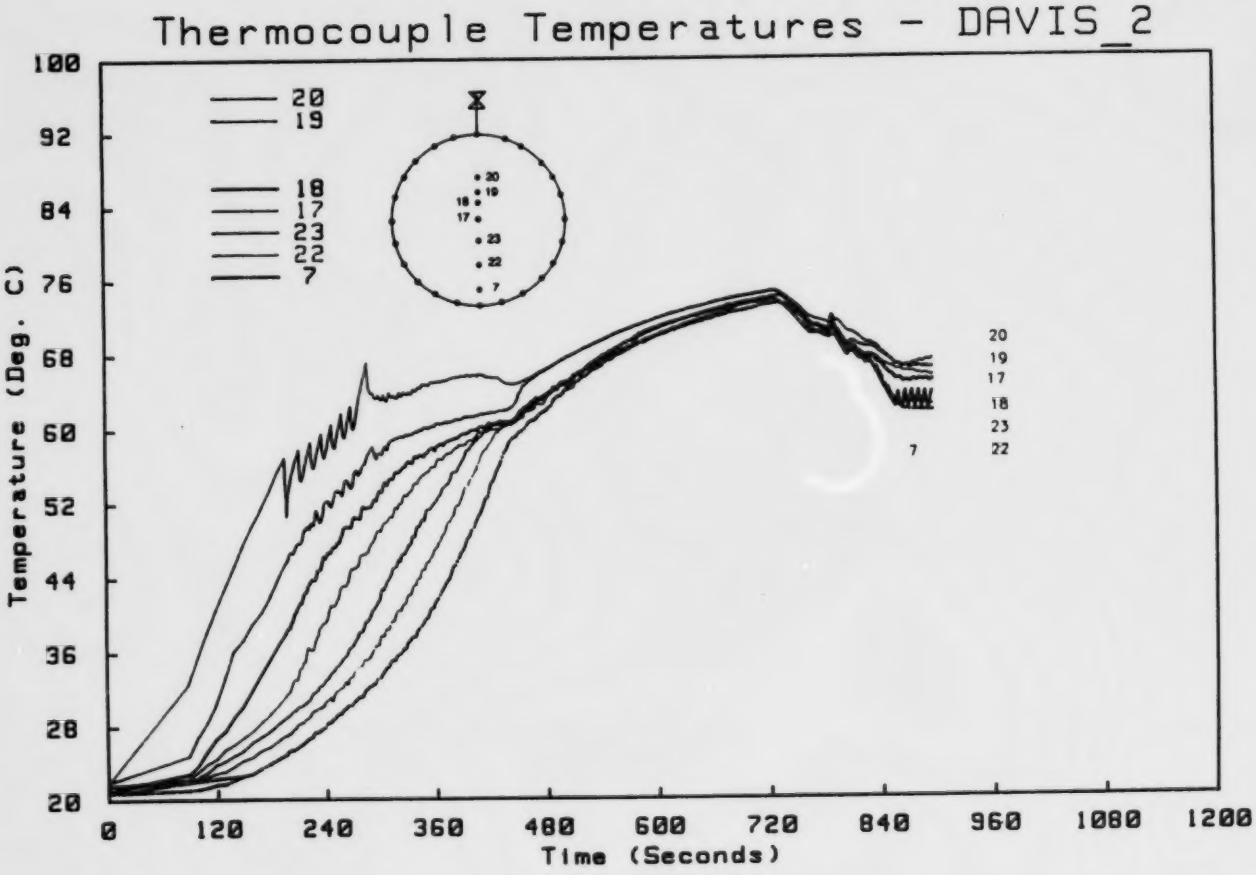

(test terminated at 720 seconds)

FIGURE 2.4-13 **TEST #2**
LADING TEMPERATURES
(VERTICAL PROFILE)VS TIME

Figure 2.4-14 presents the measured tank pressure versus time. As can be seen from the figure, the tank pressurizes rapidly until approximately 240 seconds when the pressure relief valve comes into play. For the remainder of the test, the valve cycled. The test lasted approximately 1200 seconds. During the test, there were two sudden increases in tank pressure above the valve cycling pressure. This may be due to the relief valve passing a two phase mixture, thereby reducing the valve's capacity. These pressure rises lasted only for brief periods of time and eventually the pressure came back down to the valve cycling range.

Figure 2.4-15 presents the measured tank wall temperatures versus time. The wall temperatures shown are for regions near the top of the tank. As can be seen from the figure, the wall temperatures near the top of the tank reach high values early in the test. The effect of frothing is not evident. As in Baseline #2 test, the frothing effect is not evident because initially in the test the pressure relief valve is drawing liquid rather than vapour. Because of this vapour generation is not taking place in the tank and therefore frothing is not significant. At 650 seconds into the test, instrument failure occurred.

It is clear from the results presented here that the internal shell has little effect in a rolled tank. Because froth is not generated, the internal shell cannot effectively cool the walls in the upper regions of the tank.

Figure 2.4-16 presents the measured lading temperature for Test #3. Once again, temperature gradients are clearly seen in the lading and these gradients die down at approximately 600 seconds into the test. Beyond 650 seconds the instrumentation failure causes some uncertainty in the measured temperatures.

Test #4

This test involved a tank filled to 80% capacity with Freon 11 exposed to an external heat flux of 80 kW/sq. m. The relief valve orifice diameter was 6.4 mm. The tank was not rolled and was equipped with an internal shell as described in Section 2.3. The annular gap was 13mm.

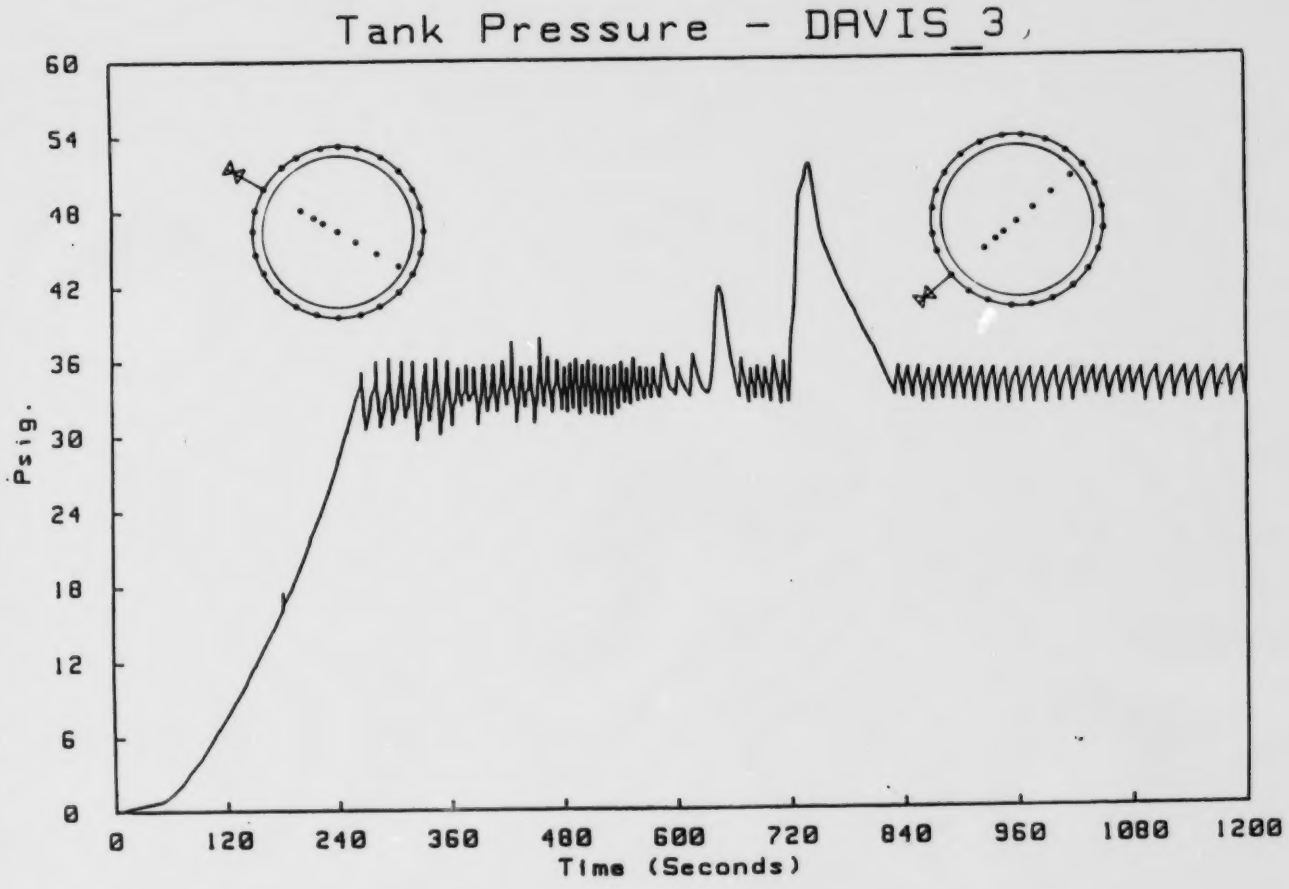

FIGURE 2.4-14 TEST #3 TANK PRESSURE VS TIME

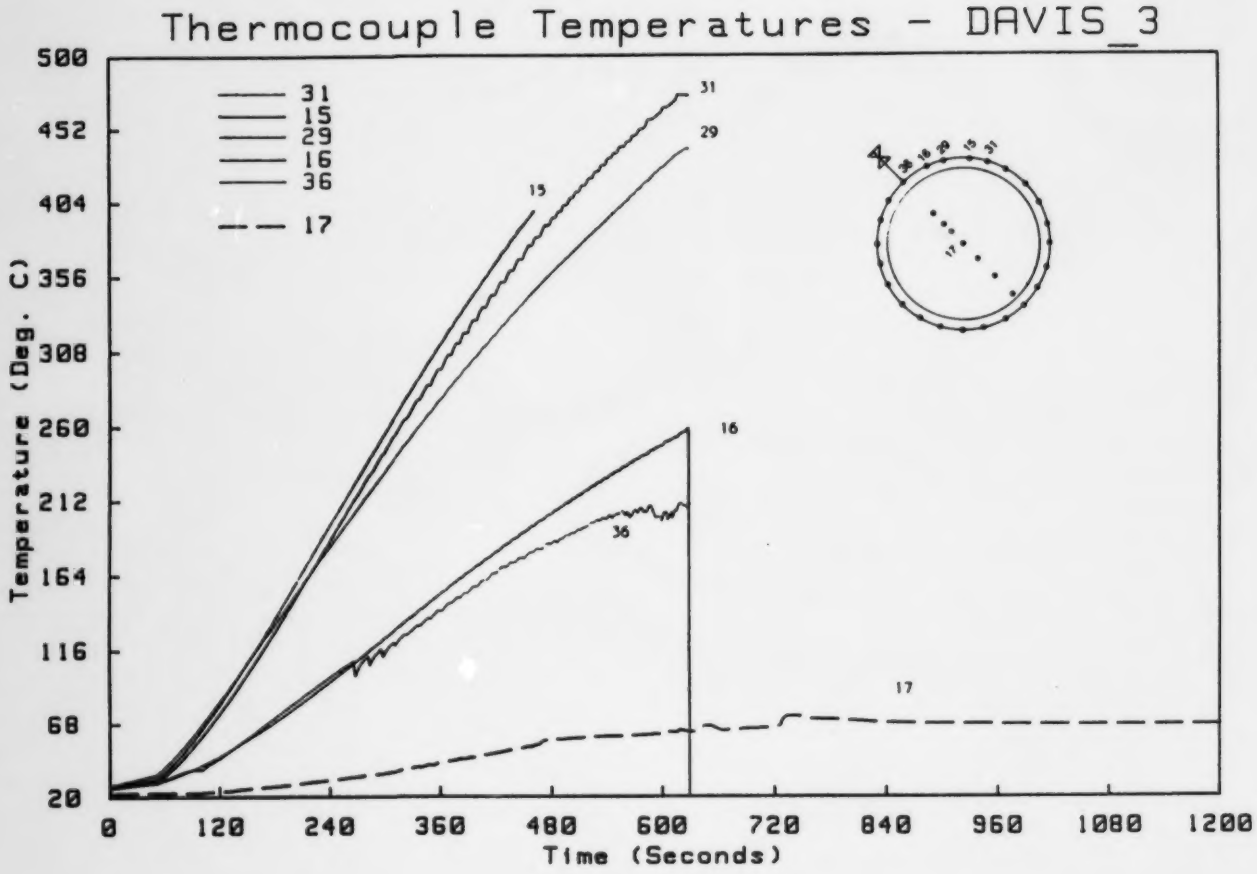

(test terminated 1200 seconds
60° roll changed to 120° roll at 650 seconds)

FIGURE 2.4-15 TEST #3 WALL TEMPERATURES (UPPER-RHS) VS TIME

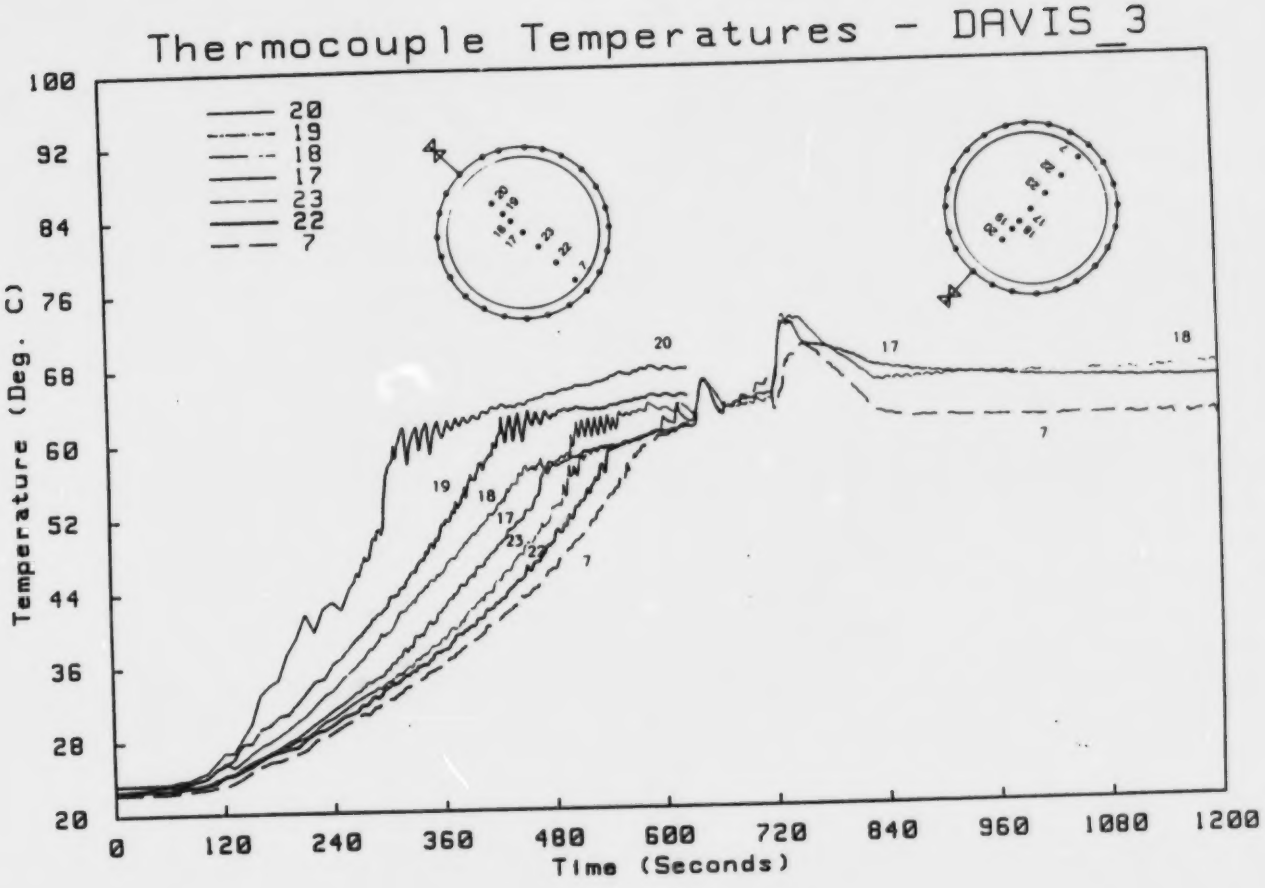

(test terminated at 1200 seconds
60° roll changed to 120° roll at 650 seconds)

FIGURE 2.4-16 TEST #3 LADING TEMPERATURES VS TIME

In this test, an attempt was made to seal off the check vents. However, during the test it was evident that the attempt to seal the check vents was not successful. The check vents continued to leak and therefore the effectiveness of the internal shell device was compromised to some degree.

Figure 2.4-17 presents the measured tank pressure versus time for Test #4. As in all the tests after the heat input was started, the tank pressurized rapidly until the relief valve came into play. First relief action occurred at approximately 180 seconds into the test. From that point on, the valve cycled until approximately 550 seconds into the test. Beyond that point the relief valve remained opened and the tank pressure rose steadily to a peak value of approximately 350 kPa. At that point in time (1000 seconds), the test was terminated because of a high pressure. Once again it appears that the presence of the internal shell device causes an increased heat flux into the tank lading and therefore the pressure relief valve capacity should be increased.

Figure 2.4-18 presents the measured wall temperatures near the top of the tank versus time. As can be seen from the figure, the tank wall temperatures near the top of the tank do not seem to be effected by froth. However, if these temperatures are compared with Baseline test #1, it will be seen that the temperatures here are significantly lower than in that test. Thermocouple locations 29 and 15 are engulfed in froth directed by the internal shell and temperatures in these areas remain close to that of the cooled liquid up until 600 seconds into the test. When comparing this to Baseline Test #1, the temperature of thermocouples mounted in similar locations exceeded or would have exceeded 300°C. In the present test thermocouples in this area measured approximately 70°C at 600 seconds into the test. Beyond 600 seconds the effect of the frothing dies down and the temperatures in these regions increase until termination of the test at approximately 1000 seconds.

Although the internal shell did not result in frothing to cover all areas of the tank wall exposed to vapour it did direct frothing over large areas. The results of this frothing were shown in the form of low wall temperatures in regions that showed high wall temperatures in the baseline test. This is an indication that the internal shell can significantly reduce wall temperatures in the

upper regions of the tank. However, it has yet to be shown what the required gap will be to insure this cooling effect over all of the wall areas wetted by vapour for the full time required to empty all the ladding. It should also be noted that in this test the check vents continued to leak thereby short-circuiting the annulus and core regions. This short-circuiting effect results in a loss in the suction build-up in the annulus which is intended to draw the liquid level in the annulus up to a level above the liquid in the core region.

Figure 2.4-19 presents the measured lading temperatures for Test #4. As can be seen from the figure, the typical temperature stratification is established and this stratification dies down once continuous venting begins.

Test #5

This test involved a tank filled to 80% capacity with Freon 11 exposed to an external heat flux of 80 kW/sq. m. In this test the relief valve orifice diameter was increased from 6.4 mm to 9.5 mm. The tank was rolled 120° and equipped with an internal shell as described in Section 2.3. Annular gap was 13mm.

In this test the internal shell had been replaced with a new shell that did not have any check vents in it. Therefore, this is the first test in which the annulus and core can only communicate through the bottom slot in the inner shell. The relief valve size was increased in this test to increase the flow velocities in the annulus during the venting process. It had originally been intended to reduce the annulus gap, however, because of interference with instrumentation and other practical considerations it was not possible to reduce the gap further.

Figure 2.4-20 presents the measured tank pressure for Test #5. As can be seen from the figure, the tank pressure rises rapidly until approximately 180 seconds into the test when the pressure relief valve comes into action. From this point on to the end of the test at 600 seconds the relief valve cycled. However, note that the relief valve cycle is very long compared with previous tests. This is because of the fact that the pressure relief valve is venting liquid and because the pressure relief valve orifice has been increased from the original 6.4 mm to 9.5 mm.

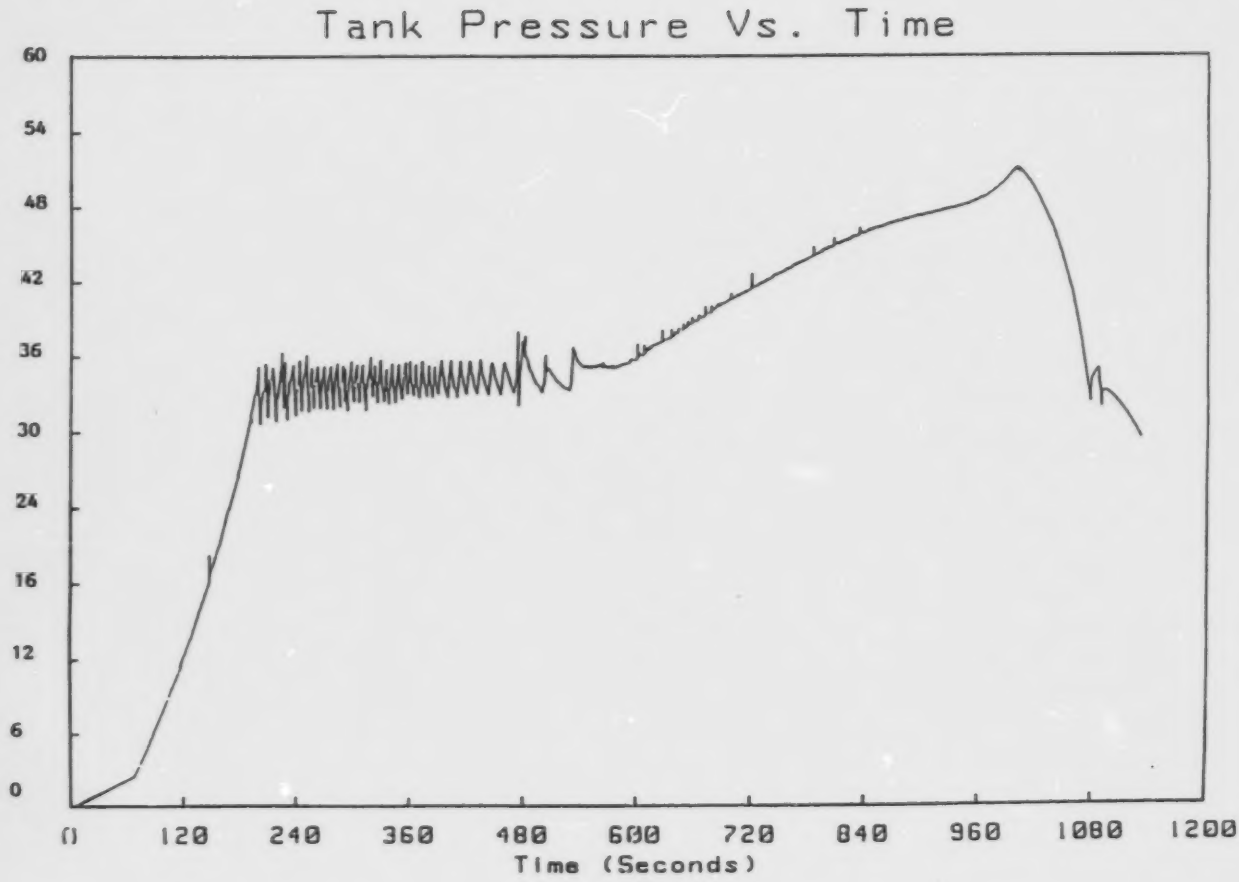

(test terminated at 970 seconds)

FIGURE 2.4-17 TEST #4 TANK PRESSURE VS. TIME

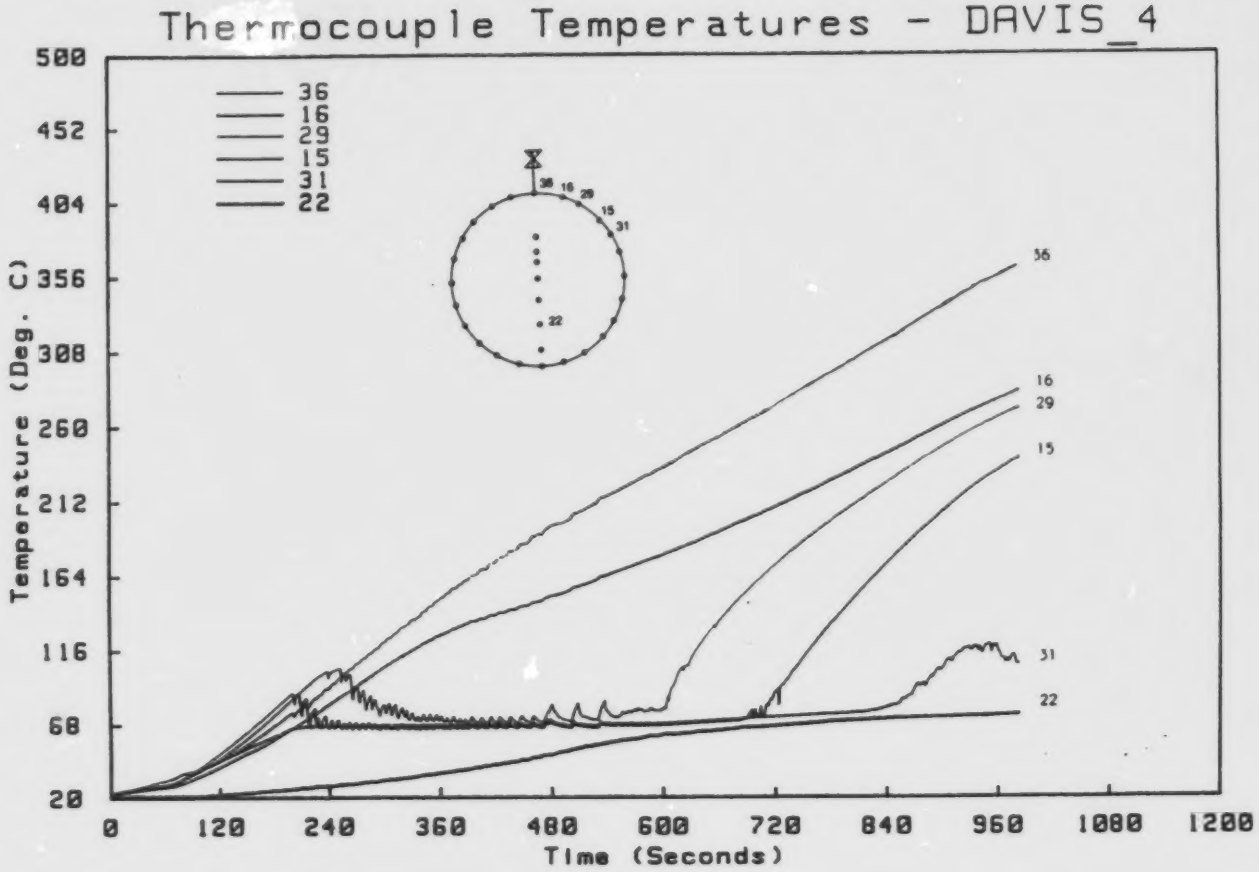

(test terminated at 970 seconds)

FIGURE 2.4-18 TEST #4 WALL TEMPERATURES (UPPER-RHS) VS TIME

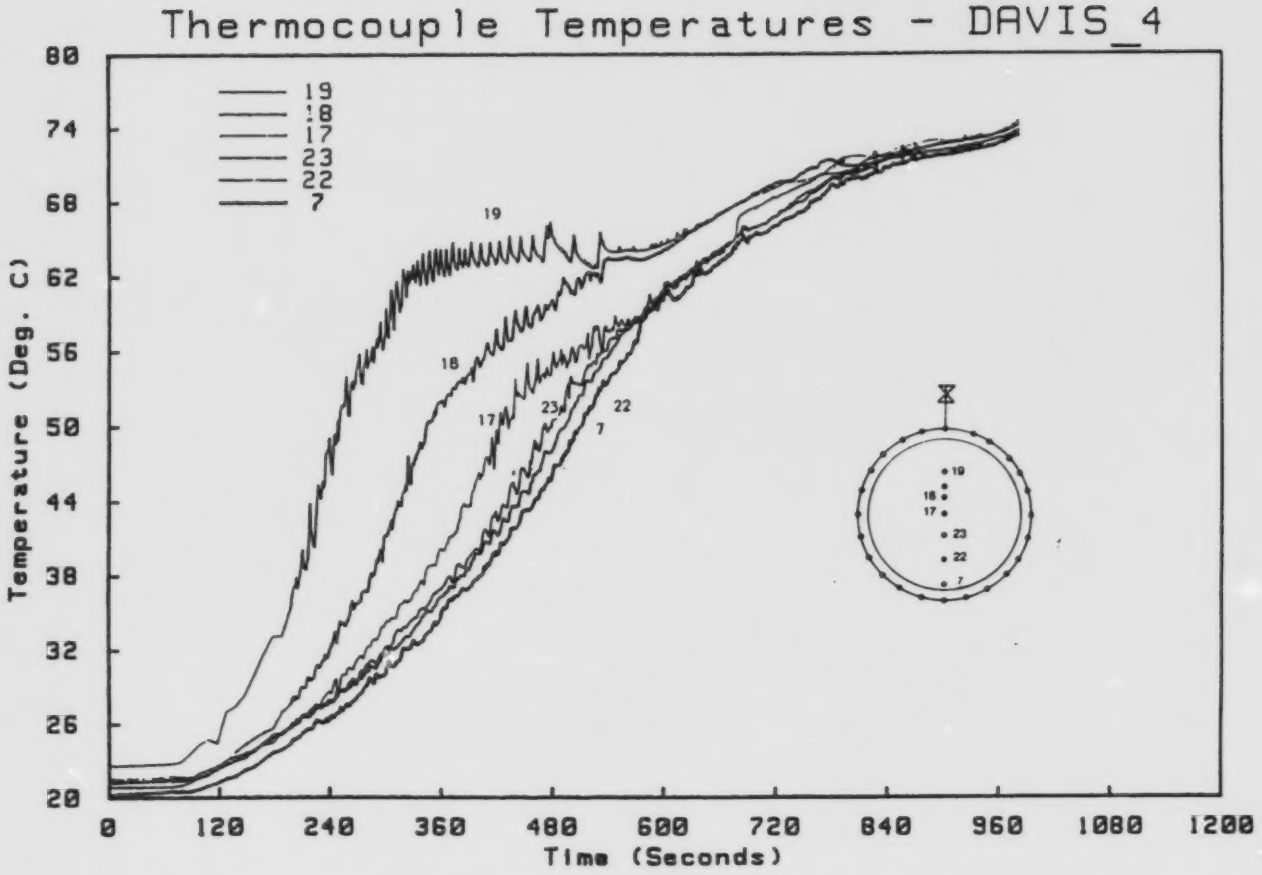

(test terminated at 970 seconds)

FIGURE 2.4-19 TEST #4 LADING TEMPERATURE VS TIME

Basically what is occurring in the test is that when the relief valve opens, liquid is drained from the annulus and the remainder of the lading is trapped in the internal shell. With the bulk of the liquid lading separated from the heat flux by the gap in the annulus, it is difficult to transfer heat to the liquid lading and increase the tank internal pressure. As a result, every time the pressure relief valve vents and reduces the tank pressure, it takes a long period of time to increase the tank pressure back to relief valve set pressure. This, of course, is a dangerous condition because, although the tank liquid lading is isolated from the heat flux thereby reducing the tank pressurization rate, the liquid is also isolated from the tank primary wall. Since it is the liquid lading that cools the tank primary wall, the tank wall temperatures rise very rapidly in this test case.

Figure 2.4-21 presents the measured tank wall temperatures in the lower portion of the tank adjacent to the internal shell slot versus time. As can be seen from the figure, the wall temperatures rise rapidly in the upper regions (vapour wetted) of the tank. The effect of the frothing is not evident from the data and this is expected because the pressure relief valve is venting liquid and vapour generation within the tank is not taking place to any significant degree. It is assumed that instrumentation failure occurred on thermocouples 5 and 22 at apprxoimately 500 seconds.

It is clear that the internal shell has little or no effect in cooling the tank wall in the upper regions of the tank; in fact, the presence of the internal shell may actually increase the wall temperatures in the lower regions of the tank because of the fact that when the annulus is drained the remaining liquid is trapped in the internal shelf. The effect of forced convection in the annulus during venting does have a slight cooling effect.

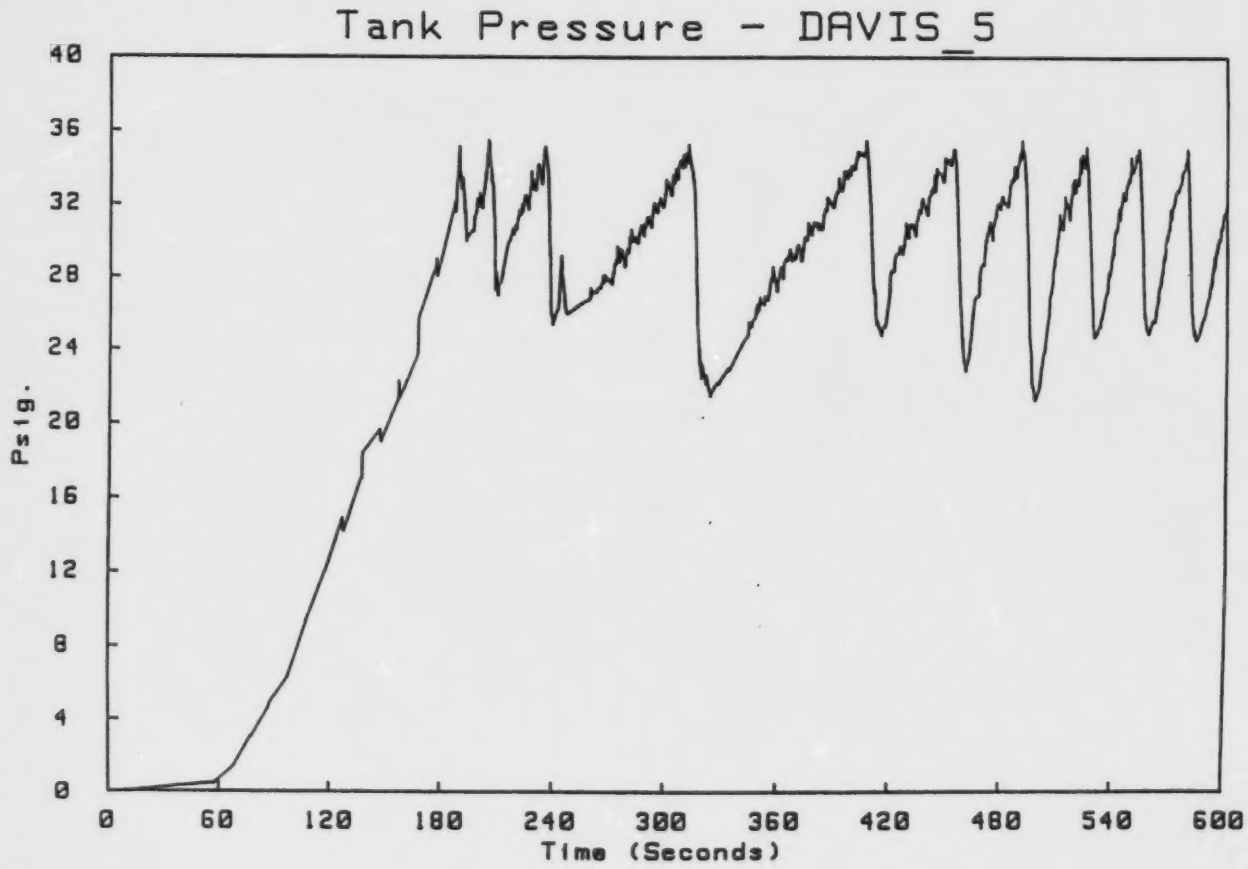

(test terminated at 600 seconds)

FIGURE 2.4-20 TEST #5 TANK PRESSURE VS TIME

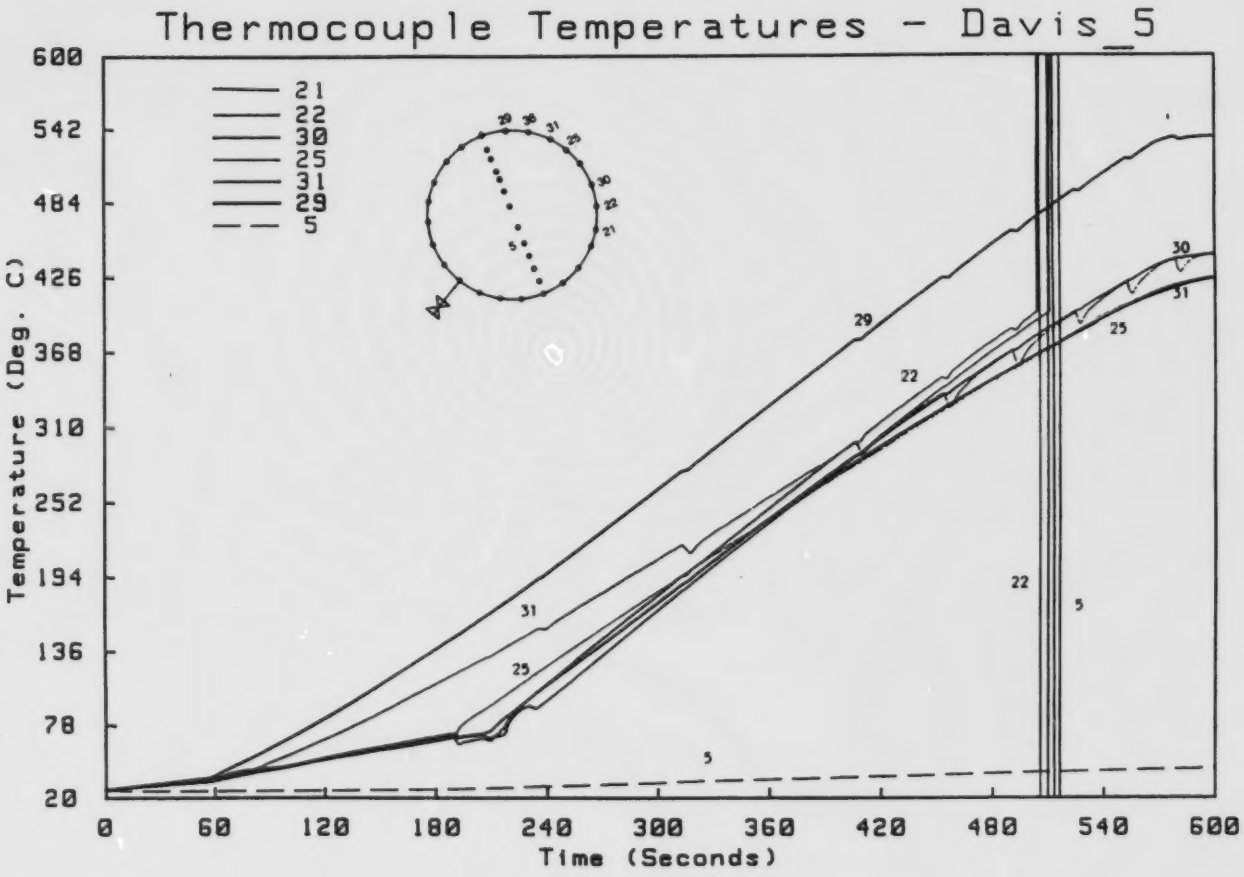

(test terminated at 600 seconds)

FIGURE 2.4-21 TEST #5 WALL TEMPERATURES VS TIME

TEST SUMMARY

In summary, the internal shell device for an upright tank did significantly reduce the peak wall temperatures in certain areas of the tank. The tests clearly showed that the internal shell acted to direct the liquid and frothing liquid along the wall during the relief valve action, thereby increasing the convective boiling coefficient for the wall and reducing the wall temperatures. It also appears that because the internal shell results in more effective cooling of certain parts of the tank wall more heat is being transferred into the lading and therefore a larger relief valve is needed.

It was clear from the tests that the internal shell in its present configuration did not direct frothing and liquid to the very top of the tank. Therefore, areas near the very top of the tank remained in contact with vapour and therefore high wall temperatures were still established. However, it should be noted that even in the areas where frothing didn't reach the tank wall, temperatures were observed to be lower in the internal shell equipped tank than they were in the unprotected tank. This is of course due to the fact that heat will be conducted from the hot regions to the cooler regions of the wall and that even though the tank wall is not visibly being sprayed by the froth and liquid, it is being affected by the misty or frothing flow that passes near the wall on its way to the pressure relief valve.

It is also clear from the present tests that the internal shell device does not effectively cool upper sections of the tank wall when the pressure relief valve is submerged in liquid. When the tank is rolled to a position where the pressure relief valve is below the liquid level in the annulus, liquid is drawn through the pressure relief valve and significant amounts of frothing and boiling do not take place. Because frothing does not take place, the internal shell does not direct froth along the wall and cool the wall in the upper regions of the tank.

As stated in the original proposal, to do these tests (see Reference 1) there was a possibility that after the annulus is drained of liquid, high velocities resulting in the annulus due to the constricted area would result in increased convective heat transfer coefficients in the upper areas of the tank. These increased convective heat transfer coefficients would have some effect in cooling

the upper regions of the tank wall. However, it is not possible from the present tests to see if this effect is significant.

It is clear from the tests that in the rolled tanks the wall temperatures in the upper regions of the tank reached very high levels. It is also clear from the tests that if the internal shell is completely sealed and the tank is rolled the liquid in the annulus will be drained and the remaining liquid will be trapped within the inner shell. As discussed in the original proposal to conduct this study, the possibility of the annulus draining and its detrimental effect on all temperatures was anticipated and it was suggested that holes be strategically placed within the internal shell to allow some leakage so that there will always be some liquid in the annulus to cool the tank wall and to absorb heat. This, however, is beyond the scope of the present test. It is believed, however, based on the results of the present tests that ensuring adequate cooling for a rolled tank would be a difficult task to achieve.

For the as tested conditions, the shell device is only effective in an upright tank where the pressure relief valve is at the top of the tank. In this tank configuration, it is possible to use the internal shell device to direct frothing and boiling liquid along the inner surface of the primary shell to provide effective cooling by convective boiling. In the present tests with gap spacing as described earlier and the pressure relief valve orifice used it was possible to have a frothing region in the annulus which existed as much as one-third of the tank diameter above the liquid level of the core. This frothing region of course has a significant effect on the tank wall temperatures in the upper sections of the tank.

It would be desirable to size the pressure relief valve and the internal shell gap spacing such that during venting the frothing region could be maintained at a height of approximately one tank diameter, therefore ensuring that the tank wall is always exposed to frothing liquid for all filled conditions. This, of course, could result in the pressure relief valve drawing a two-phase mixture and the sizing of the pressure relief valve would have to be established accordingly.

Based on the results of these limited scope experiments a computer model was developed in an attempt to predict the performance of the internal shell concept in a full scale tank-car. Details of this computer model and the results obtained are presented in the following section.

3.0 COMPUTER MODELLING

This section describes the internal shell as it was modelled for the purposes of the preliminary thermal feasibility study. The object of the thermal model was to allow for initial analytical study of the internal shell concept before any detailed experimental work is conducted. The thermal model of the internal shell was developed in parallel with small scale testing of the internal shell at the University of New Brunswick. Details of these tests are present in Chapter 2 of this report.

3.1 MODELLED SYSTEM

The internal shell system as it was modelled includes the tank primary shell, the internal shell, internal shell check vents (before any experiments were conducted the author concluded based on certain model assumptions that the check vents would be required to maintain the core region pressure below or equal to the annulus pressure; however, subsequent test results showed this not to be the case) and the primary shell pressure relief valve. The system was modelled as 2-dimensional, that is no axial gradients were considered and no end effects were considered. It is fully realized that the internal shell system is truly 3-dimensional; however, for the purposes of the preliminary thermal feasibility study, the 3-D effects were not considered. It was originally intended that the present model would be used to study the gross performance of the internal shell concept under the influence of such parameters as tank roll, relief valve size and gap spacing.

Figure 3.1-1 presents a sketch of a cross section through a tank with the internal shell in place. The sketch shows the presence of the relief valve, the annular gap, the bottom slot, the check vents, and the core region. In the sketch, the liquid level is shown to be equal in both the annulus and the inner core. A differential in liquid level will occur if for any reason liquid flows from the core to the annulus or vice versa, or if differential thermal expansion occurs. A difference in level will also occur if boiling occurs in the annulus on the inner surface of the primary shell resulting in the generation of a frothing layer in the annulus.

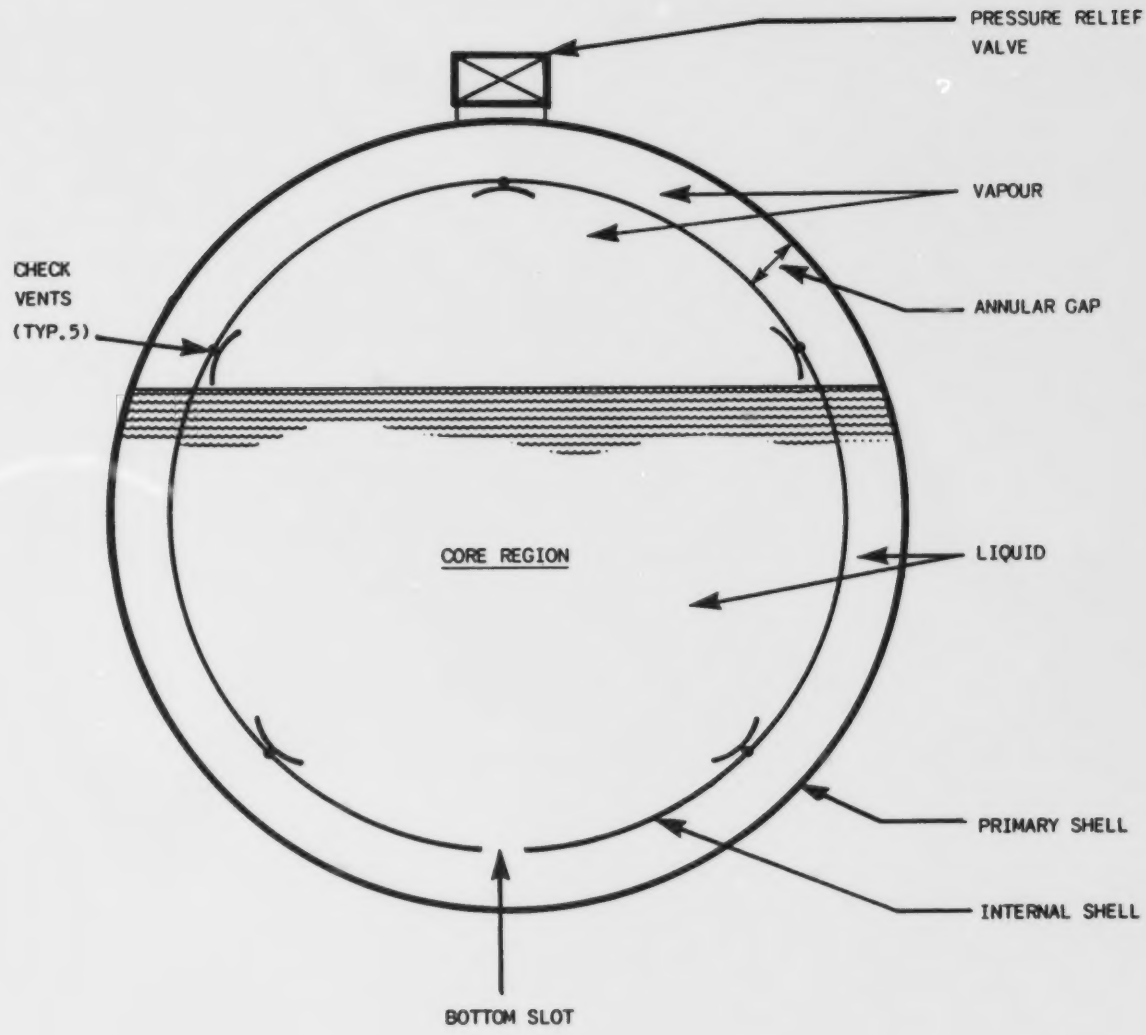

FIGURE 3.1-1 CROSS SECTION OF TANK WITH INTERNAL SHELL

Flow from one region in the tank to another can take place through the bottom slot, and the check vents. Material can only leave the primary shell through the relief valve.

It was the objective of this modelling exercise to predict the overall response of the tank and its lading to fire impingement when the tank is equipped with an internal shell device.

3.2 MODES OF OPERATION

Figure 3.2-2 shows a series of sections through the internal shell equipped tank. These views are intended to show the various modes of operation the shell can be in. In total there are six possible significant modes depending on the location of the liquid level and tank roll. The mode of operation is important because it effects the various flows in and out of the tank. In all cases it was assumed that the bottom slot is diagonally across from the relief valve. The modes are summarized as follows:

Mode 1 both liquid levels (core and annulus) below the bottom slot with Hc > Ha

Mode 2 both liquid levels (core and annulus) below the bottom slot with Hc < Ha

Mode 3 annulus level below slot and core level above slot

Mode 4 annulus level above slot and core level is below the slot

Mode 5 both levels above the slot with Hc > Ha

Mode 6 both levels above the slot with Hc < Ha

where, Hc = vertical liquid height in core
Ha = vertical liquid height in annulus

Each of these modes will now be discussed separately so that their significance can be illustrated.

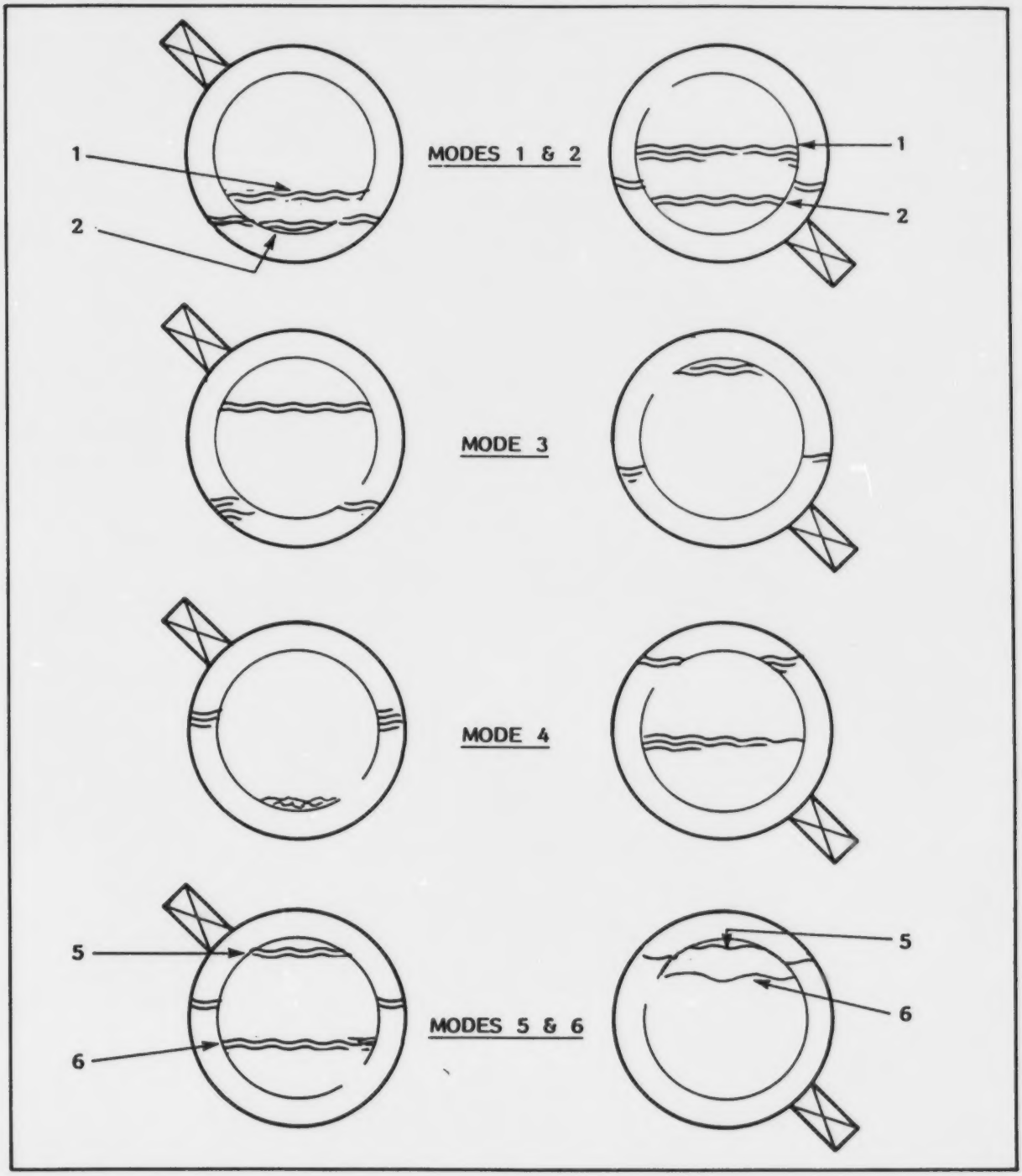

FIGURE 3.2-2 MODES OF OPERATION

MODE 1:

When the internal shell is operating in this mode, liquid is trapped in the core and it can only leave the core as a vapour through the bottom slot. If there are no openings in the inner shell and if the relief valve operates, the annulus is drained of liquid by the venting operation. If the annulus is drained, then the primary shell will only be cooled by radiation to the inner shell and by forced convection due to the flow of vapour in the annulus due to the relief valve action. The liquid in the inner core will effectively be insulated from the heat input and this will result in a reduction in the tank pressurization rate. Vapour will be flowing through the relief valve which is desirable. However, one major problem is that the primary shell is likely to get very hot unless the forced convection is very strong.

MODE 2:

This mode is similar to Mode 1 except that the annulus liquid level is above that in the core. This, of course, means that the annulus has not drained yet. If the relief valve is acting, the Mode 2 operation will eventually lead to Mode 1 unless some opening in the inner shell allows liquid to drain into the annulus.

MODE 3:

This mode is a physically unrealistic mode where the liquid level in the core is above the bottom slot and the level in the annulus is below the bottom slot. In this mode liquid would be spilling out of the core through the bottom slot into the annulus.

MODE 4:

In this mode, liquid in the annulus is above the bottom slot while the core liquid is below the slot. This could happen, for example, if the suction created in the annulus by the relief valve action is so strong that the core is drained completely before the annulus level drops appreciably. In this case, the primary shell wall would be very effectively cooled by the liquid in the annulus.

MODE 5:

In this mode, both liquid levels are above the bottom slot but the core level is above the annulus level. Such a situation could occur if the annulus pressurized faster than the core thereby forcing liquid to flow from the annulus to the core. It could also happen if relief valve operation resulted in material being removed from the annulus faster than the bottom slot flow from the core could replenish it. This possibility is eliminated if the bottom slot is made large enough to ensure adequate flows from the core to the annulus. In any event, this mode is undesirable because it leaves more of the primary shell wall exposed to vapour than it would be if the internal shell were not present. This, of course, leads to higher wall temperatures.

Because both levels are above the bottom slot, only liquid passes through the slots. It is because of this mode of operation that the inner shell check vents were introduced. It was concluded that this mode is possible when the relief valve is closed. If heat is only added at the primary shell then the liquid in the annulus will heat up more rapidly than the liquid in the core, thus causing the pressure in the annulus to rise more rapidly than that in the core. The check vents were intended to relieve the overpressure in the annulus thereby eliminating the possibility of mode 5 occurring. It is undesirable to have mode 5 because it results in the primary shell being exposed to more vapour than it would normally see and this would result in higher wall temperatures. This is exactly opposite to what the internal shell was designed to do.

MODE 6:

Mode 6 is similar to mode 5 except that the core level is below the annulus level. When the internal shell is operating in this mode it is performing its intended function. In this mode, the primary shell is wetted by liquid more than it would be if the internal shell were not present. This wetting action results in reduced wall temperatures.

3.3 MODELLING APPROACH

The internal shell system was modelled using the tank-car thermal model TANKCAR. Details of this model can be found in Reference 3. A brief summary of this model will be given in the following section.

For the purposes of modelling the internal shell, TANKCAR was modified to include the presence of the internal shell. The modifications were limited to the thermodynamic process model, the internal surface heat transfer and the calculation of the liquid levels. The software developed for these purposes is presented in Appendix A.

3.4 TANK-CAR THERMAL MODEL TANKCAR

The tank-car thermal model TANKCAR can simulate a long cylindrical tank filled partially with vapour exposed to either an engulfing type fire, such as caused by a burning pool or a torch type fire, such as that caused by a relief valve flare from a neighbouring tank. The model can account for the effects of a number of thermal protection devices such as pressure relief valves, thermal insulation, radiation shielding, temperature sensing relief valves, and novel internal protection devices including heat dissipating matrices. The model can simulate the effects of roll and pitch of the tank.

The overall thermal model is made up of a series of sub-models which represent the various processes taking place within the tank.

The flame-to-tank heat transfer sub-models can account for either an engulfing pool fire or a two-dimensional torch. The pool fire model accounts for thermal radiation and convection. The thermal radiation is calculated as a function of the circumferential position on the tank by accounting for the typical shape of large pool fires in the absence of cross wind effects. The convection calculations are based on empirical relations for convection to horizontal cylinders in a crossflow. The torch sub-model is based on empirical relations for a jet impinging on a flat plate. The geometry of the jet/plate system in the sub-model is similar to the U.S. DOT Transportation Test Center Torch Simulator.

The temperature distribution of the tank wall and associated coverings is calculated using finite difference techniques. The finite difference solution accounts for pure conduction through the tank wall and insulating layers. The finite difference solution also accounts for the heat transfer from the fire to the tank outer surfaces, and from the tank inner surface to the lading. The interior surface heat transfer submodels account for convection and radiation in the vapour space, and convection and boiling in the liquid region.

The thermodynamic process sub-model treats the lading as three distinct regions, the vapour space, the liquid boundary, and the liquid core. It is assumed that the vapour and liquid boundary (near wall and free surface) are in thermodynamic equilibrium and saturated. The core is assumed to be subcooled initially, but after some period of venting, it is assumed to be in equilibrium with the liquid boundary and vapour space.

The pressure relief valve sub-model accounts for both the mechanical action of a relief valve and the fluid mechanics. The valve mechanics are accounted for using a steady state model. Valve cycling dynamics are not accounted for explicitly, but rather implicitly by having a model valve that sits partially open to represent the reduce flow capacity during cycling, and fully open when in reality the valve is fully open. The opening fraction is determined by the lading vaporization rate which relates to the valve cycling frequency. The valve flow sub-models can account for dry vapour flow and for frozen liquid flow.

The wall stresses are calculated at the point on the wall circumference which experiences the highest temperature, and includes pressure induced (hoop) stress and stresses due to radial temperature gradients in the tank wall. The tank failure analysis is based on the maximum normal stress theory of failure. Degradation in the wall material strength with increases in temperature is accounted for using available data for tank-car steel.

The computer model is capable of predicting the tank internal pressure, mean lading temperatures, wall temperature distribution, relief valve flow rates, liquid level, tank wall stresses and tank failure all as functions of time from initiation of the fire impingement. The model has been extensively validated by comparing its predictions with the results of numerous fire tests involving full and fifth-scale rail tank-cars exposed to engulfing fires.

For further details of the tank-car thermal model, the reader is directed to Reference 3.

3.5 INTERNAL SHELL THERMAL MODEL

The thermal model for the internal shell is based on the fundamentals of thermodynamics, fluid mechanics and heat transfer. The governing equations for the model satisfy conservation of mass, conservation of energy, and process. Special constitutive relationships have been assumed for the bottom slot and check valve flows. In general, the bottom slot flow must satisfy hydrostatic pressure considerations and must satisfy flow requirements to satisfy these hydrostatic pressure considerations when venting is taking place.

In all cases it was assumed that a frothing region existed in the annulus above the liquid level when vapour was passing through the relief valve. The height of the frothing region was assumed constant for a particular shell gap size. Further details of the assumed froth height are given in the Results section.

Because the mode of operation effects the processes taking place the assumptions are presented on an operating mode basis. For details of the equations and the methods of solution the reader is directed to the computer listing in Appendix A.

Process and Assumptions for MODES 1 and 2

For these modes, we effectively have two liquids isolated from one another and a vapour space common to both. The vapour space spans both the inner core and the annulus with the bottom slot acting as an interconnecting channel.

For these modes, it has been assumed that the core and annulus pressures are the same and equal to the saturation pressure for the annulus liquid. The vapour is assumed to be in saturated equilibrium with the annulus liquid. The core being at a lower temperature will be a subcooled liquid. Condensation of vapour on the core liquid is neglected. Heat added to the system is partially taken in by the annulus and partially taken in by the core. The actual distribution of the heat is set by a constant. Material vented from the tank is taken from the annulus only.

Closure is obtained by noting that the process occurs at constant total volume.

Process and Assumptions for MODES 3, 4, 5, and 6

For these modes, we effectively have two liquids communicating through the bottom slot and the check vent. Both liquid and vapour flows can occur between the two regions. It has been assumed that the liquid and the vapour in the annulus are in saturated equilibrium. Material vented from the tank comes from the annulus. Closure for the annulus equations is obtained by specifying that the annulus volume is constant. Note that the annulus properties can be calculated explicitly without regard for the core properties. However, also note that constitutive relationships for the check vent and bottom slot mass flows must be established.

For the core material, it has been assumed that the pressure is equal to the annulus pressure. The liquid in the core is therefore subcooled. The vapour in the core is assumed to be in thermal equilibrium with the vapour in the annulus. Closure for the core is obtained by requiring that the process takes place at constant core volume.

Check Vent and Bottom Slot Flow Relationships

The process and energy equations for the different modes of operation contain terms for the mass flows through the check vents and the bottom slot. For the thermal model to work, it is necessary that constitutive relationships for these flow rates be determined. These relationships will depend on the mode of operation and are strongly effected by the action of the relief valve. The basic assumptions used to establish these relationships are discussed separately for the different modes of operation. For details of the equations used the reader is directed to the program listing in Appendix A.

Modes 1 and 2:

For these modes the liquid is below the bottom slot and vapour is free to pass through it. The check vents in this case do not perform any function (i.e. it assumed that no flow takes place). In the thermodynamic model for these modes, it was assumed that the vapour region acts as a single region and therefore there is no coupling effect caused by flow through the bottom slot (since vapour is one region there is no need to calculate the flow through the bottom slot).

Mode 3:

If this mode were to occur, then fluid would spill through the bottom gap into the annulus. The flow rate through the gap would be similar to that of an open channel flow spilling over the crest of a dam plus a correction term in the event that the annulus pressure may be different than that of the core.

The check vent flow would be zero if the core pressure was above the annulus pressure. If the core pressure was less than or equal to the annulus pressure then the check vent volume flow would balance the bottom slot volume flow.

Mode 4:

In terms of the check vent and bottom slot flows, mode 4 is similar to mode 3 except that the liquid spills into the core from the annulus. The governing equations for the flow remain the same only the sign of the flow changes.

Modes 5 and 6:

As discussed earlier, when the internal shell is performing its intended function it is operating in mode 6. In mode 6 the action of the relief valve is causing liquid to flow from the core into the annulus.

It has been assumed that the flow through the bottom slot is caused by relief valve action. It was assumed that if the relief valve is open the volume of liquid removed from the annulus due to venting is just replaced by liquid flowing from the core through the bottom slot. In other words, it has been assumed that no lifting of the annulus level takes place due to suction in the annulus during venting. This is an agreement with the test results discussed earlier. Differences in the liquid levels of the annulus and core are due only to thermal expansion effects.

3.6 MODEL VALIDATION AND TESTING

Upon completion of the model development, an attempt was made to validate the internal shell model. However, since the internal shell device is a new concept in internal protection, no data was available that could be used to quantitatively validate the model. As stated elsewhere in this report, the objectives of the limited scope

experiments were to provide qualitative data so that the performance of the internal shell could be further understood. The experiments conducted in this study did not use a test fluid that TANKCAR can account for and the test apparatus scale was smaller than can presently be handled by TANKCAR. Therefore, a qualitative validation of the internal shell model using the experimental results was not possible. However, observations taken from the tests can be used to qualitatively validate the model predictions.

3.7 RUN CASES

Table 3.7-1 presents a summary of the runs cases considered in the modelling study of the internal shell equipped tank. All runs involved a full-scale tank filled initially to 95% capacity with propane. The tanks were exposed to a simulated engulfing fire.

Run #	Valve Area	Shell Gap (%D)	Shell Bottom Slot (%D)	Roll Angle (deg)	Fire Type
1	std	5	20	0	engulf
2	1.25 x std	5	20	0	engulf
3	std	3.33	20	0	engulf
4	1.25 x std	3.33	20	0	engulf
5	1.25 x std	5	20	90	engulf
6	1.25 x std	5	20	120	engulf
7	std	5	20	0	torch @ TDC

TABLE 3.7-1 SUMMARY OF MODEL RUN CASES

3.8 RESULTS AND DISCUSSION

Before the results of the internal shell simulations are discussed and presented, two Baseline cases will be considered. Baseline A involves a simulation of a full scale unprotected tank exposed to an engulfing fire. The tank is filled to 95% capacity with propane and the tank is equipped with a standard size relief valve. These two cases will be presented so that the simulations involving the internal shell device can be compared with simulations for an unprotected tank. The simulation results from Baseline A have been validated against available results from fire tests conducted on full scale unprotected tanks. Further details of this validation can be found in Reference 3.

Baseline A

Figures 3.8-1 to 3.8-4 present the results of the simulation for the Baseline A involving a full scale unprotected tank exposed to an engulfing fire.

Figure 3.8-1 presents the predicted tank pressure versus time for this baseline case. As can be seen from the figure initially there is a rapid increase in the tank pressure until the pressure relief valve comes into place. Up until approximately 10 minutes into the fire, the relief valve cycles because the vapour generation rate within the tank is not sufficient to maintain the pressure at a level that ensures that the relief valve remains open. However, at 10 minutes into the fire, the pressure relief valve remains open and the vapour generation within the tank is sufficient to cause a steady increase in the tank pressure even with the pressure relief valve open. At approximately twenty minutes into the fire the tank pressure peaks and begins to drop slowly. This gradual drop in pressure is due to the fact that as the liquid level in the tank drops, the total heat flux to the liquid lading is reduced and therefore the vapour generation rate is reduced. This drop in the vapour generation rate results in the drop in the tank pressure during continuous venting through the relief valve. At approximately thirty minutes into the fire, the simulation results indicate that the pressure relief valve once again begins to cycle.

Figure 3.8-2 presents the predicted wall temperatures for the Baseline A case. The figure shows predicted wall temperatures at different positions around the circumference of the tank. The different positions are at

0, 30, 60, 90 and 120 degrees around the side from the top of the tank. As can be seen from the figure, the wall temperature at the tank top dead centre or at 0 degrees rises rapidly once the simulation begins. Further around the side of the tank the wall temperatures remain low until the liquid level drops below that point on the tank wall due to venting of lading from the tank. At approximately 10 minutes into the fire simulation, the wall temperature at the 30 degree location increases rapidly. This is because at approximately 10 minutes into the fire the liquid level drops below the 30 degree mark in the tank. Similar trends are seen for the 60, 90 and 120 degree locations. The peak wall temperature occurs at the tank top dead centre and the temperature value reached is approximately 620 degrees Celcius.

Figure 3.8-3 presents the predicted liquid level versus time for the Baseline A simulation case. The Figure shows the angle from top dead centre to the point on the tank wall where the liquid level exists versus time from fire admission. As can be seen from the figure during the first 10 minutes of the simulation, when either the pressure relief valve is closed or cycling, the liquid level in the tank actually rises because of thermal expansion. However, beyond approximately 10 minutes continuous venting is occurring and the liquid level in the tank is dropping. The liquid level is dropping of course, because the venting rate far outweighs the rate of expansion of the liquid due to its increase in temperature. Extrapolating from the figure, it was estimated that the tank would have emptied at approximately 42 minutes into the fire.

Figure 3.8-4 presents the predicted wall stresses and strength versus time for the Baseline A case. The figure shows the tank wall stresses at the inner and outer fibres of the tank wall. The stresses include pressure induced stresses and thermal stresses due to radial temperature gradients. The figure also shows the tank wall material tensile strength at the point on the tank wall that experiences the highest wall temperature (at top dead centre). As can be seen from the figure, the tank wall tensile strength drops rapidly after approximately 12 minutes into the simulation. This is because of the rapidly increasing wall temperatures at that point in the simulation. At approximately 25 minutes into the simulation, the tank wall tensile strength drops below the maximum stresses predicted for the tank wall. By the maximum normal stress theory of failure, the tank failed at that point. This time to predicted failure agrees well

with the actual failure in the fire tests conducted on a full scale unprotected tank. In test the tank failed at approximately 24 minutes into the fire. Further details of the full scale fire tests and their comparison to predictions to using the thermal model can be found in Reference 1.

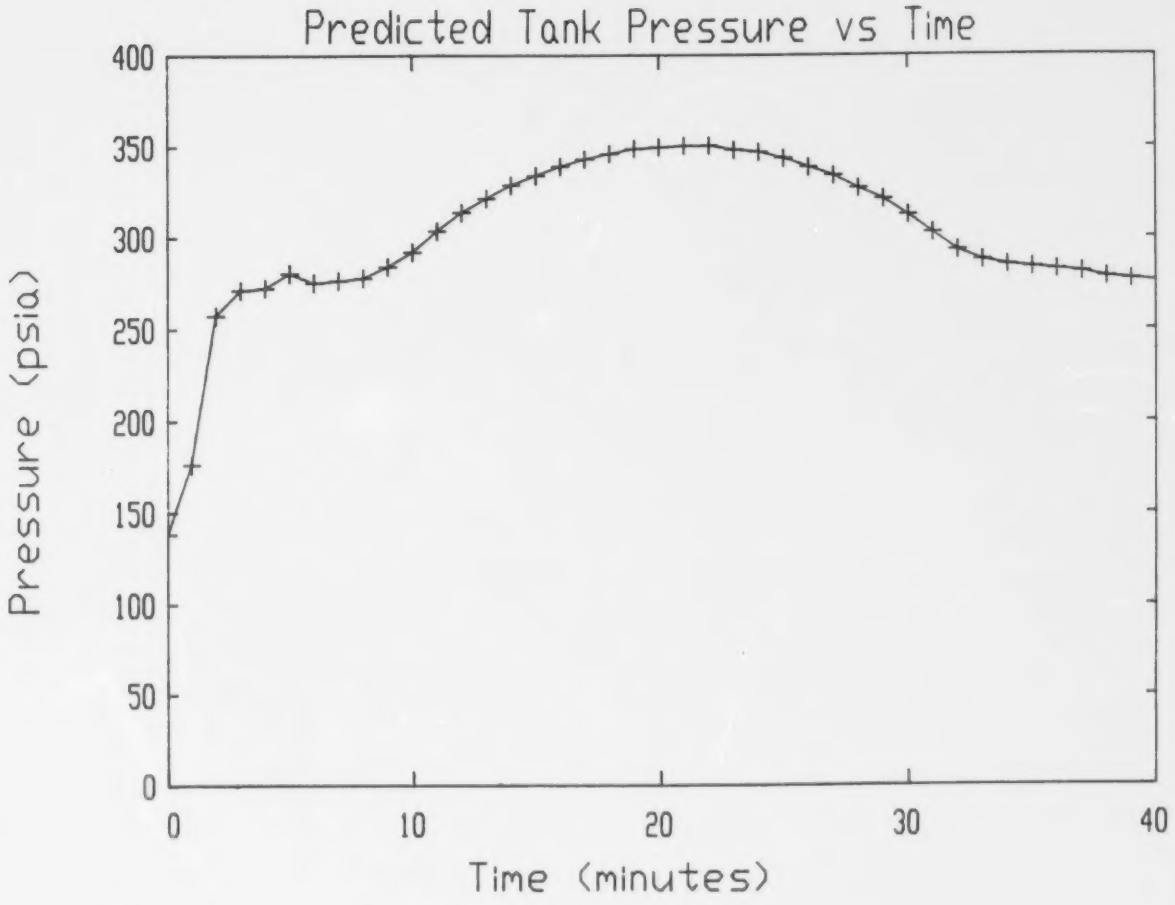

FIGURE 3.8-1 BASELINE A CASE

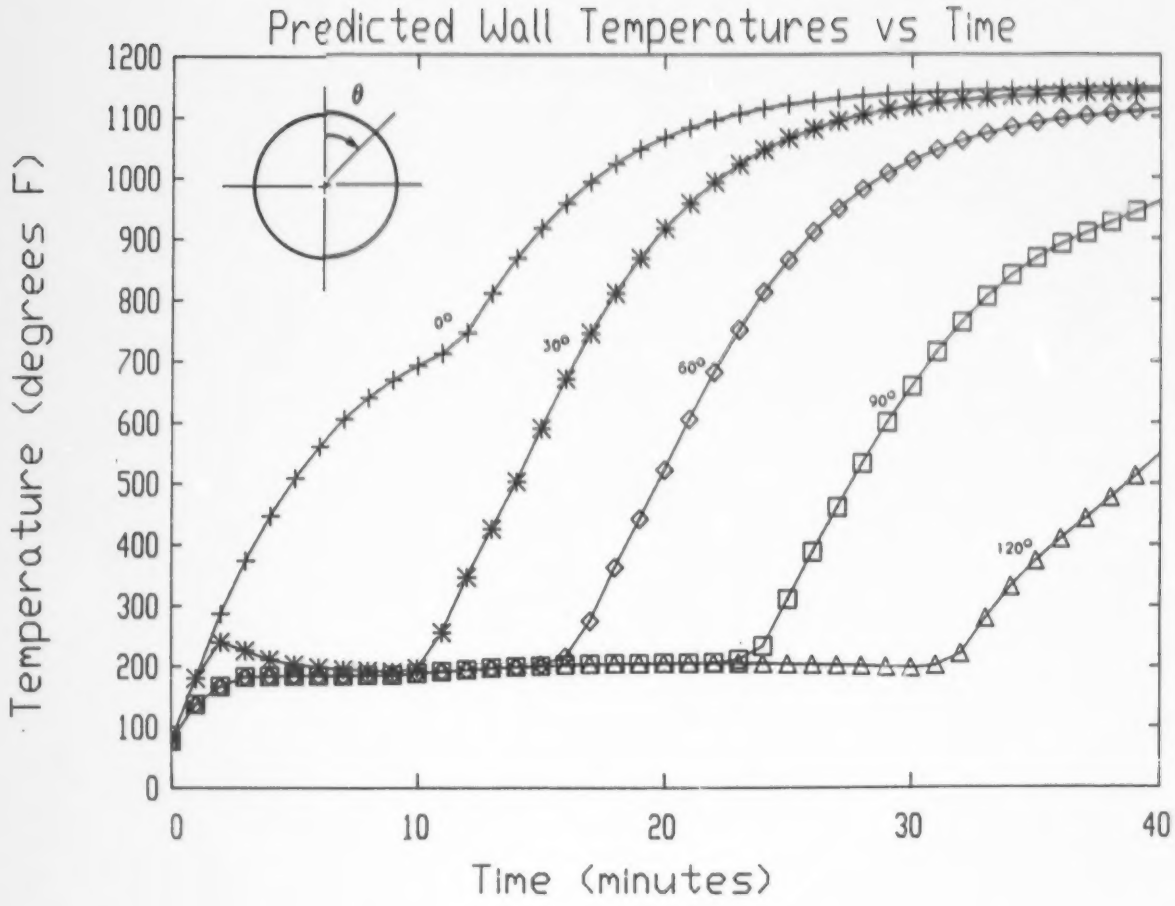

FIGURE 3.8-2 BASELINE A CASE

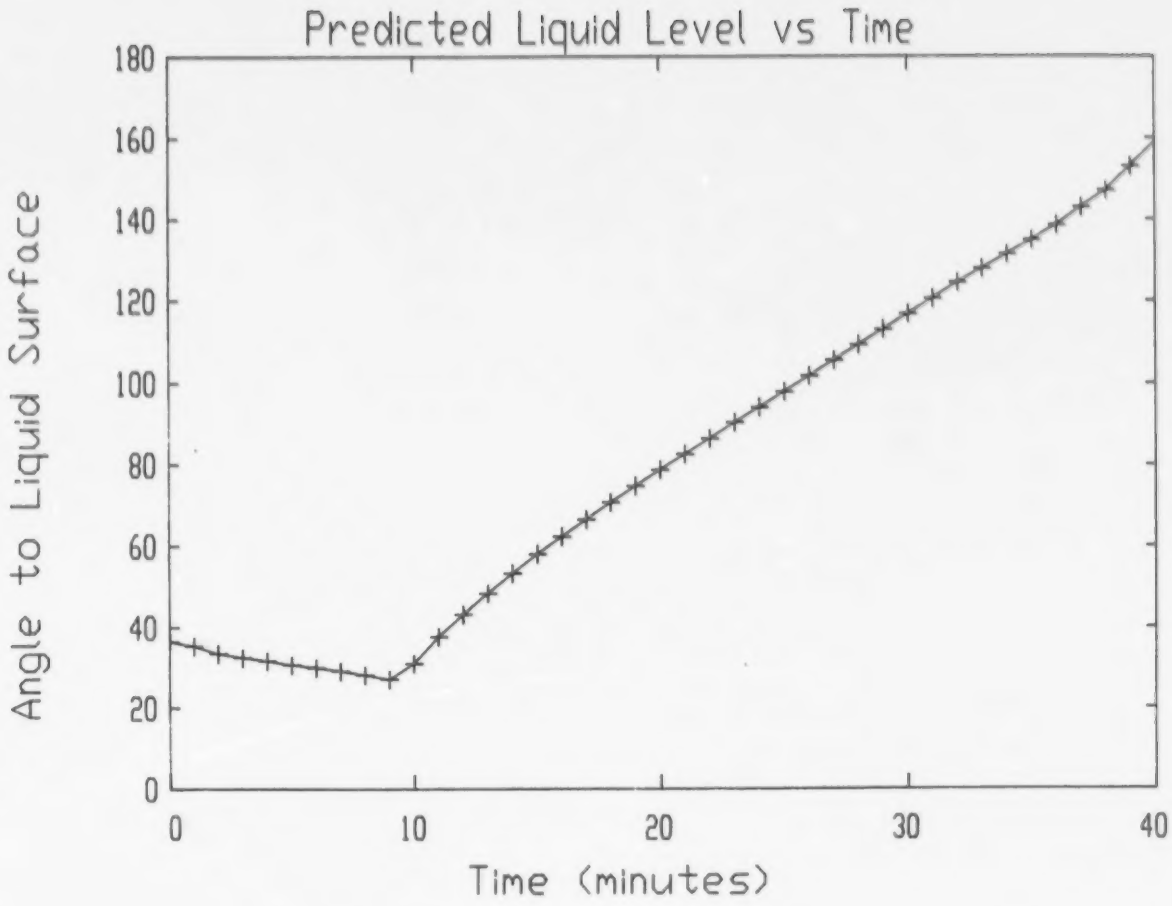

FIGURE 3.8-3 BASELINE A CASE

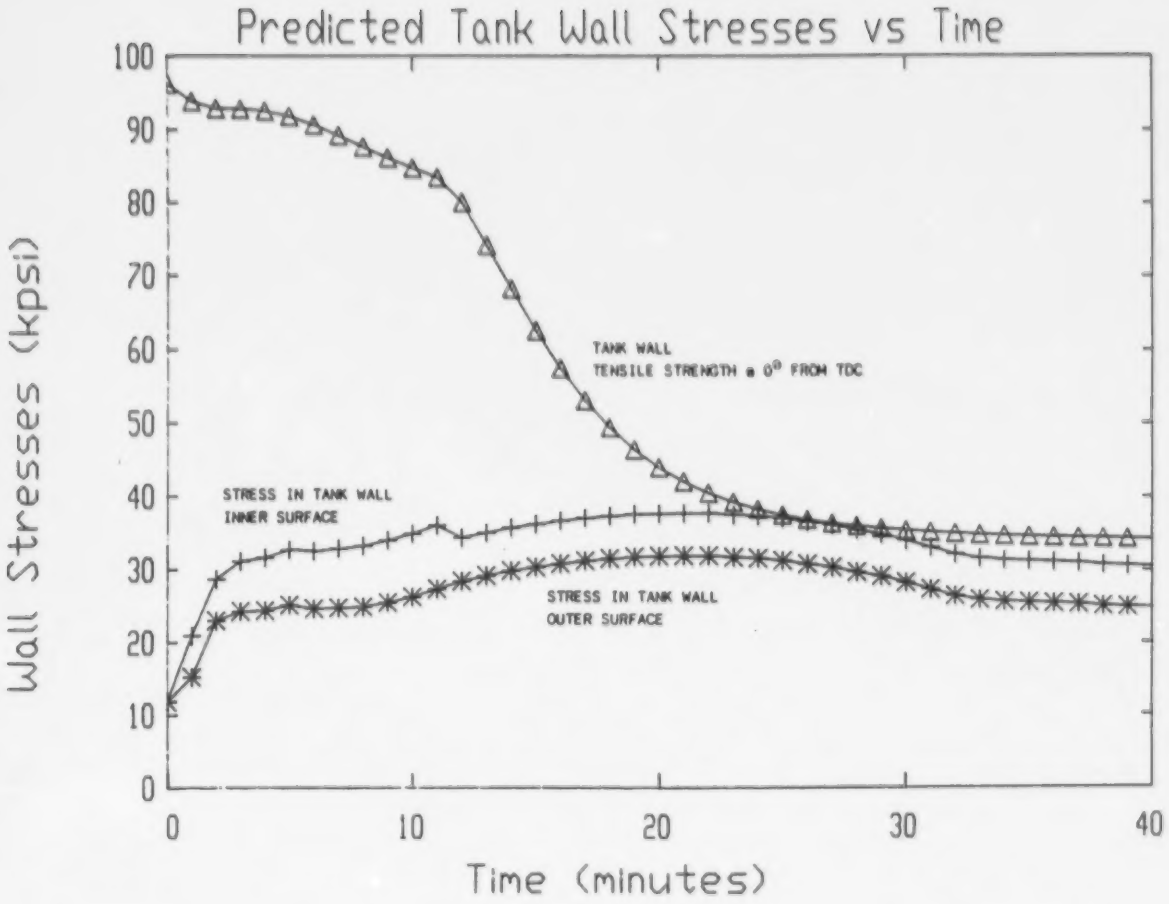

FIGURE 3.8-4 BASELINE A CASE

Baseline B

Baseline B involved a simulation of a full scale unprotected tank filled to 95% capacity with propane. The tank was equipped with a pressure relief valve that was 25% larger in terms of flow area than the standard pressure relief valve. The same opening setting of approximately 270 psi was used in this simulation. In other words, the only difference between Baseline B and Baseline A is that Baseline B has a slightly larger pressure relief valve.

Figures 3.8-5 to 3.8-8 present the simulation results for the Baseline B case. Figure 3.8-5 presents the predicted tank pressure versus time for the fire ignition for the simulation. As can be seen from the figure, the predicted pressure is similar to that in Baseline A; however, because of the increased pressure relief valve size the peak pressure reached in the tank is less than the Baseline A case. This is, of course, because the capacity of the pressure relief valve is increased when the flow area is a lower pressure in the tank during continuous venting. In addition, it can be seen from the figure that relief valve begins to cycle again at approximately 20 minutes into the fire. This did not occur in the Baseline A case until after 30 minutes into the fire.

Figure 3.8-6 presents the predicted tank wall temperature versus time for the Baseline B case. As can be seen from the figure, the predicted wall temperatures are very similar to those presented for the Baseline A case. This is because the increasing of the size of the pressure relief valve has little effect on the tank wall temperatures other than a slight shift of the temperature response along the time scale. This, of course, is because the larger pressure relief valve has some effect on the rate at which lading is vented from the tank. The peak wall temperature is not affected by the larger pressure relief valve.

Figure 3.8-7 presents the predicted liquid level versus time for the Baseline B case. As can be seen from the figure, the position of the liquid level is slightly effected by the larger pressure relief valve. However, the figure indicates that the tank does not empty more rapidly if larger pressure relief valve is installed. This is because the larger pressure relief valve results in a reduced tank pressure. Since the flow rate through the pressure relief valve is a function of the tank

pressure by reducing the tank pressure you also reduce the flow rate through the relief valve. Therefore, the effect of the larger flow area is offset by the reduced pressure to push the lading through the relief valve. The net results is that there is not a dramatic difference at the rate which the tanks empty into the two Baseline cases. The simulations indicate that the Baseline B case actually empties slightly slower than the Baseline A case.

Figure 3.8-8 presents the predicted tank wall stresses and tank wall tensile strength. As can be seen from the figure, the tank wall tensile strength still drops to a relatively low value once the high wall temperatures are established in the tank. The exact value to which the tensile strength drops is identical to that for the Baseline A case. In other words, increasing the pressure relief valve size has no effect on the ultimate tank wall tensile strength due to increasing wall temperatures. However, as can be seen from the figure, the predicted tank wall stresses are reduced by the fact that the pressure induced hooped stresses are less than in the Baseline B case. As a result of that, the simulation results indicate that the tank wall tensile strength does not drop below the predicted tank wall stresses. Therefore, the simulation suggests that the tank would not fail by the maximum normal stress criteria. However, the predicted tank wall tensile strength and the predicted maximum wall strength comes so close to one another that there is no safety margin in this case. Therefore, one could justifiably say that this is an unacceptable situation.

The Baseline A and Baseline B cases were presented so that following results for internal shell equipped tanks could be compared directly to these cases. If the reader desires to compare the following simulation results for internal shell equipped tanks with that of the thermally insulated tank, the reader is directed to Reference 1 that shows the results of predictions and the results of experiments for thermally insulated tanks.

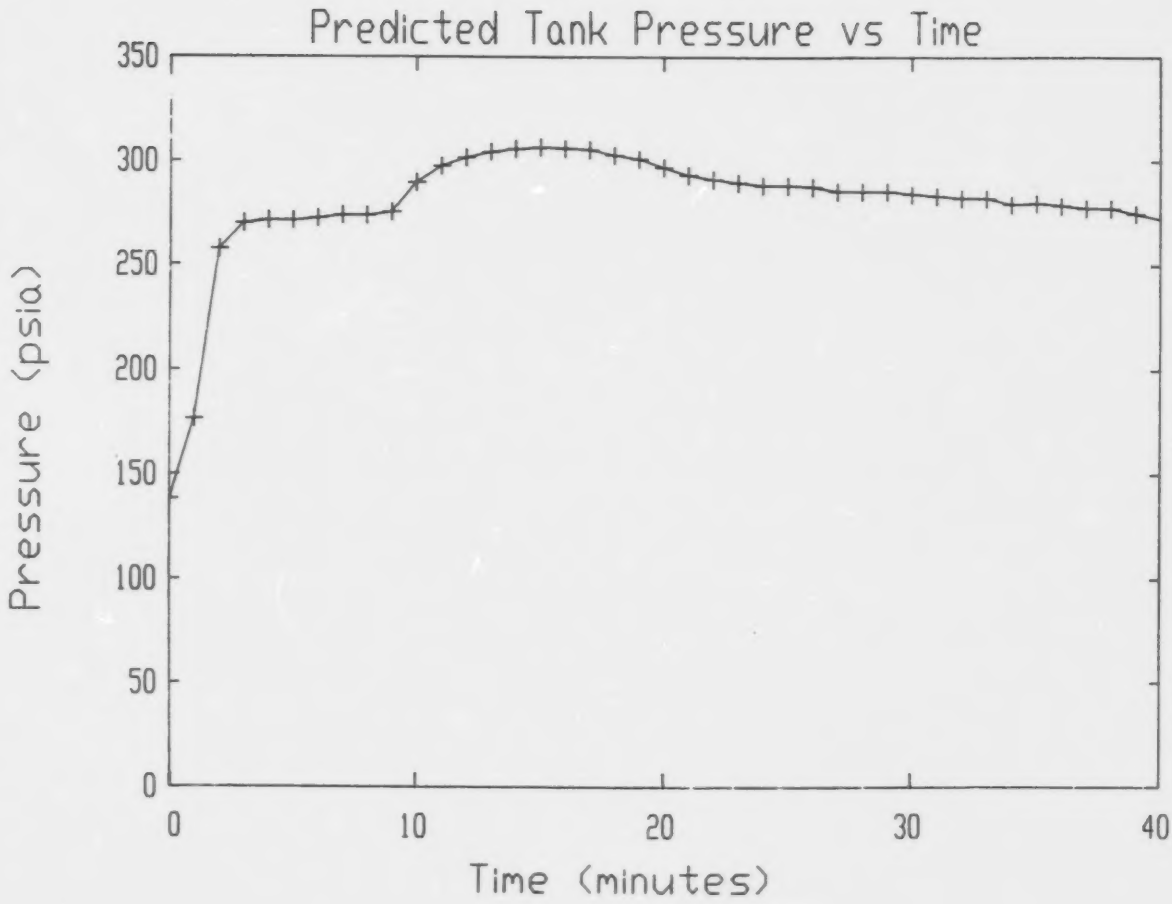

FIGURE 3.8-5 BASELINE B CASE

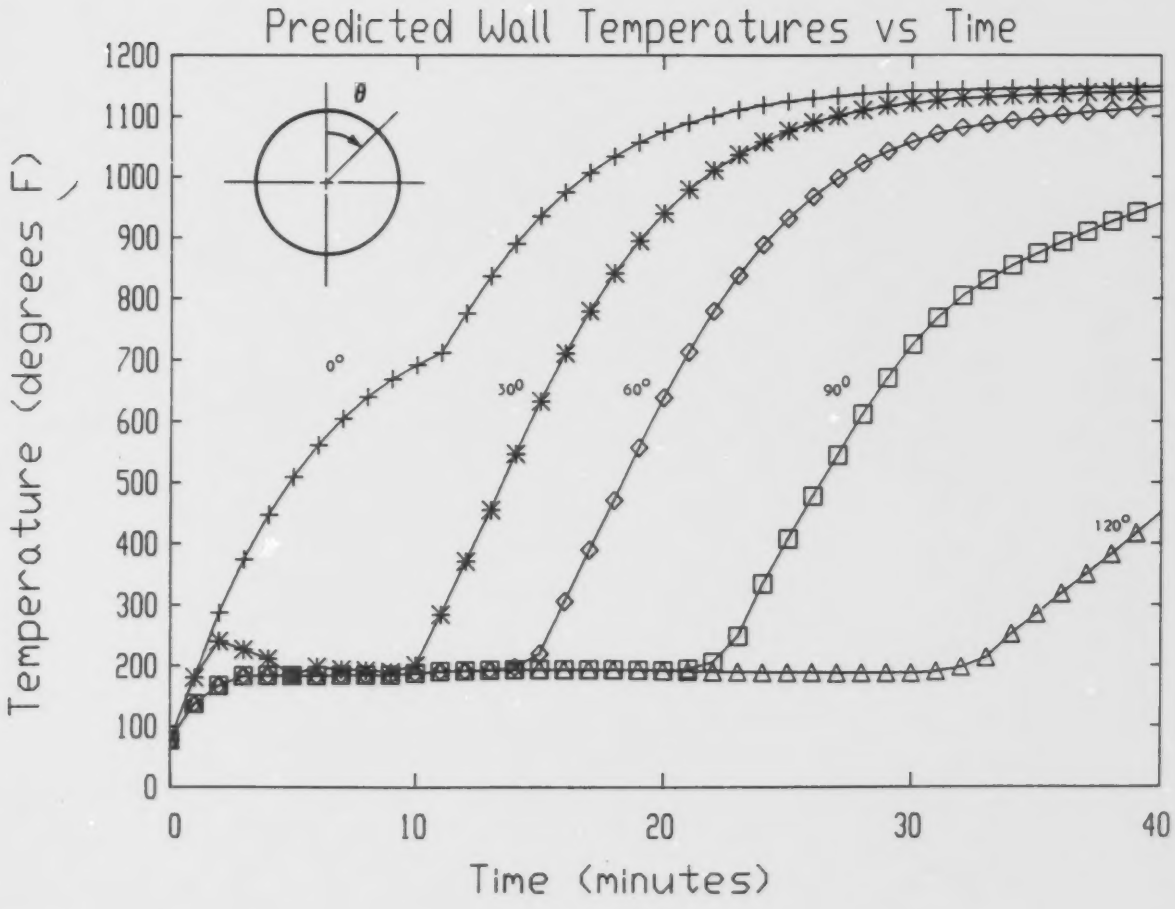

FIGURE 3.8-6 BASELINE B CASE

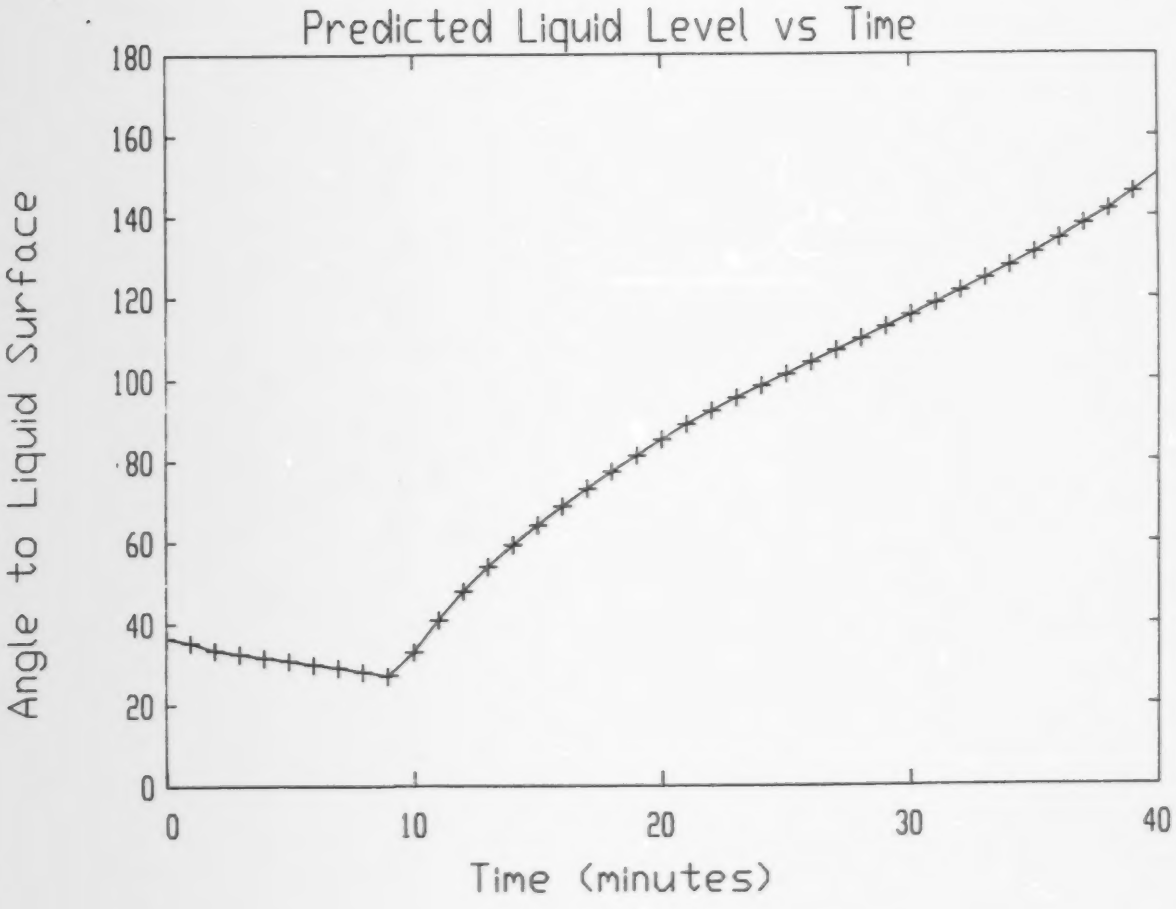

FIGURE 3.8-7 BASELINE B CASE

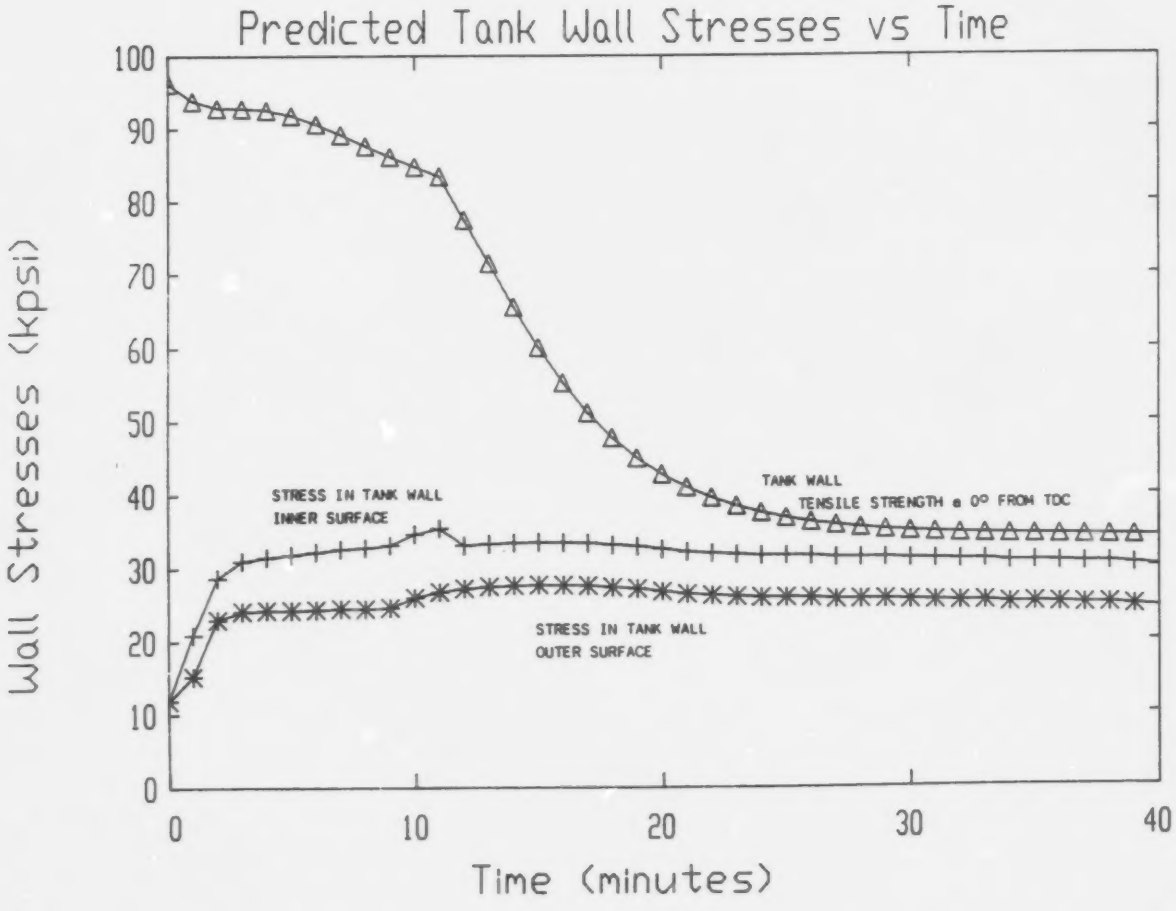

FIGURE 3.8-8 BASELINE B CASE

Run Case #1

This simulation involved the full scale tank equipped with an internal shell thermal protection device. The case involved a full scaled tank filled to 95% capacity with propane equipped with a standard size pressure relief valve with an internal shell. The internal shell gap was 5% of the tank diameter and the shell bottom slot was 20% of the tank diameter. The tank roll angle was 0 degrees and the tank was exposed to the simulated engulfing fire. Figures 3.8-9 and 3.8-13 present the predicted response of the internal shell equipped tank.

Figure 3.8-9 presents the predicted tank pressure versus time in the internal shell equipped tank. As can be seen from the figure, the tank pressure rapidly rises during the first few minutes of the simulation. At approximately 4 minutes into the simulation, the tank relief valve begins to cycle and at approximately 10 minutes into the simulation, the pressure relief valve remains open for continuous venting. Beyond that time, the pressure within the tank increases slowly to a peak at approximately 20 minutes and then the tank pressure begins to drop off slowly. The trends shown in the figure are very similar to those presented for the Baseline A case of an unprotected full scale tank. The only things to note are that during the relief valve cycling period, the pressure within the tank rose slightly in the case of the internal shell equipped tank but remained nearly steady for the Baseline A case. The reason for this is that during venting with the internal shell equipped tank the heat flux into the tank lading is slightly higher because of the frothing in the annulus within the tank. This results in additional vapour generation and a slight increase in pressure in the tank.

Figure 3.8-10 presents the predicted tank wall temperatures for the run one case involving an internal shell equipped tank. As can be seen from the figure, the tank wall temperatures increase with trends that are similar for the baseline cases. However, it is clear from the figure that the peak wall temperatures are lower than those observed in the baseline case. This is is because in the internal shell equipped tank, the frothing that takes place during venting through the pressure relief valve is directed along the tank wall because of the presence of the internal shell. This frothing directed along the wall results in an increase heat transfer coefficient in the regions of the wall that would normally be in contact with vapour. This increase heat transfer

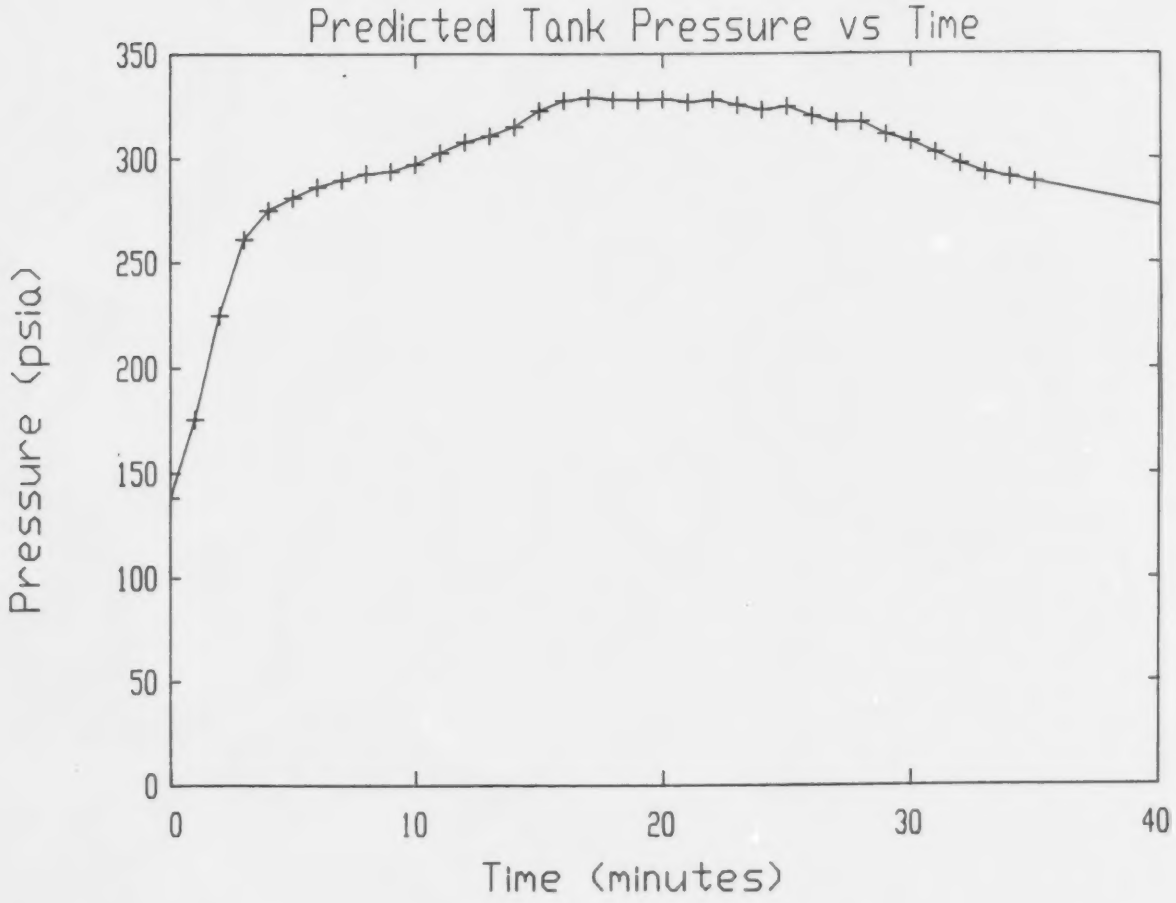

FIGURE 3.8-9 RUN CASE #1

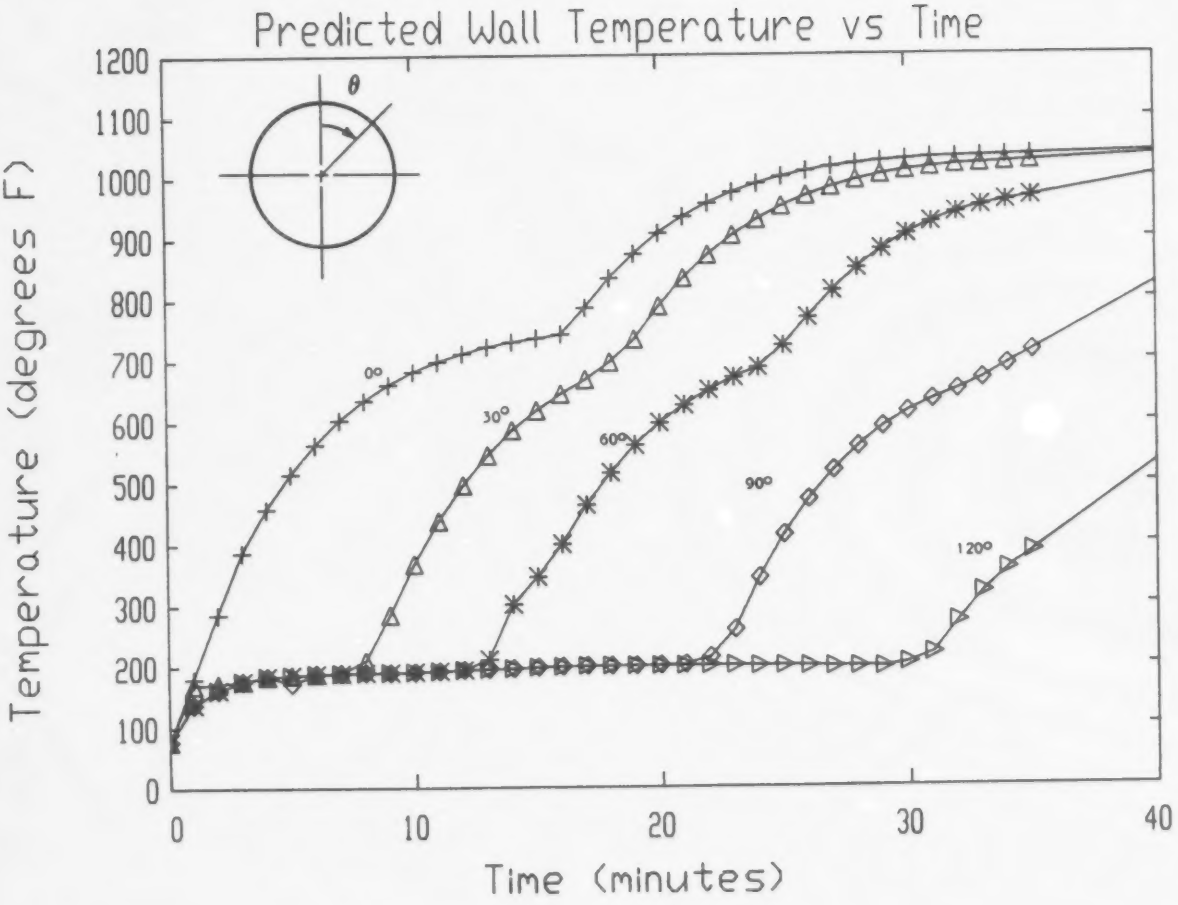

FIGURE 3.8-10 RUN CASE #1

coefficient results in frothing above the liquid level with a height of approximately 1/3 the tank diameter. This is based on observations from the UNB test results. In addition to the reduction in the peak wall temperature, it is clear from the results presented in the figure that wall temperatures throughout the tank are effected by the presence of the internal shell device. This is evident from the presence of the bend in the temperature response curves for all of the wall locations from 0 degrees to 120 degrees from top dead centre. In the baseline case, this bend is only observed at the top dead centre further around the curve the bend is not observed. This is because the bend is a result of the frothing layer and in the internal shell equipped tank the frothing layer is much deeper and effects a much larger portion of the tank wall. Further discussion of the effects of the frothing layer can be found in Reference 2.

Figure 3.8-11 presents the predicted liquid level versus time for the run case #1. In this figure, the liquid level is actually the liquid level in the annulus space. As can be seen from the figure the liquid level in the annulus drops with the pattern similar to that observed in the baseline cases. However, in the figure there are sudden changes in the liquid level at approximately 9 and 12 minutes into the simulation. These sudden changes are due to instabilities in the mathematical model used to simulate the changes in the liquid level in the annulus and in the inner core regions. These sudden changes in the liquid level should be ignored.

Figure 3.8-12 presents the predicted liquid levels in the annulus base and inner core region. The liquid levels are measured from the bottom of the tank. As can be seen from the figure, the liquid levels in the annulus and inner core follow one another very closely. The liquid level in the annulus region is slightly higher during the initial periods of simulation because of density differences between the fluid in the annulus and in the core. As in the previous figure showing the liquid level in the annulus, we see sudden changes at approximately 9 and 12 minutes in the liquid levels in the annulus space. These are again a result of instabilities in the mathematical model and should be ignored. The important thing to note here is that during the simulation it has been assumed that the action of the pressure relief valve does not significantly lift the liquid level in the annulus. This is based on the observations from the UNB scale model tests. From the UNB tests, it was observed that the action of the pressure relief valve did not result in a significant drop in the annulus and therefore was not a

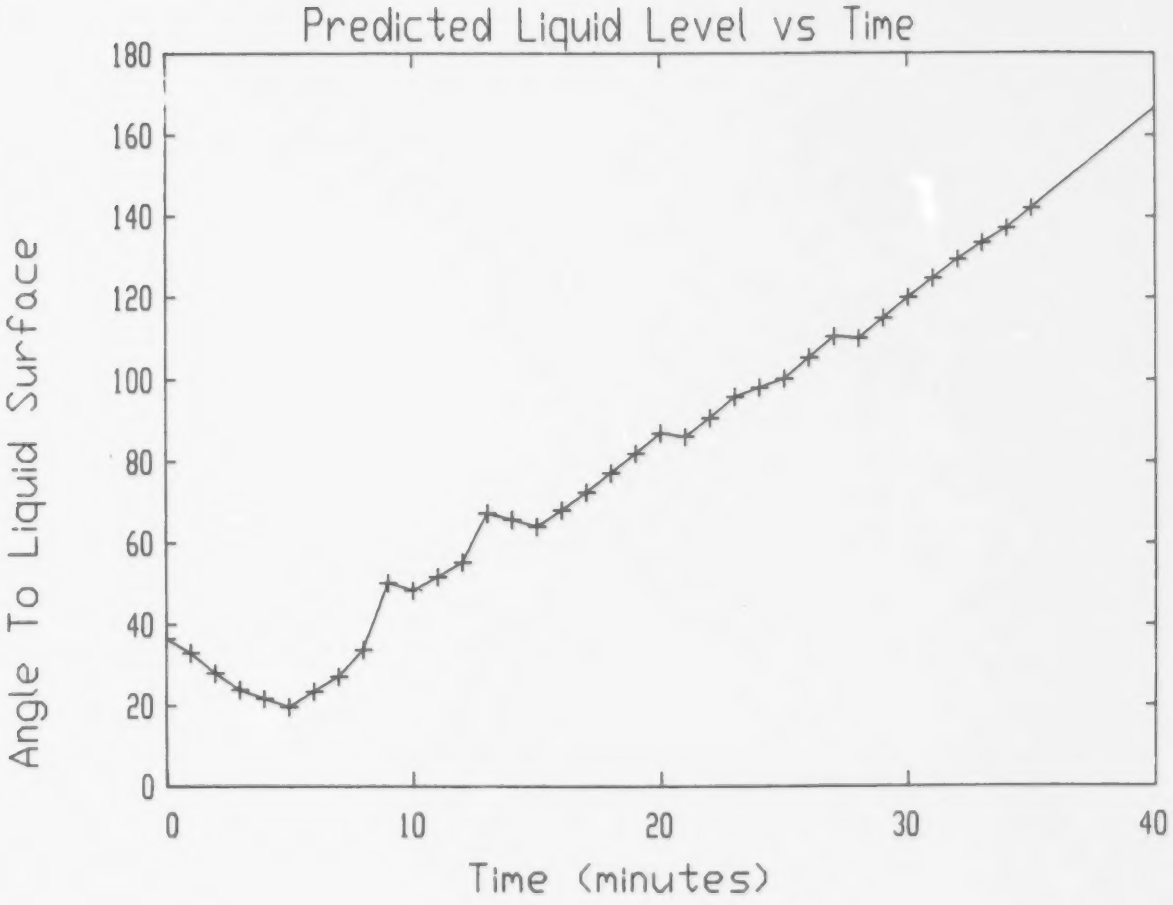

FIGURE 3.8-11 RUN CASE #1

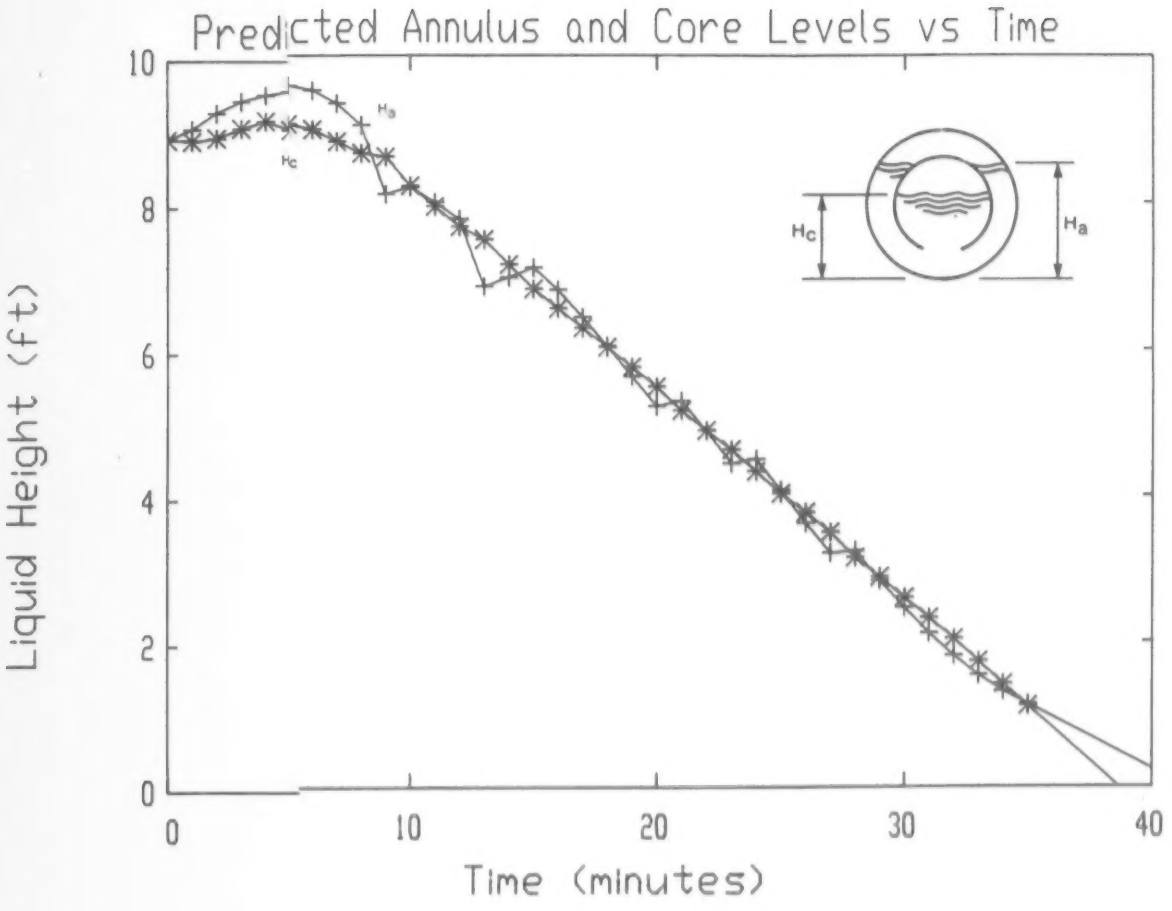

FIGURE 3.8-12 RUN CASE #1

a significant difference in the liquid levels between the annulus liquid and the core liquid. A small difference in liquid level was observed and it is believed that this small liquid level difference was due to density differences between the annulus liquid and the core liquid. This is because the annulus liquid heats up more rapidly and has a lower density than the fluid in the core and therefore the liquid column in the annulus must be higher to give the same hydrostatic pressure at the bottom of the tank. It should be noted that it is not for certain that suction in the annulus can not be generated to lift the liquid level in the annulus. The present simulations were performed assuming that there is no significant change in the annulus liquid level because they were not observed in the UNB tests. It should be recalled that the UNB tests for the upright tanks involved internal shells with check vent devices and these devices leaked thereby short-circuiting the annulus and the core regions. This short-circuiting effect resulted in no appreciable pressure differential being generated between the annulus and the core during venting. Additional testing is required to establish whether or not some suction can be generated.

Figure 3.8-13 presents the predicted wall stresses versus time for the Run Case #1. As can be seen from the figure, the predicted tank wall stresses are quite similar to those predicted for the Baseline cases. This is because the pressures generated within the tanks are similar for the internal shell equipped tank and for the unprotected tank. However, as can be seen from the figure, the tank wall tensile strength is significantly different from the internal shell equipped tank. As can be seen from the figure, the tank wall tensile strength drops because of increasing wall temperatures; however, because the wall temperatures in the internal shell liquid tank are not as high as in the unprotected tank, the tank wall maintains a higher strength level in the internal shell equipped tank case. Therefore, the predictions are that the internal shell equipped tank will not fail. Once again, it should be noted that this simulation assumed that there was no appreciable lifting of the liquid level in the annulus and that frothing could only be generated for a height of one-third the tank diameter. These assumptions are based on the UNB tests which were of course very limited in scope. Further experimentation is required to validate these assumptions, especially for a full case scale involving propane.

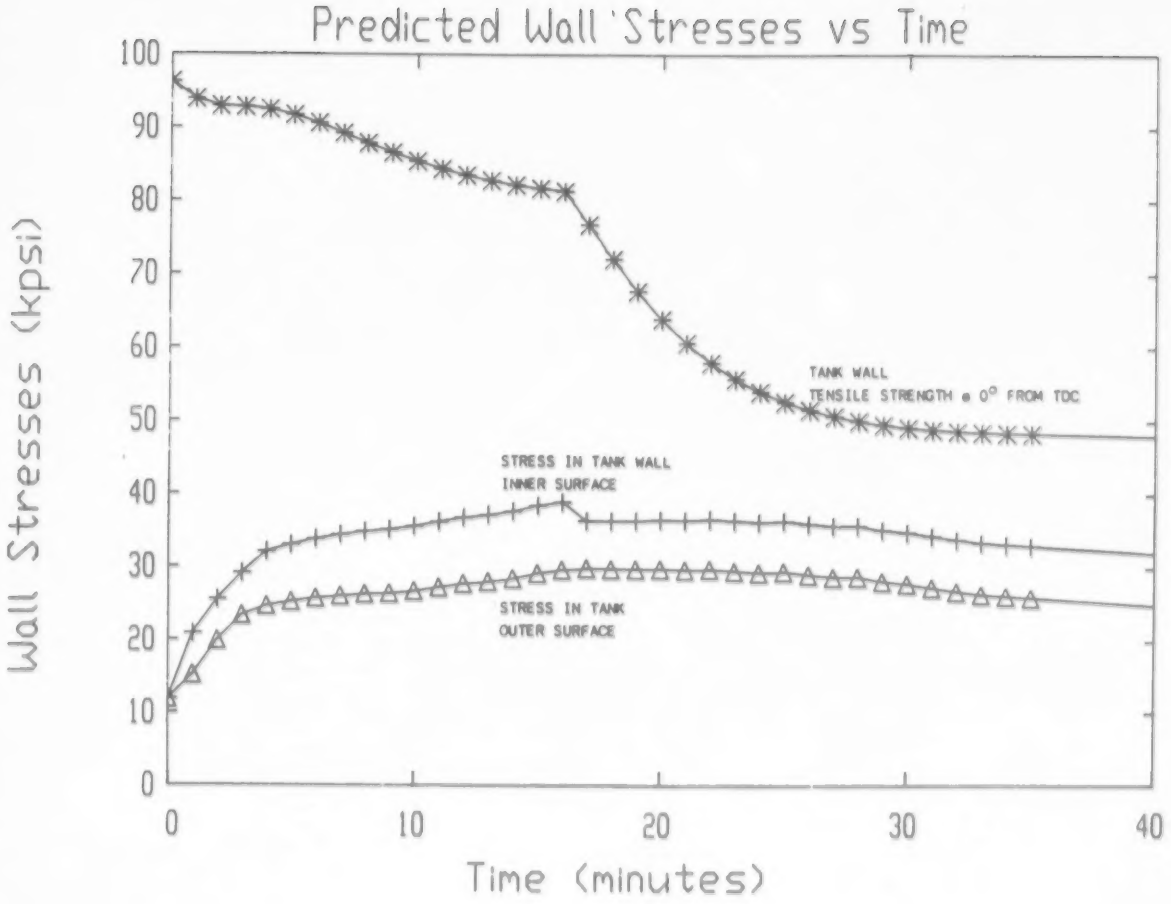

FIGURE 3.8-13 RUN CASE #1

In summary, it appears that by putting in an internal shell in an upright full scale filled with propane the internal shell device will in fact reduce the risk of thermally induced rupture in this tank without significantly changing the rate at which the tank empties its lading during pressure relief. In other words, by having an internal shell device in the tank the tank will empty quickly and the tank wall material strength will not be reduced as much as it would be in an unprotected tank case.

Run Case #2

This run case involved a simulation of a full scale tank identical to that of run case #1 except that the pressure relief valve flow area has been increased by 25%. The results of the simulation are presented in Figure 3.8-14 to 3.8-18.

Figure 3.8-14 presents the predicted tank pressure versus time for Run Case #2. As can be seen from the figure, the predicted tank pressure rises rapidly during the initial minutes of the simulation and levels off once the pressure relief valve comes into play. The simulation showed that the pressure relief valve would cycle for the entire fire event. The reason for this is that the internal shell device trapped the bulk of the lading in the inner core which effectively isolates and insulates it from the fire. As a result, the majority of the vapour generation takes place within the annulus during continuous venting. This, of course, has not been validated in any way and this must be considered as preliminary. It appears from this simulation that increasing the pressure relief valve beyond what is used in this case is unnecessary.

Figure 3.8-15 presents the predicted tank wall temperatures versus time from fire ignition. As can be seen from the figure, predicted wall temperatures for Run Case #2 are almost identical to those for Run Case #1. It appears that increasing the relief valve flow area for an internal shell tank has very little effect on the wall temperatures. It should be noted at this point that this conclusion is a result of the simple assumptions that went into the internal shell thermal model. In reality, the action of the pressure relief valve will have a significant effect on the depth and persistence of the frothing layer that will exist in the annular region. A significant amount of experimentation would have to be performed before such a model could be developed. In any event, as in the Run Case #1, the peak wall temperatures in Run Case #2 have been reduced below those for the baseline cases. In addition, the presence of the frothing layer in the annulus has an effect over a large area of the tank wall.

Figure 3.8-16 presents the predicted liquid level in the annulus versus time for fire ignition. As in Run Case #1 the predicted liquid level follows the trend similar to that of the baseline cases. Once again, we see instabilities in the mathematical solution.

Figure 3.8-17 presents the predicted annulus and core liquid levels versus time from fire ignition. As in Run Case #1, the annulus and core levels follow one another closely during the entire simulation. As in Run Case #1 this is a consequence of the assumption used in the simulation that no appreciable suction is generated within the annulus during venting. This was of course one of the observations from the UNB small scale tests.

Figure 3.8-18 presents the predicted tank wall stresses and strength versus time from fire ignition. As can be seen from the figure, the tank wall tensile strength drops because of high wall temperatures established. The level to which the tensile strength drops is identical to that for Run Case #2 are very similar to those predicted for Run Case #1. The two run cases differ in the predicted tank wall stresses. As can be seen from the figure, the predicted tank wall stresses are somewhat lower than those predicted for Run Case #1. This is because of the lower tank temperature predicted for Run Case #2 when compared to Run Case #1. The lower predicted tank pressure is, of course, a result of the increased pressure relief valve size. Since the predicted tank wall stresses include both pressure induced hoop stresses, it is therefore reasonable to conclude that the reduced tank wall stresses are a result of the reduced tank pressure. In any event, the simulation results indicate that this tank would not fail.

In summary, the presence of the internal shell device results in the tank not failing. By increasing the pressure relief valve size the factor of safety is slightly increased. However, it appears from the predicted tank pressure that increasing the pressure relief size beyond that used in this example is unnecessary.

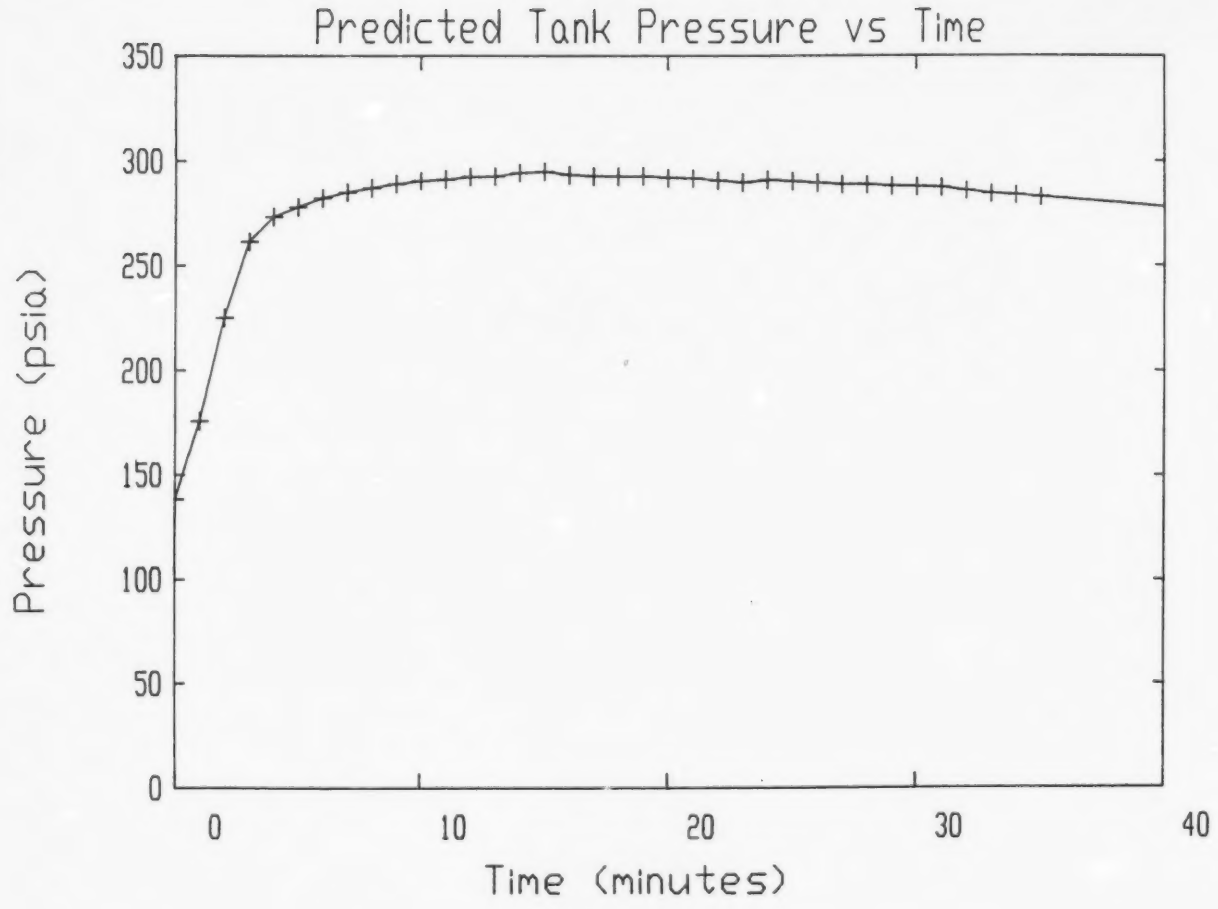

FIGURE 3.8-14 RUN CASE #2

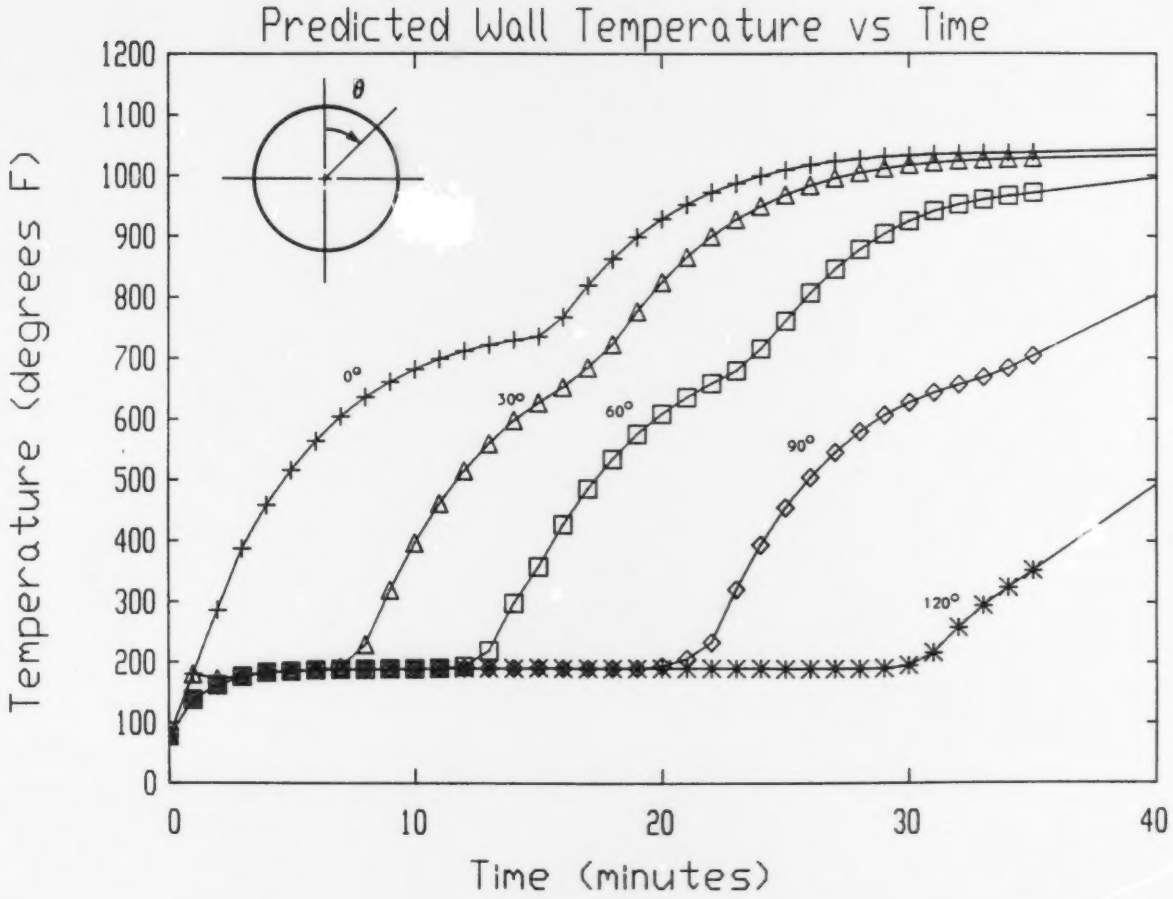

FIGURE 3.8-15 RUN CASE # 2

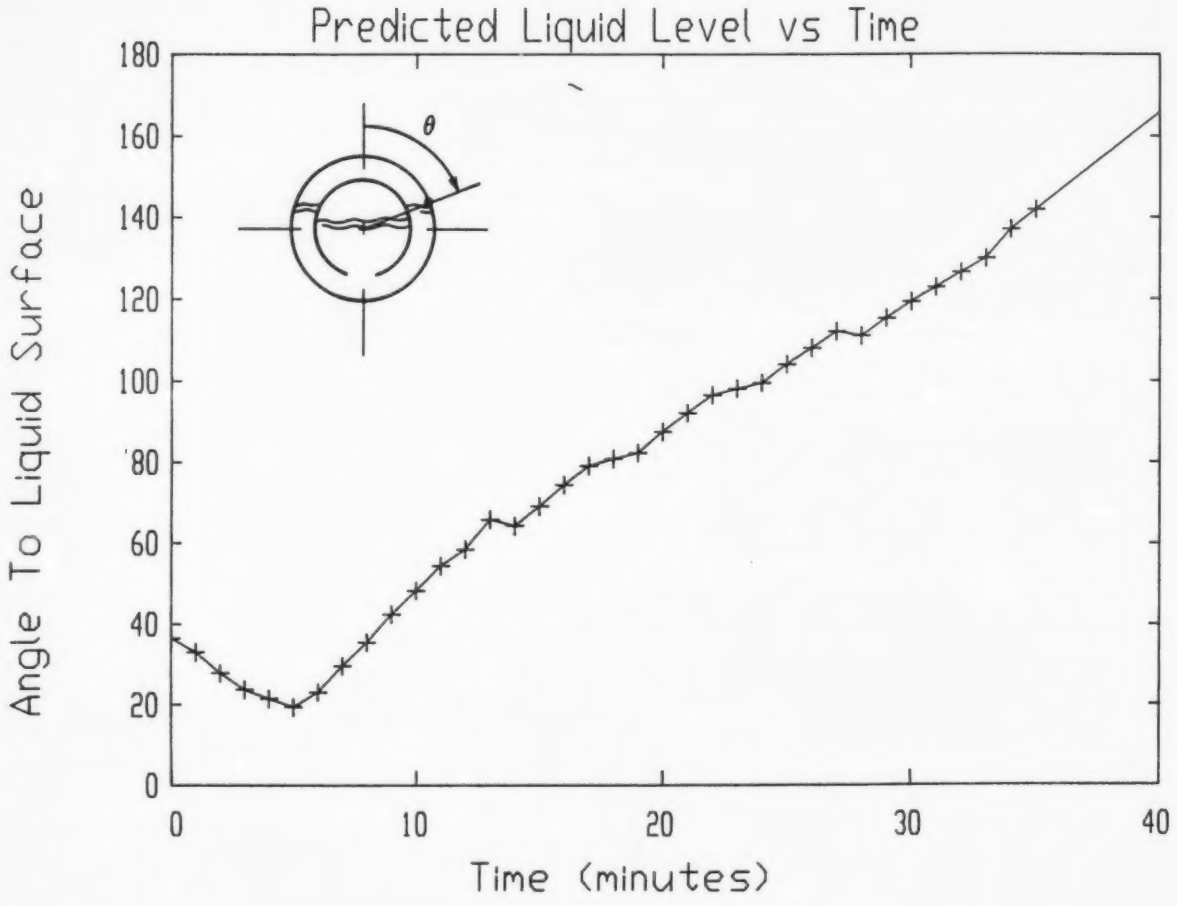

FIGURE 3.8-16 RUN CASE # 2

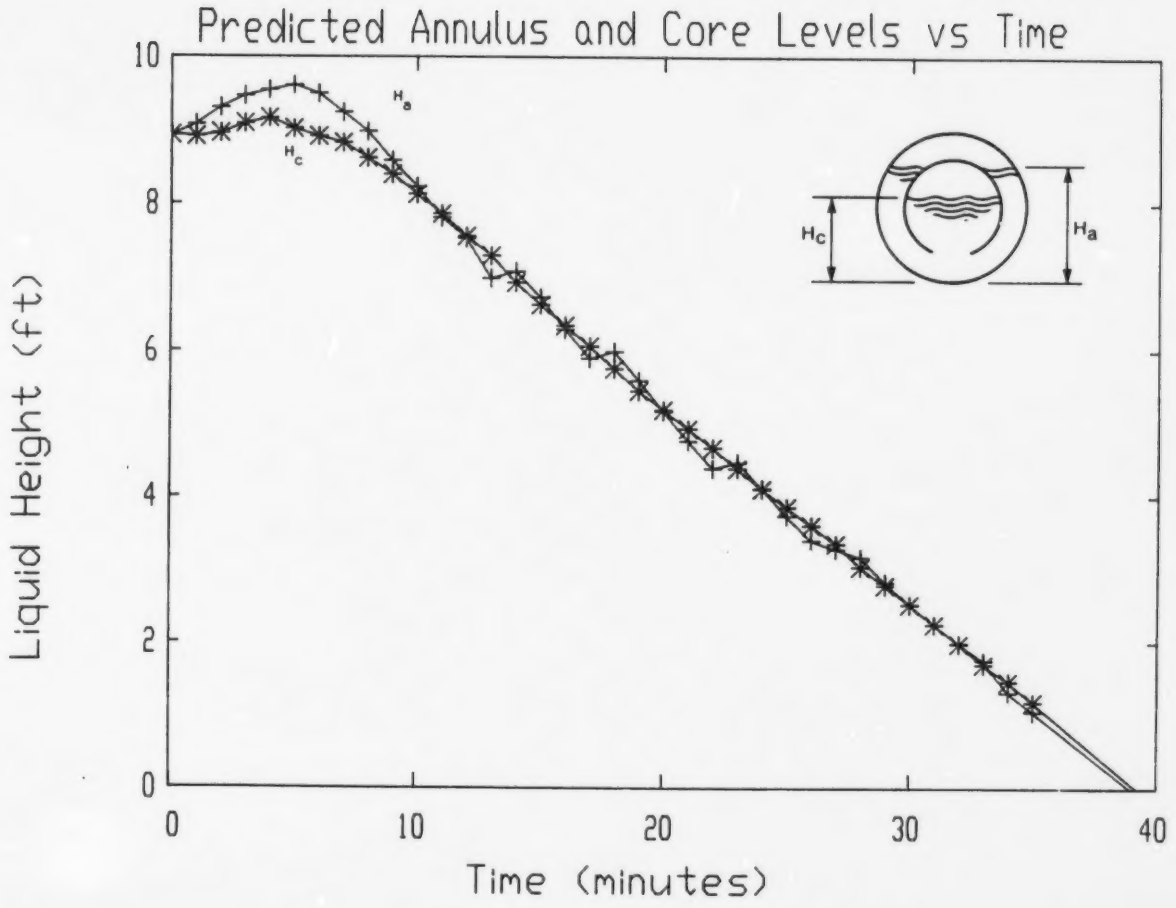

FIGURE 3.8-17 RUN CASE # 2

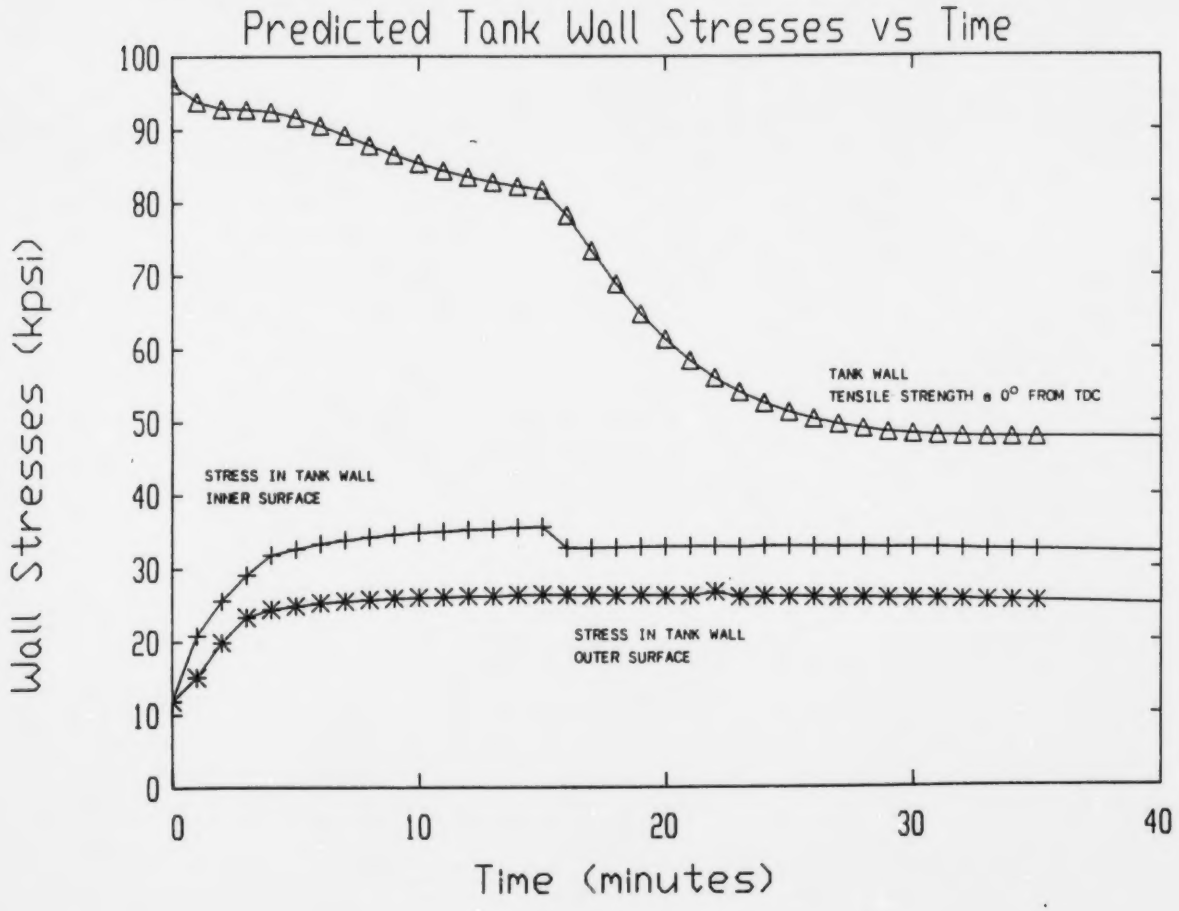

FIGURE 3.8-18 RUN CASE # 2

Run Case #3

This simulation was identical to that of Run Case #1 except that the shell gap spacing had been reduced from 5% of the tank diameter to 3 1/3% of the tank diameter. As in Run Case #1 the simulation involved a full scale upright tank filled to 95% capacity with propane. The tank was equipped with a standard size pressure relief valve. The simulation involved a fully engulfing fire. Results of the simulation are presented in Figures 3.8-19 to 3.8-23.

Before the results of the simulation are presented the following items should be noted. In carrying out out the simulation it was assumed that the shell gap size effects the height of the frothing layer. It was assumed that for the same heat flux the same volume of froth would be generated. It was therefore assumed that if the gap size is reduced and since the total volume of froth remains constant that the height of the frothing layer would increase for the reduced gap size. Therefore, it was assumed that the height of the frothing layer is inversely proportional to the gap. Starting from Run Case #1 where it was assumed that the frothing layer would be one-third the diameter of the tank, the frothing height in this case was calculated by multiplying the one-third tank diameter dimension times the ratio of the gap sizes for the two cases; in other words, in this case it was assumed the frothing layer would be equal to one-half the tank diameter. It should be noted that this assumption is not based on any experimental results. Therefore, the results of this simulation should be considered as preliminary only. They are intended for discussion purposes only and are presented for comparison purposes. In other words, the simulation is meant to show the effect of increasing the height of the frothing layer on the response of the tank lading system.

Figure 3.8-19 presents the predicted tank pressure for Run Case #3. As can be seen from the figure, the tank pressure versus peak tank pressure is slightly greater than that observed for Run Case #1.

Figure 3.8-20 presents the predicted tank wall temperature versus time from fire ignition. As can be seen from the figure, the increased frothing height has a significant effect on the tank wall temperatures. The peak tank wall temperature is reduced from that of Run Case #1 and the time duration for reduced wall temperatures is longer. The effect of the frothing layer is of course seen over a larger area of the tank wall for a longer period of time.

Figure 3.8-21 presents the liquid level in the annulus. Once again, the predicted liquid level is similar to that observed for the other run cases and for the baseline case. Again, some instabilities in the mathematical solution are observed.

Figure 3.8-22 presents the predicted annulus and core levels versus time from fire ignition. As in the previous run cases, the liquid levels in the annulus and core follow one another closely during the entire simulation. Once again, it is observed that the liquid level in the annulus stays slightly above the liquid level in the core region during the initial period of the simulation because of the effects of density differences.

Figure 3.8-23 presents the predicted tank wall stresses and strength versus time from fire ignition. Because of the reduced wall temperatures it is clearly seen in the figure that the tank wall strength remains higher than in the previous run cases. The predicted tank wall stresses are similar to the previous cases because of the similar pressures obtained in the tank. Once again, the predictions indicate that the tank will not fail. The margin of safety in this case appears to be higher than in the previous run cases involving internal shell equipped tanks.

In summary, the results of this prediction indicate that by increasing the height of the frothing layer the margin of safety is improved. Therefore, in an upright tank it appears to be advantageous to size the shell in such a manner to maximize the height of the frothing layer.

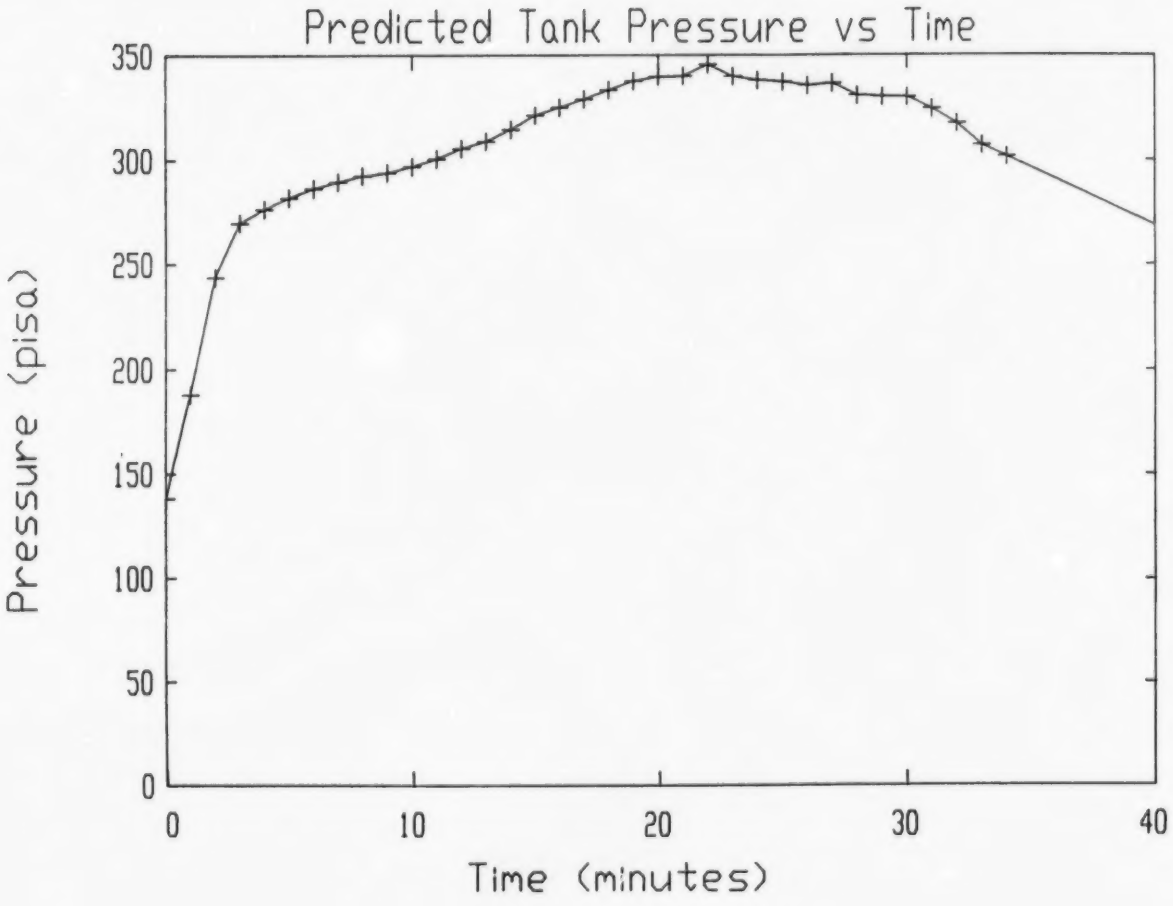

FIGURE 3.8-19 RUN CASE # 3

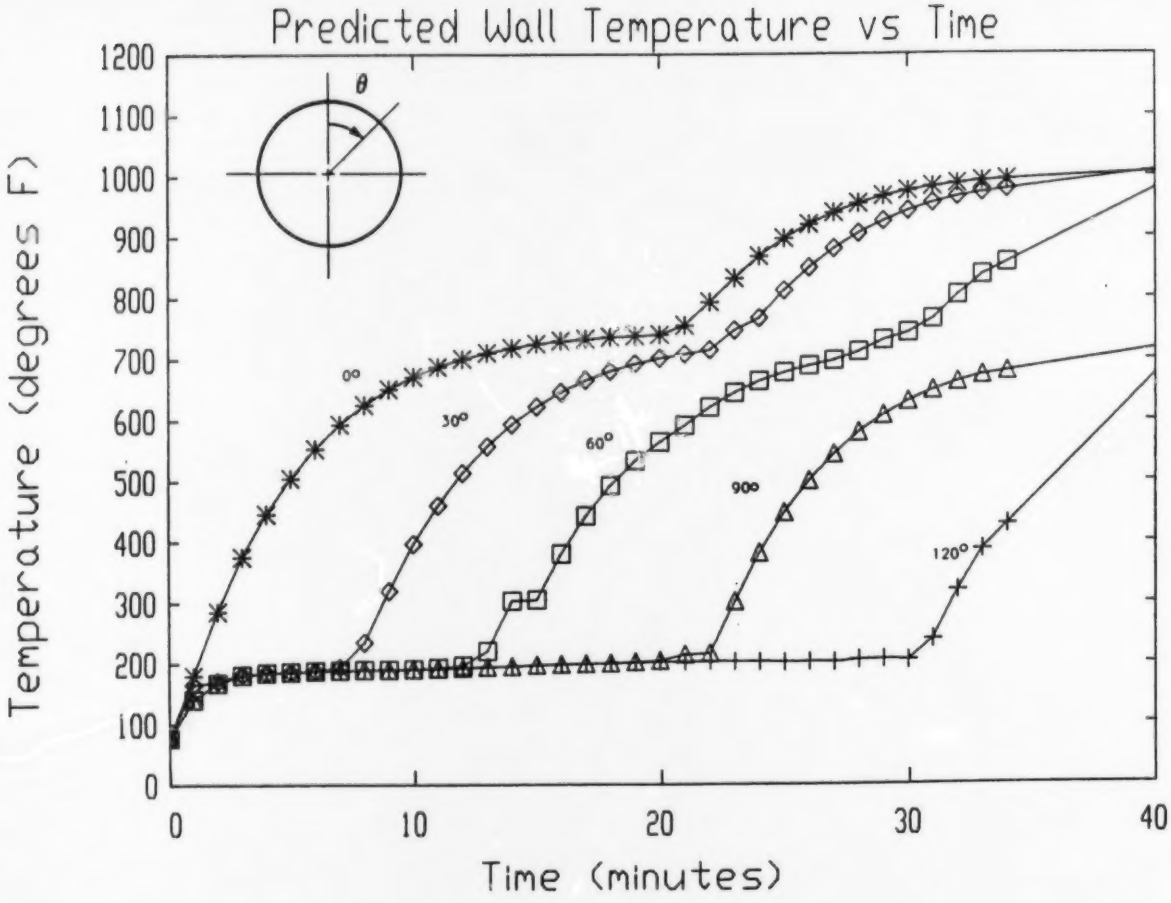

FIGURE 3.8-20 RUN CASE # 3

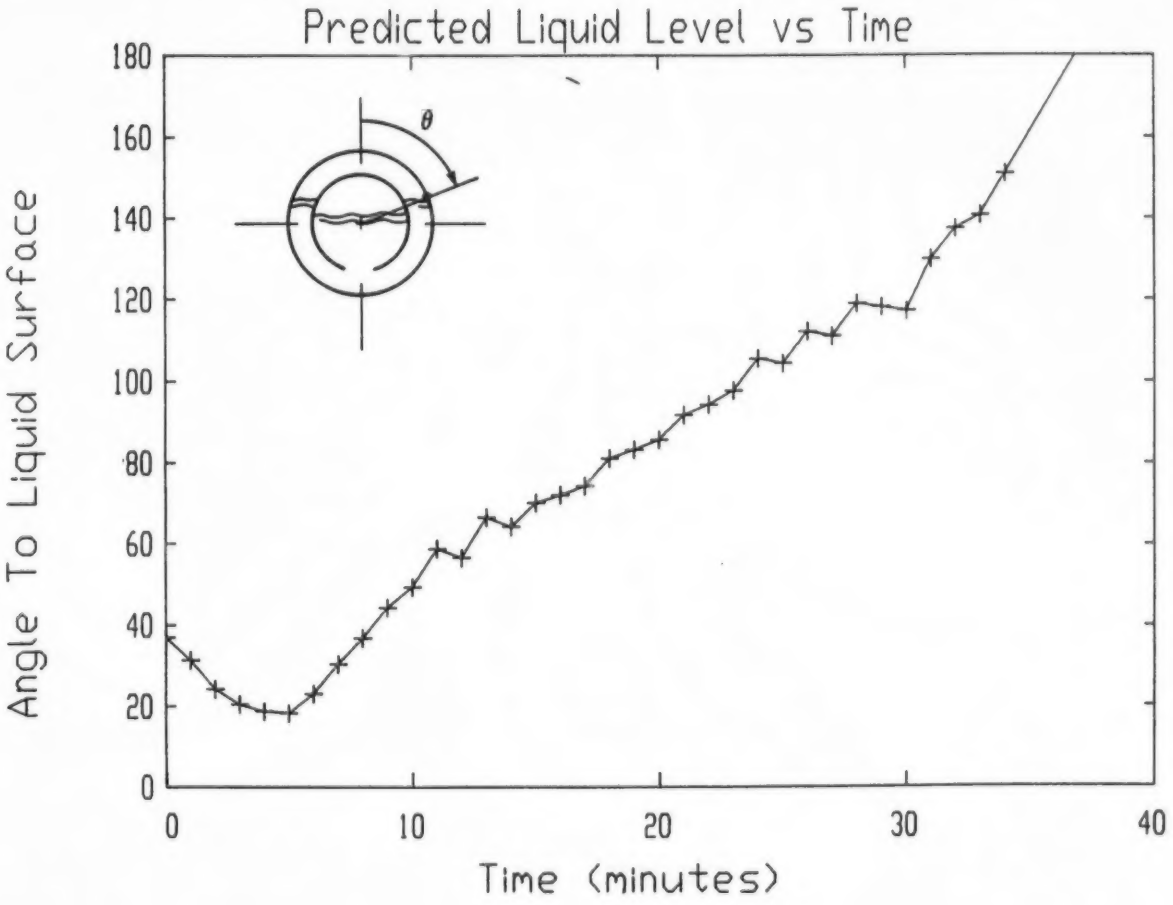

FIGURE 3.8-21 RUN CASE # 3

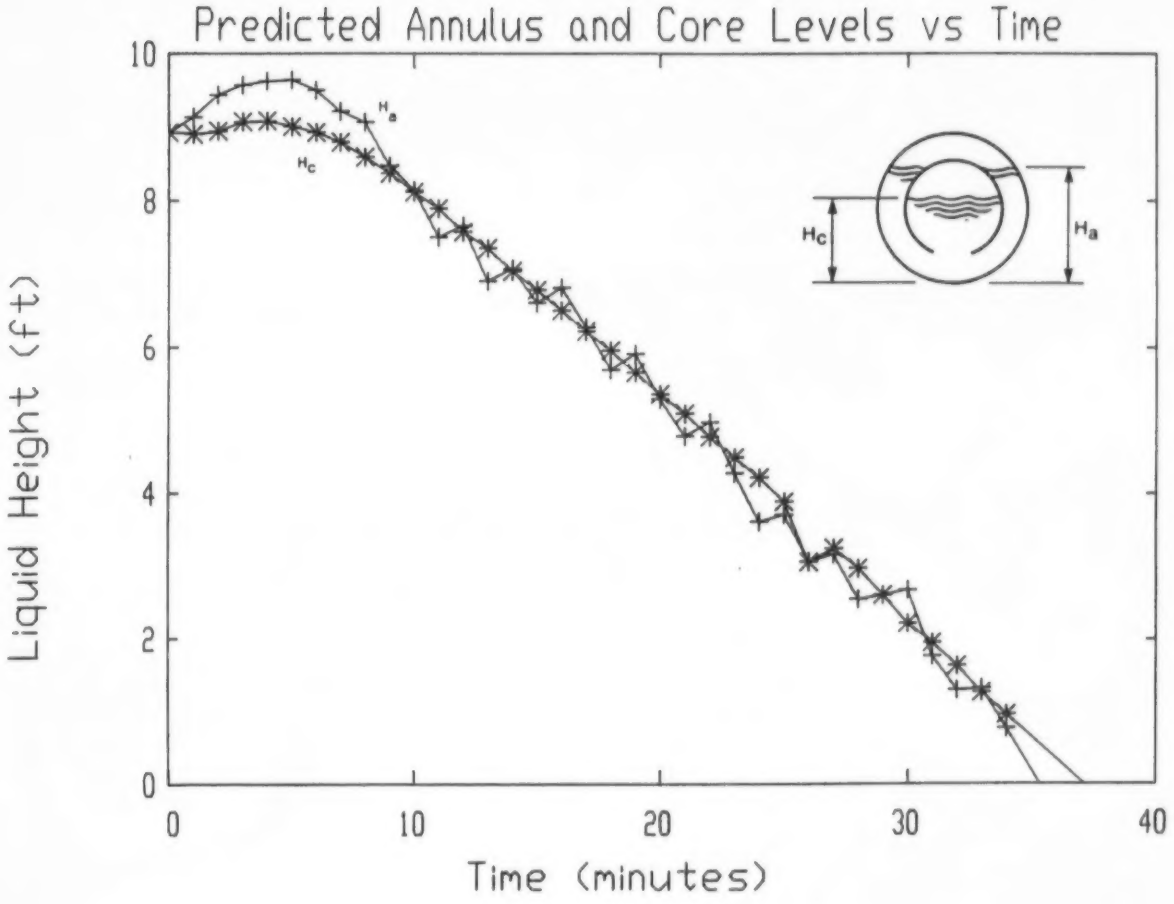

FIGURE 3.8-22 RUN CASE # 3

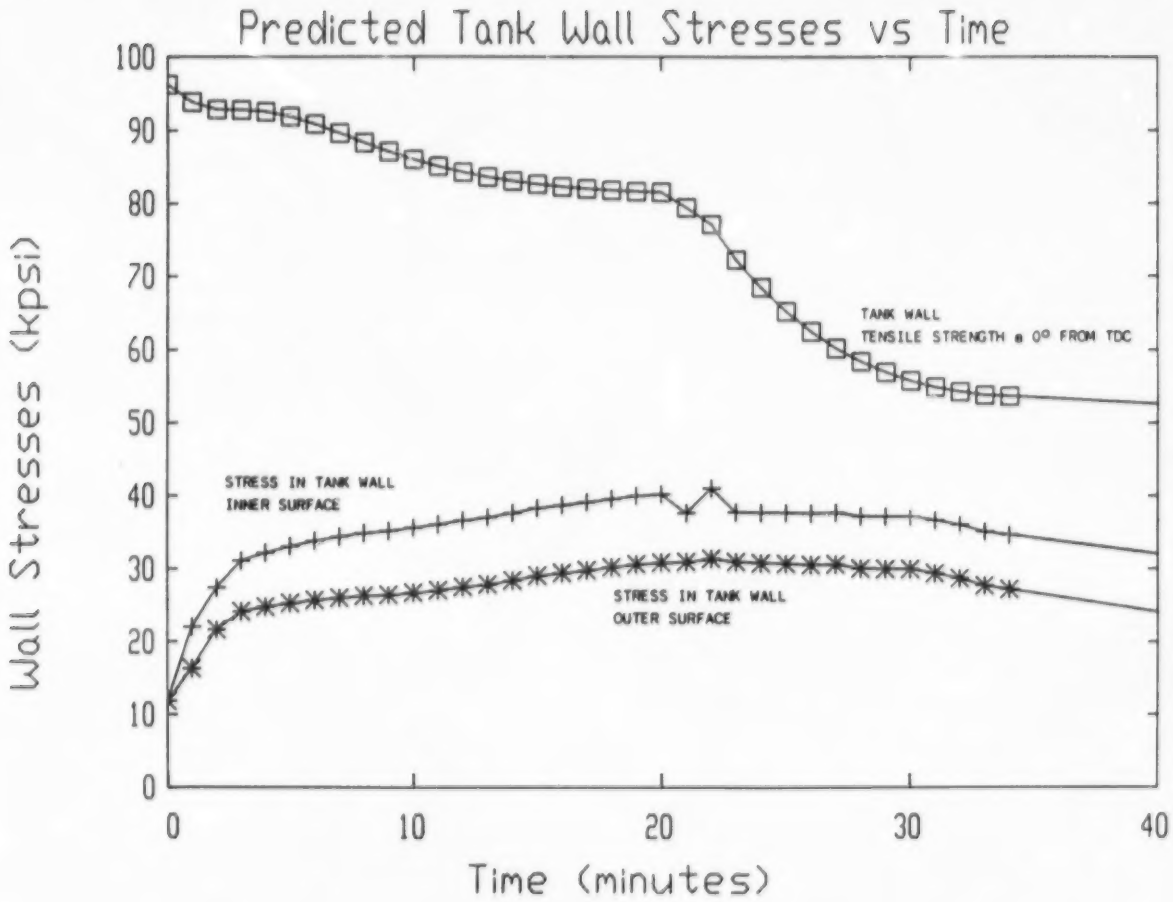

FIGURE 3.8-23 RUN CASE # 3

Run Case #4

This run case is identical to that of Run Case #3 except that the pressure relief valve size has been increased by 25%. The simulation involved the full scaled upright tank equipped with an internal shell device with the gap being 3 1/3% of the tank's diameter. The simulation involved a fully engulfing fire. The same assumptions as used for Run Case #4 regarding the height of the frothing layer were used in this run case. Once again, it was assumed that increasing the size of the pressure relief valve had no effect on the height of the frothing layer. The results of the simulation are presented in Figure 3.8-24 to 3.8-28.

Figure 3.8-24 presents the predicted tank pressure for Run Case #5. As can be seen from the figure, the increased valve capacity results in the peak pressure being significantly reduced from Run Case #3. The difference in peak pressure is very similar to that observed in Run Cases #1 and 2.

Figure 3.8-25 presents the predicted tank wall temperatures versus time from fire ignition. The predicted tank wall temperatures appear to be unaffected by the increased valve capacity. The peak wall temperatures are unaffected by the increased valve capacity. The only effect of the increase valve capacity on the wall temperatures is a slight shifting of the temperature response along the time scale.

Figure 3.8-26 presents the predicted annulus liquid level during the fire simulation. As can be seen from the figure, the annulus liquid level follows a trend similar to that for previous run cases and for the baseline cases. Once again, some mathematical instabilities are observed.

Figure 3.8-27 presents the predicted annulus and core liquid level versus time from fire ignition. Once again, the figure shows that the liquid level in the annulus and core follow one another very closely during the entire simulated fire event. The results here are very similar to those shown previously for Run Cases #1 through 3.

Figure 3.8-28 presents the predicted tank wall stress and strength versus time from fire ignition. As can be seen from the figure, the tank wall strength is almost identical to that predicted for Run Case #4 and this, of course, is because the tank wall temperatures for this case are very similar to those for Run Case #3. However, the predicted wall stresses are lower in this case than in Run Case #4 because the increase in pressure relief valve capacity results in a lower tank pressure. As a result, the thermal model predicts that the tank will not fail and that the margin of safety in this case is higher than in Run Case #3. Therefore, it appears that by increasing the relief valve capacity and therefore reducing the peak tank pressure, this results in an increased margin of safety.

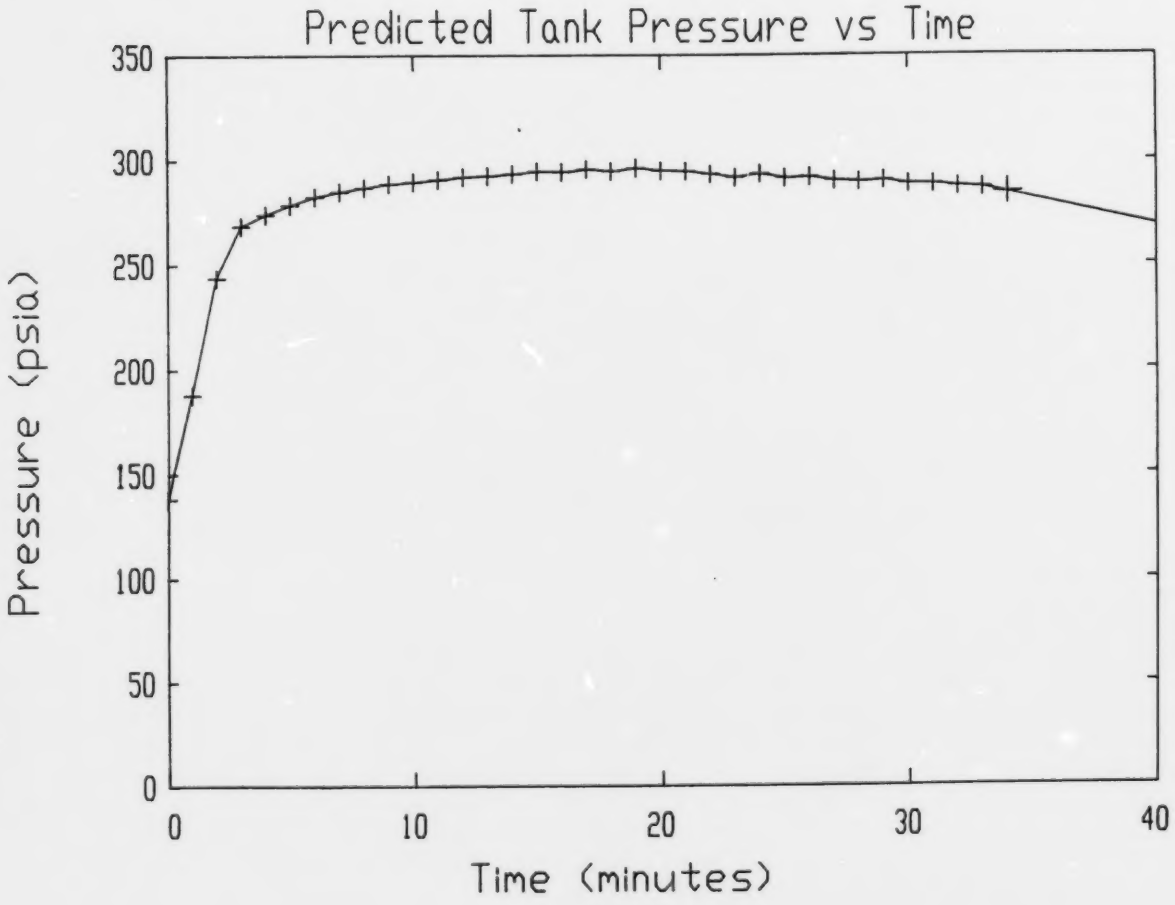

FIGURE 3.8-24 RUN CASE # 4

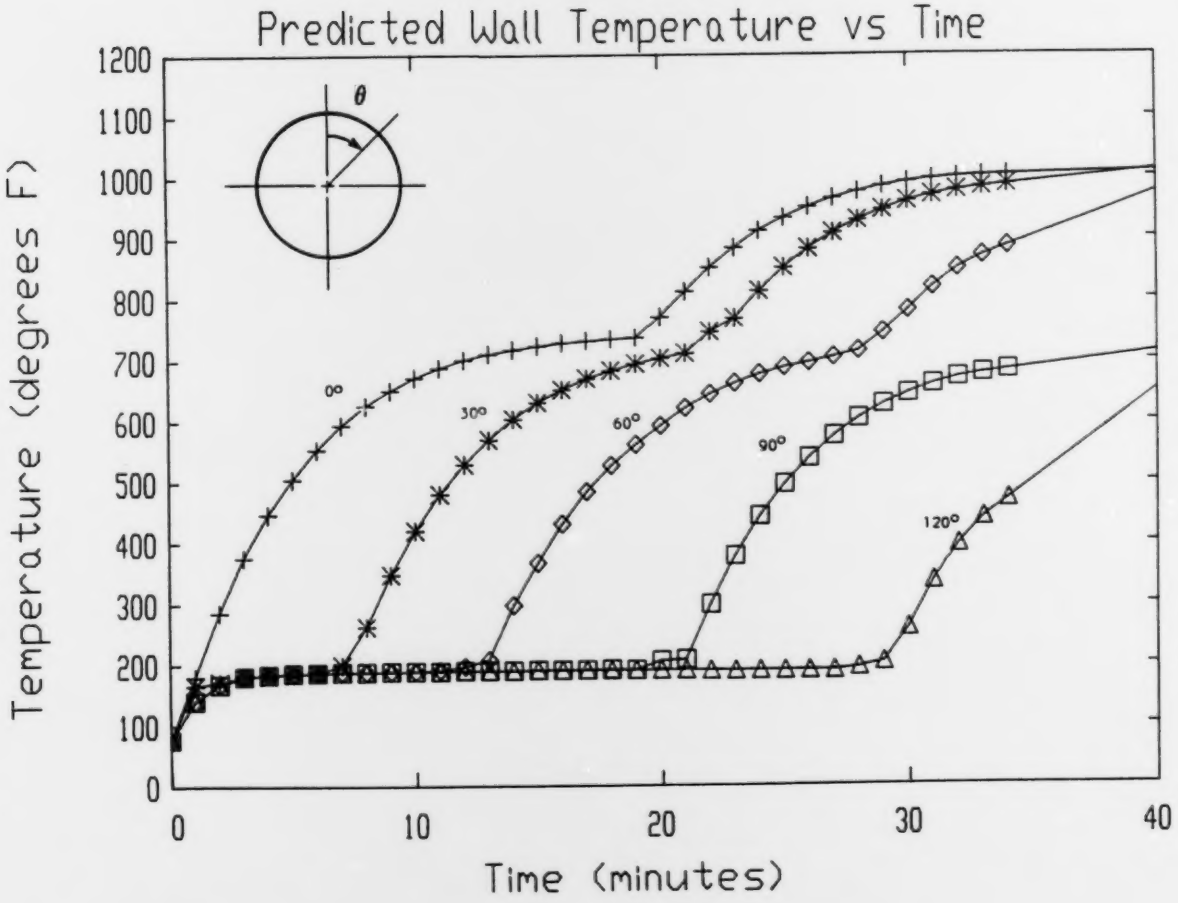

FIGURE 3.8-25 RUN CASE # 4

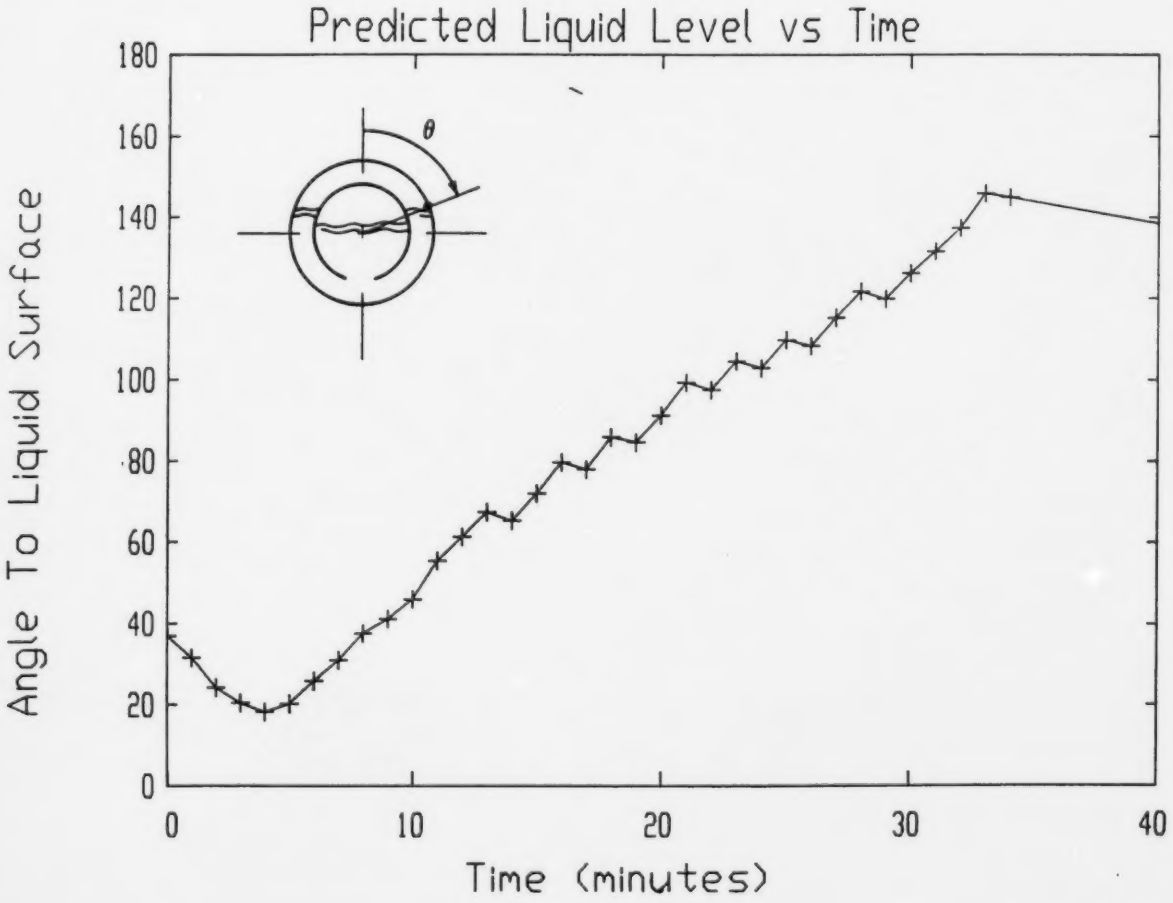

FIGURE 3.8-26 RUN CASE # 4

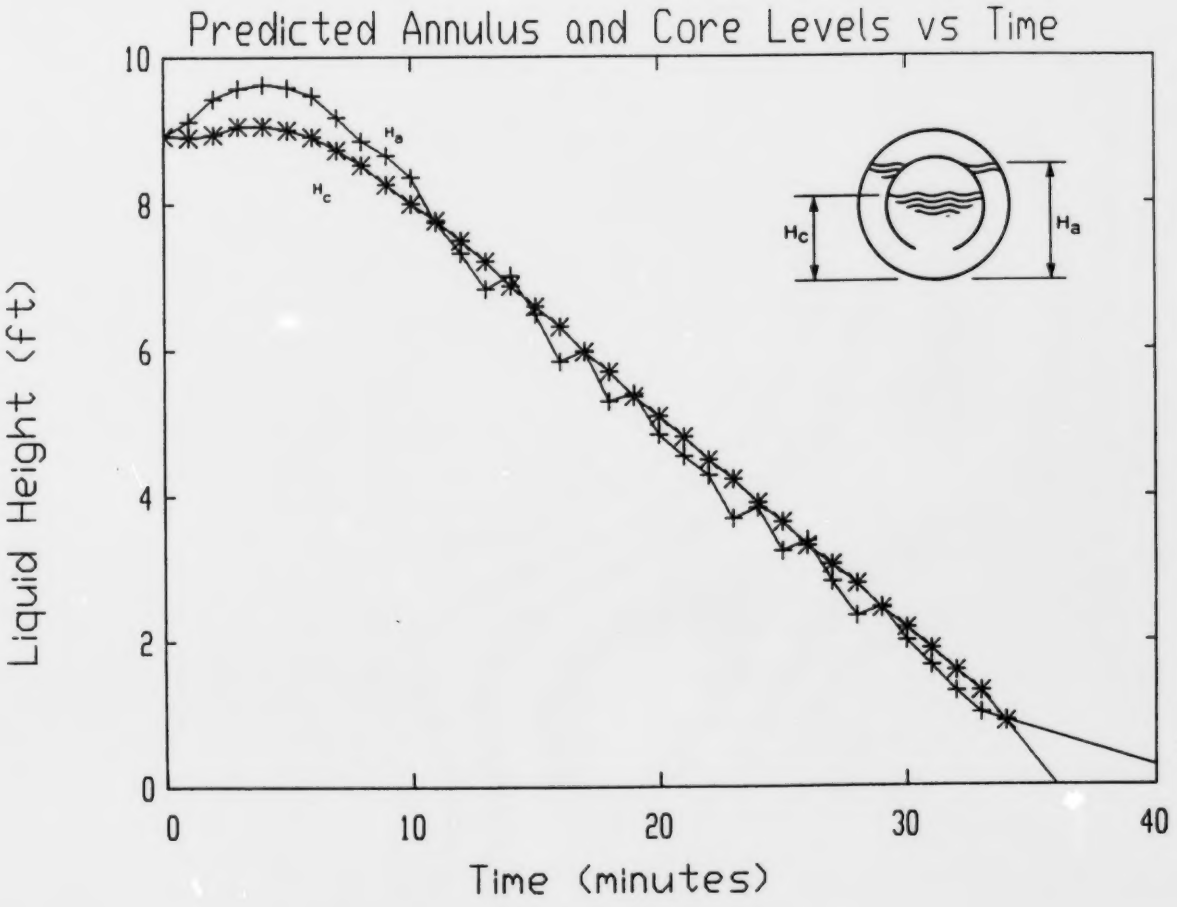

FIGURE 3.8-27 RUN CASE # 4

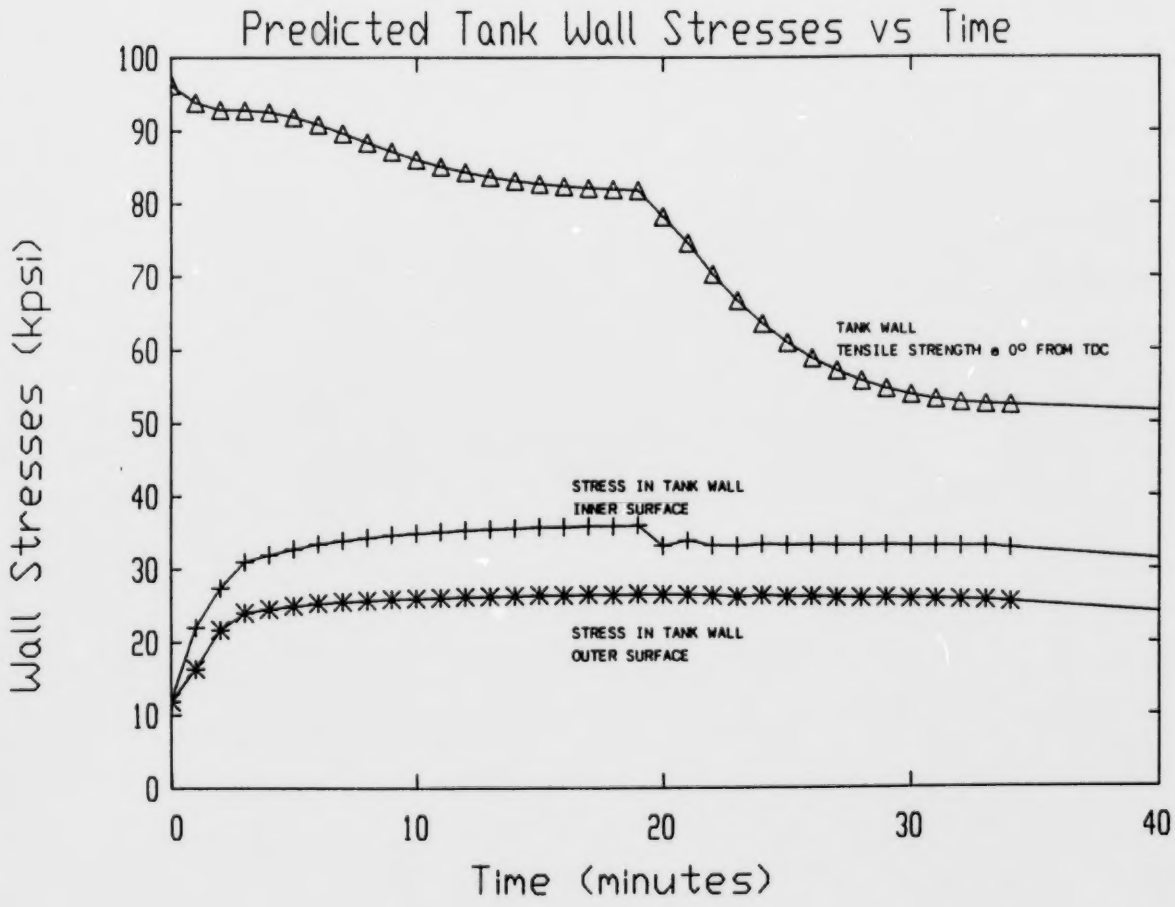

FIGURE 3.8-28 RUN CASE # 4

Run Case #5

This run case involved a full scaled tank equipped with internal shell device. The shell gap was 5% of the tank diameter filled to 95% capacity with propane. The tank was equipped with a relief valve that has a flow area of 25% greater than a standard size pressure relief valve. The tank was rolled 90 degrees to one side. Therefore, this run case differs significantly from previous run cases because in this case the tank is rolled and the pressure relief valve is initially below the liquid surface. In the simulation it is assumed that if the pressure relief valve is below the liquid surface and therefore venting liquid, no appreciable frothing is generated within the tank. Because of this, the benefits of the internal shell device are reduced because they are no longer directing froth along the inside of the tank primary wall. A concern is that in this type of situation the internal shell device may even make the situation worse than in an unequipped tank. The results of the simulation are presented in 3.8-29 to 3.8-33.

Figure 3.8-29 presents the predicted tank pressure for Run Case #5. As can be seen from the figure during the initial period of simulation the tank pressure rose rapidly until the pressure relief valve came into play. Once the pressure relief valve opened, the tank pressure was maintained at or near the pressure relief valve setting. It should be noted at this point that the pressure relief valve flow was assumed to be 'frozen liquid' flow and that two phase flow through relief valve was not accounted for in this simulation. This, of course, is a weakness of the existing tank car thermal model.

Figure 3.8-30 presents the predicted tank wall temperatures versus time from fire ignition for Run Case #5. As can be seen from the figure, the internal shell device does not act to significantly reduce the tank wall temperatures in the rolled tank during the initial periods of the simulation. Wall temperatures in the upper regions of the tank rise very rapidly. Because it has been assumed that liquid is passing through the pressure relief valve the tank will empty very rapidly because the mass flow rates are high when only liquid is passing through the relief valve. As a result, wall locations lower in the tank wall experienced earlier increases in temperature for the case of a submerged pressure relief valve. Eventually, however, the liquid level in the annulus drops below that of the pressure relief valve location and

therefore the pressure relief valve eventually begins to vent vapour. At that point in time, the vapour going through the relief valve must flow around the tank through the annulus thereby resulting in forced convected heat transfer in the annulus. As a result of this forced convection the simulation predictions indicate that the tank wall temperatures at the top of the tank remain slightly below those predicted for an unprotected upright tank car. This decrease in the peak wall temperatures is approximately 30 degrees Celcius. Although this is a small temperature difference, it does have an effect on the predicted tank wall material strength to be discussed later.

Figure 3.8-31 presents the predicted liquid level from the annulus versus time from fire ignition. As can be seen from the figure initially the liquid level in the annulus rises because of acts of thermal expansion. However, once the pressure relief valve comes into play, especially when the the pressure relief valve is submerged, the liquid level in the annulus drops very rapidly because of the high mass flows associated with liquid flow through the relief valve. When the liquid level in the annulus reaches the bottom slot flow from the core region maintains the liquid level in the annulus approximately constant at the lower lip of the bottom slot in the internal shell. The liquid level in the annulus then remains stationary because of the replenishing flow from the inner core. At approximately twenty minutes the liquid level in the core is such that it can no longer flow into the annulus the remaining liquid in the core is trapped in the annulus. At this point, the liquid level in the annulus again drops rapidly. Sometime during this period, the pressure relief valve begins to vent vapour because the liquid level is below the entrance to the relief valve. Once vapour is being vented from the tank, it is assumed that froth is established and therefore some cooling effect is experienced. As can be seen from the figure eventually the liquid is totally drained from the annulus and the only liquid remaining is that trapped in the inner shell core.

Figure 3.8-32 presents the predicted annulus and core levels versus time from fire admission. As can be seen from the figure, liquid levels in the annulus and core regions differ significantly for the case of a rolled tank. During the initial period of time, the liquid level in the annulus rises slightly above that in the core because of thermal expansion effects. However, once the

pressure relief valve comes into action, the liquid level in the annulus drops rapidly below that in the core. This is because the valve is draining liquid from the annulus. However, at some point the level in the core spills out into the annulus and this maintains the level in the annulus at least until the point where the liquid level in the core reaches the lower lip of the inner shell and therefore the remaining liquid in the inner core is trapped. This is observed to happen at approximately 20 minutes into the simulation. Beyond this, the liquid level in the annulus is drained very rapidly because it is assumed that all the material that is being vented comes from the boiling in the annulus. Once the liquid level in the annulus has dropped to the bottom of the tank, the material for venting comes from the core region and therefore beyond approximately 23 minutes into the test the core liquid level beings to drop until eventually the core itself is drained and at this point the tank is empty. The results shown in this figure seem reasonable; however, during the time period approximately 6 and 20 minutes the rate at which the liquid level in the core drops as the liquid spills from the core to the annulus seems rather slow. This appears to be a problem in the flow models used to represent the mass flow between the annulus and core region. However, because there is no experimental data available to validate this, the model was considered to be sufficient for the present purposes.

Figure 3.8-33 represents the predicted tank wall stresses and strength versus time from fire admission. As can be seen from the figure, the tank wall strength drops rapidly once high wall temperatures are established in the tank; however, the tank wall strength is not dropped as far as it does for the case of an upright unprotected tank. This is because in the present case the simulated predictions indicate that forced convected heat transfer in the annulus does play a role in reducing the tank wall temperatures. This, of course, needs to be substantiated with testing. If forced convected heat transfer in the annulus were ignored, then the wall temperatures in this particular case involving a rolled tank with an internal shell device would reach the levels predicted for the upright unprotected tank. If the wall temperatures did reach the high levels experienced in the baseline cases, then the tank wall strength would have dropped and it is possible that the tank would fail. Therefore, it is very difficult at this point to substantiate the present predictions.

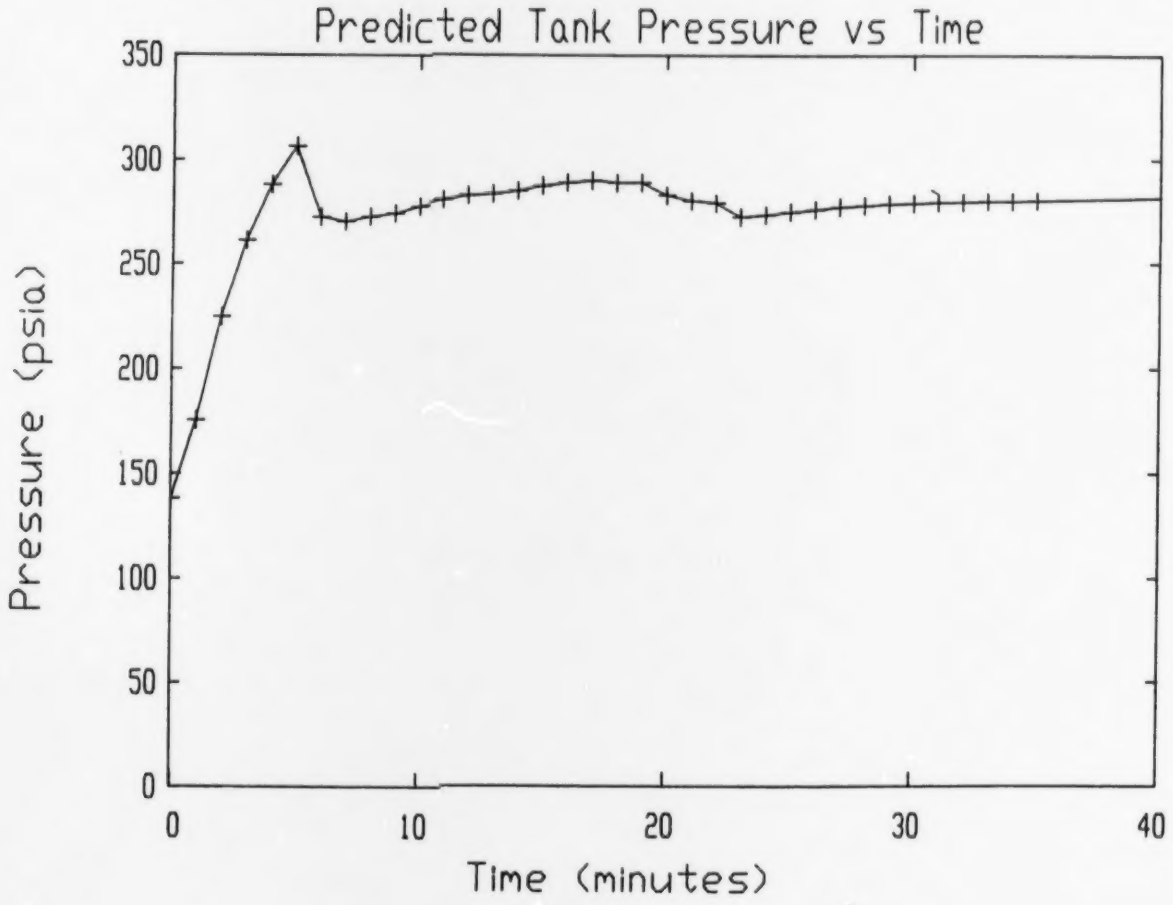

FIGURE 3.8-29 RUN CASE # 5

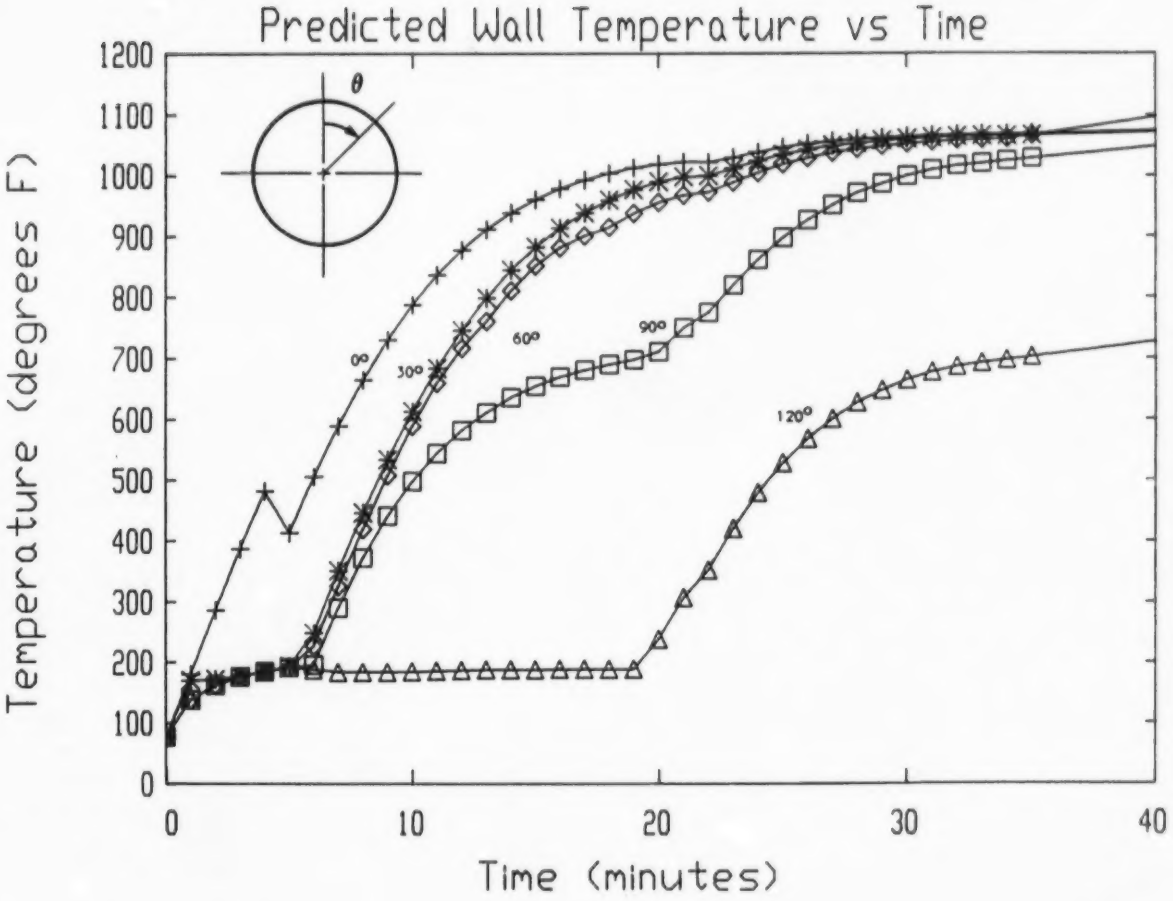

FIGURE 3.8-30 RUN CASE # 5

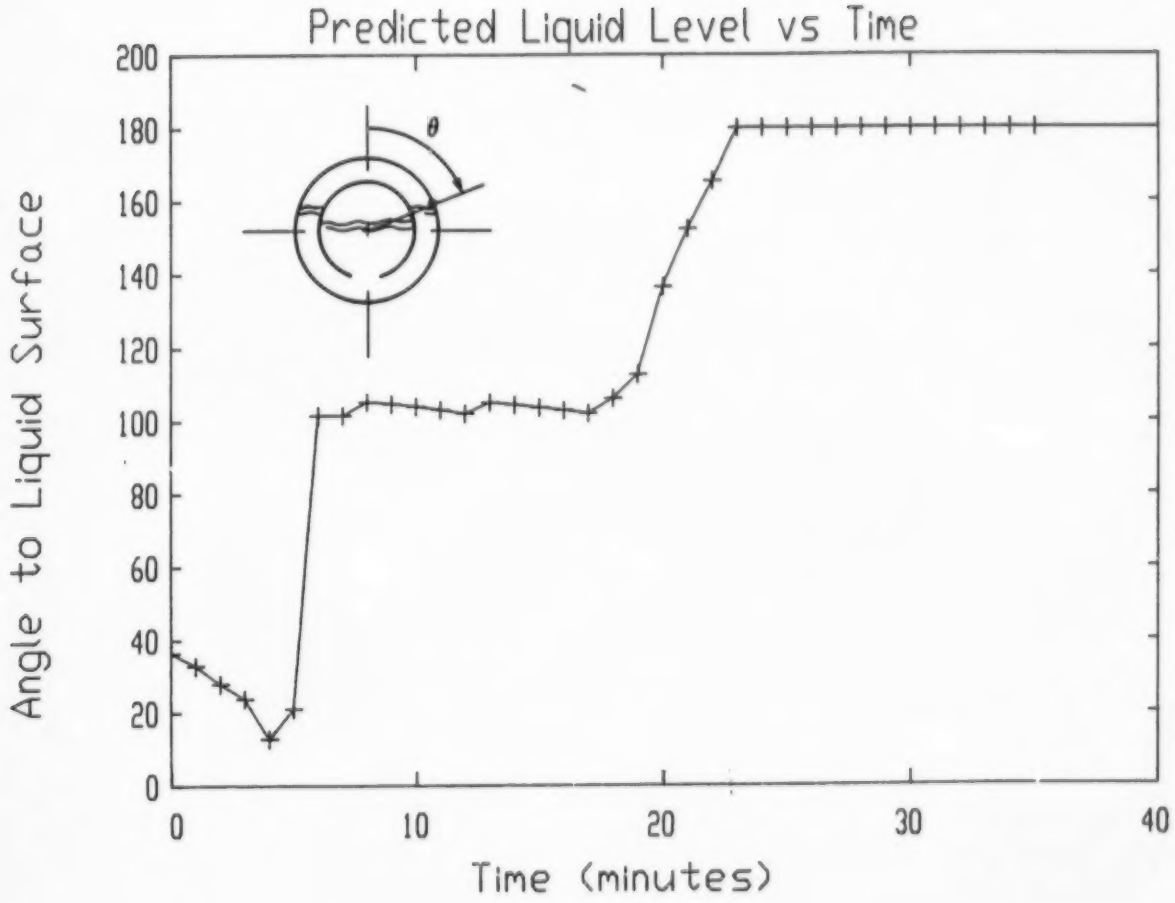

FIGURE 3.8-31 RUN CASE # 5

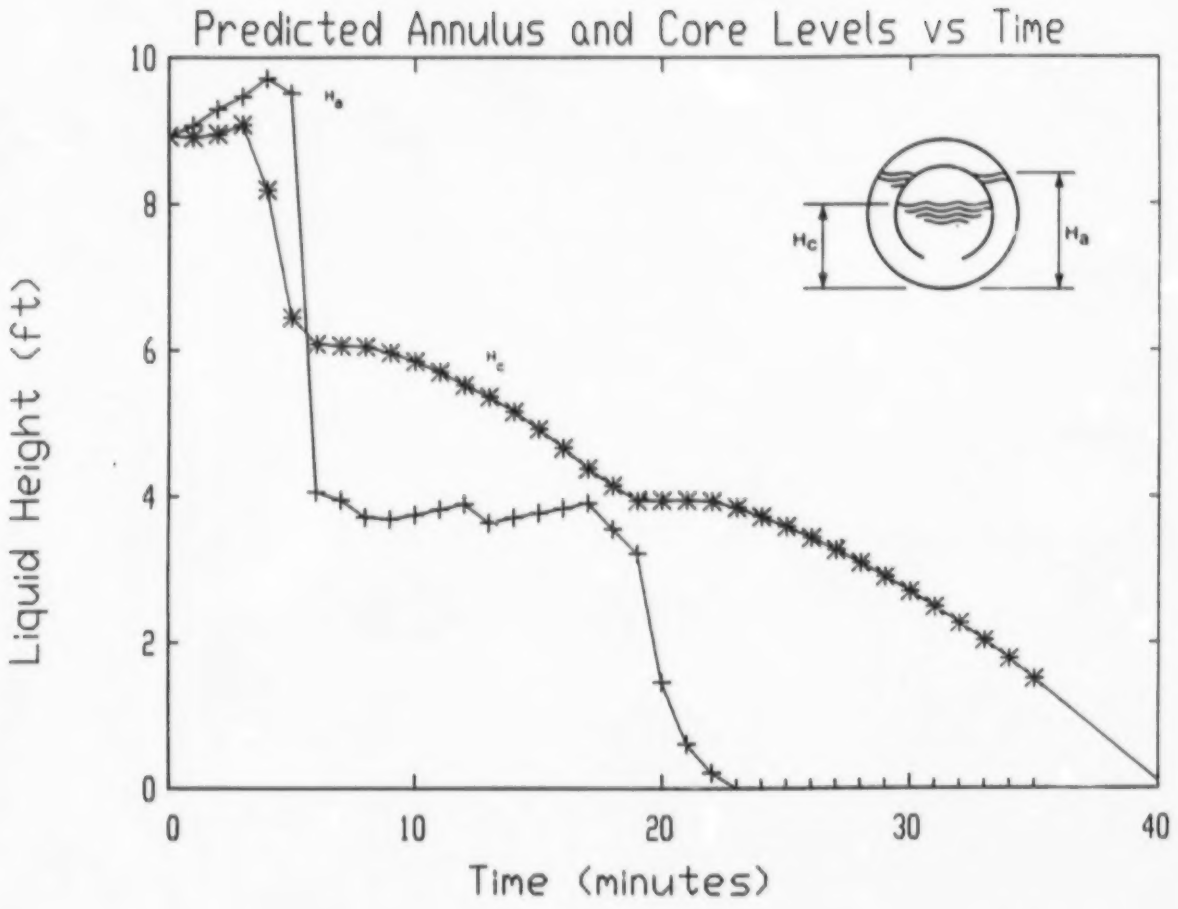

FIGURE 3.8-32 REN CASE # 5

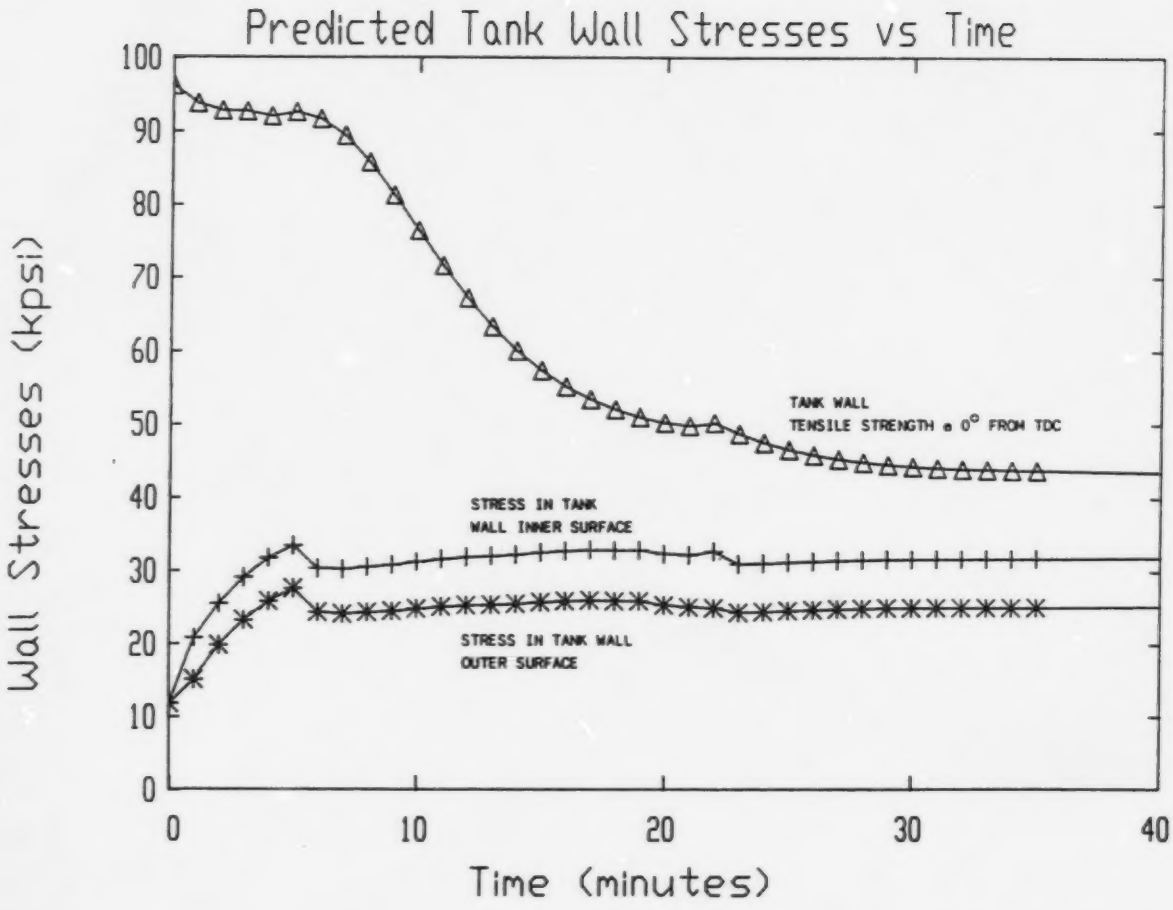

FIGURE 3.8-33 RUN CASE # 5

Run Case #6

This run case involved a tank equipped identically with that of Run Case #5, except in this case the tank is rolled to 120 degrees to one side. In this case, therefore, more liquid will remain trapped within the inner core and the annulus will be drained much more quickly. The results of this simulation are presented in figures 3.8-34 to 3.8-38.

Figure 3.8-34 represents predicted tank pressure versus time from fired admission. As can be seen from the figure, the predicted tank pressure is very similar to that of Run Case #5. It appears that the pressure relief valve cycled during much of the simulation.

Figure 3.8-35 represents predicted tank wall temperatures versus time from fired admission. As can be seen from the figure, the tank wall temperatures rose very rapidly to high levels. The wall temperatures in the lower regions of the tank increased much earlier than the baseline cases because the liquid was being drained from the annulus. As with Run Case #5, the predicted peak tank wall temperatures are slightly below those predicted for the baseline cases because of the effects of forced convection in the annulus. As before, this is unsubstantiated by experimental results. Further experimental testing is necessary to validate these predictions. If the forced convection in the annulus were ignored, the peak wall temperatures would reach or exceed the levels predicted for the unprotected upright tank of the baseline run cases.

Figure 3.8-36 presents the predicted liquid level in the annulus versus time. As can be seen from the figure, the liquid level in the annulus initially rises due to thermal expansion but once the pressure relief valve comes into action the liquid level in the annulus drops very rapidly. At the point liquid is being drained from the core. For a short period of time between 6 and 8 minutes the liquid level when the annulus remains stationary or near stationary and then eventually the remaining liquid in the core is trapped and in the core and the liquid level in the annulus once again drops very rapidly. Beyond approximately 12 minutes there is no longer liquid in the annulus region. The venting action has completely drained the annulus and the only liquid remaining is trapped in the inner shell core.

Figure 3.8-37 represents the predicted annulus and core levels versus time from fire admission. As can be seen from the figure the annulus liquid level drops very rapidly once the pressure relief valve comes into action. The tank annulus is empty after approximately 12 minutes of the simulation. After the annulus is drained, the remaining liquid trapped in the core is slowly vented from the tank as the tank cycles.

Figure 3.8-38 represents the predicted tank wall stresses and strength versus time from fire admission. As in Run Case #5, the simulation predictions indicate that the tank does not fail even though liquid is flowing through the pressure relief valve for much of the time. The reason the tank does not fail is that with forced convection in the annular space the tank wall temperatures remain slightly below those for an unprotected upright tank and the tank pressure also remains relatively low.

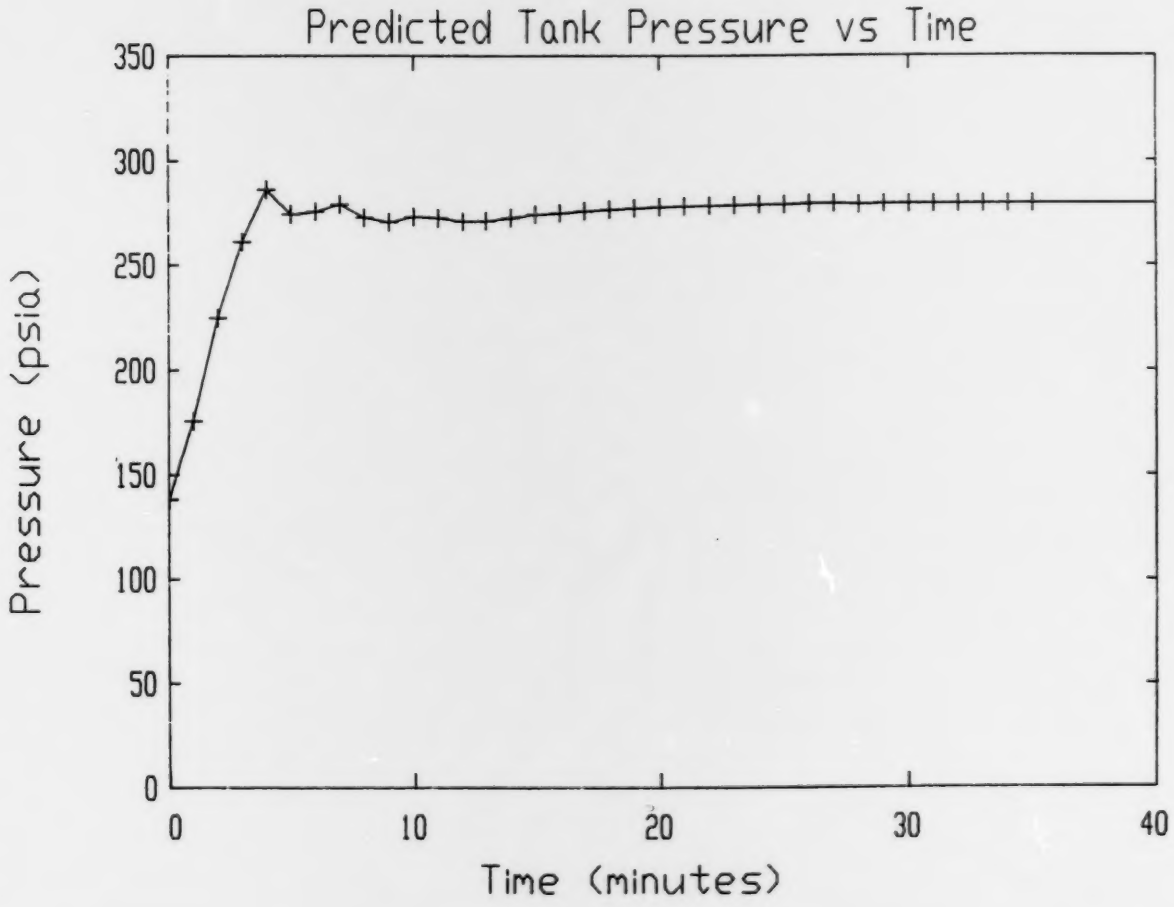

FIGURE 3.8-34 RUN CASE # 6

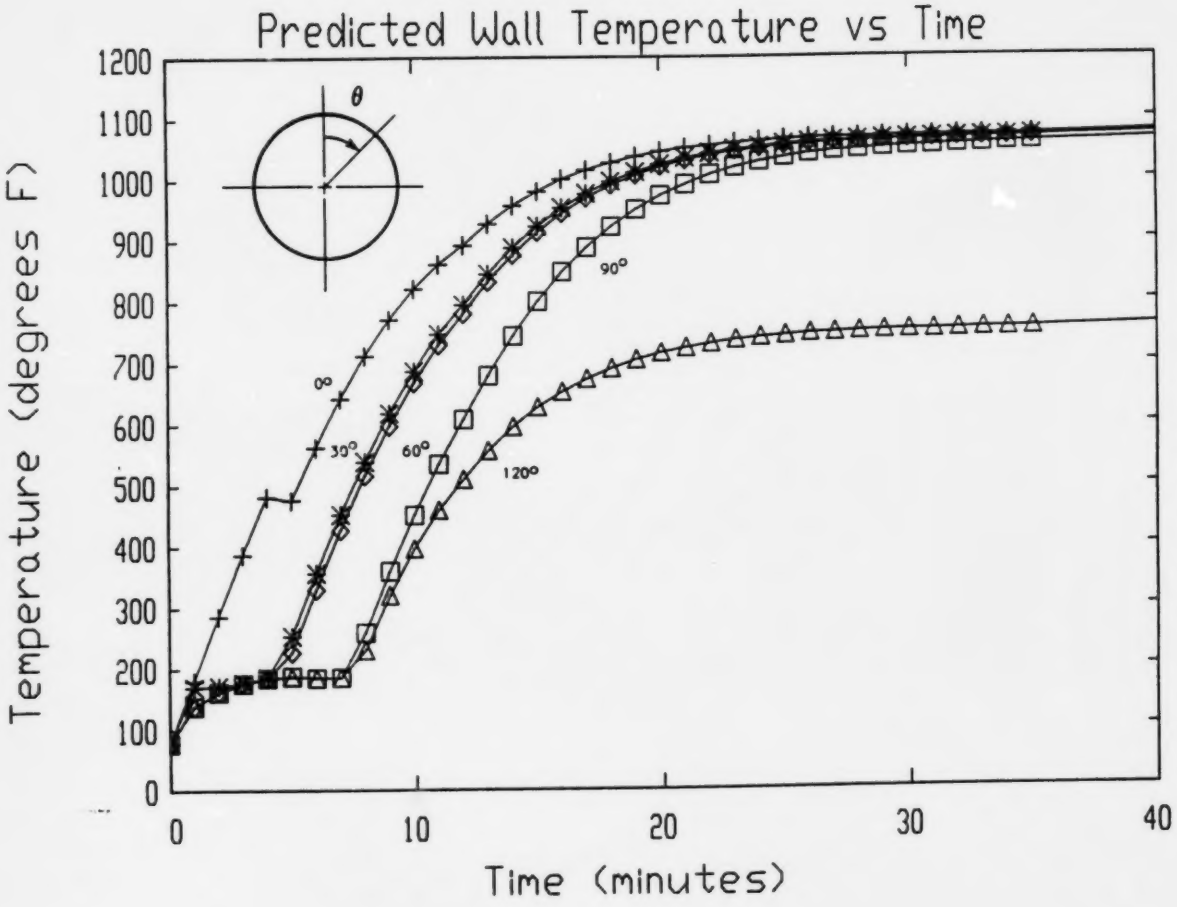

FIGURE 3.8-35 RUN CASE # 6

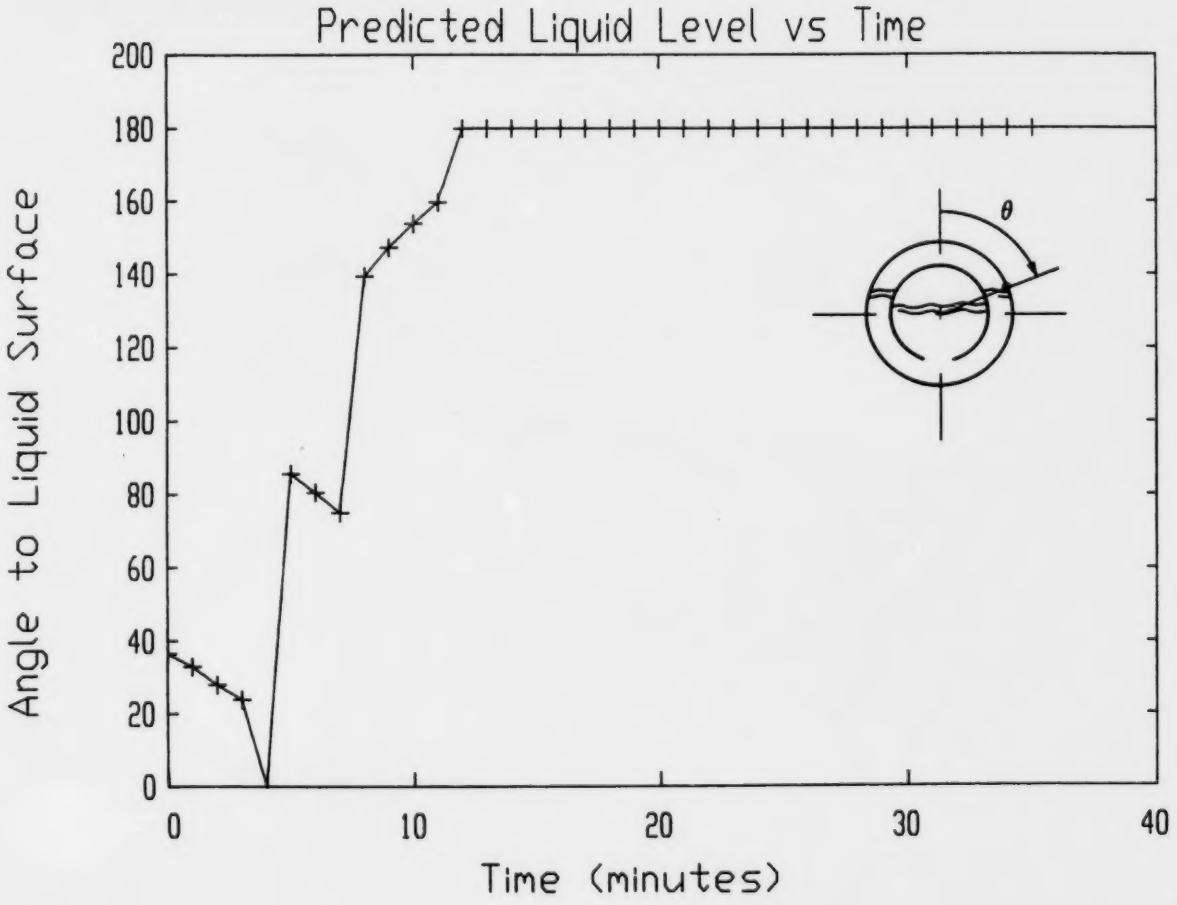

FIGURE 3.8-36 RUN CASE # 6

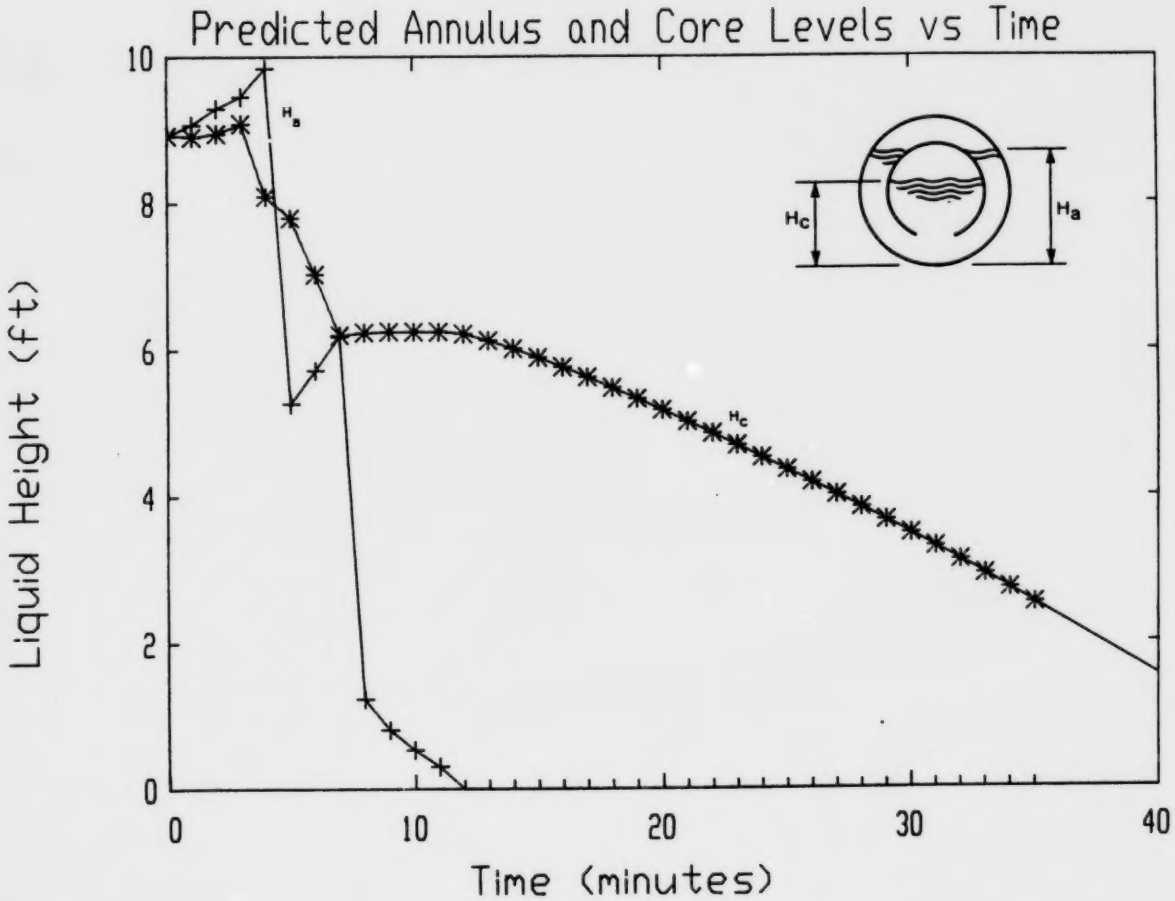

FIGURE 3.8-37 RUN CASE # 6

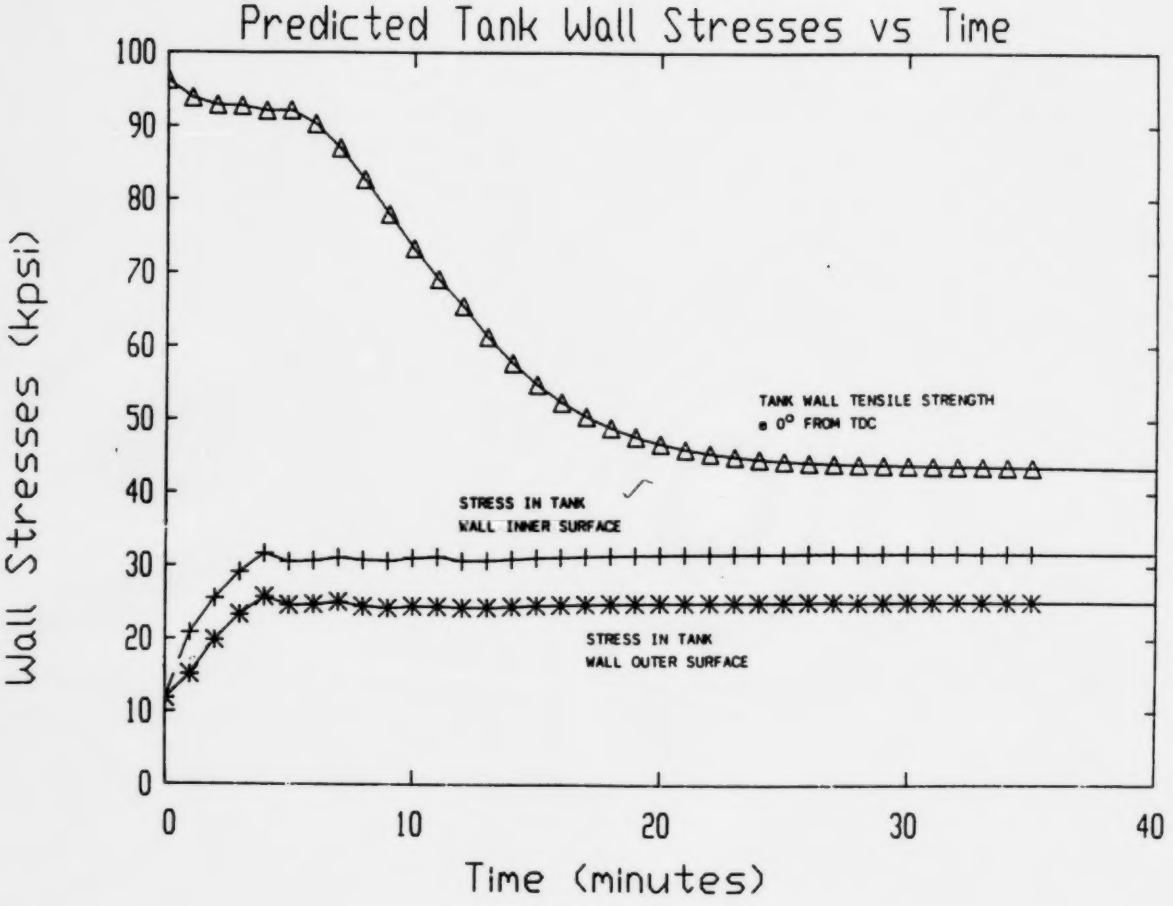

FIGURE 3.8-38 RUN CASE # 6

Run Case 7: (Simulation of Shell Equipped Tank Exposed To Torch Fire Impingement)

This run case involves simulation of a full scale shell equipped tank exposed to torch fire impingement. The torch fire application was at the top dead centre of the tank. The tank was equipped with a standard size pressure relief valve. The internal shell gap size and bottom slot dimensions are as presented in Table 3.7-1.

This simulation was performed in response to concerns that an internal device would not be able to protect the tank if the tank were exposed to torch fire impingement near the top of the tank where the wall is in contact with vapour. It should be noted that this type of impingement is unlikely because of geometry. It is difficult to construct a scenario where the burning relief valve flare from a tank impinges directly on the top or near the top of a neighbouring tank. It is more likely that the burning relief valve flare from a tank would impinge on the side of a neighbouring tank.

Figure 3.8-39 presents the predicted tank pressurization for the case of a shell equipped tank exposed to torch fire impingement at the top dead centre of the tank. As can be seen from the figure, the tank pressurizes slowly until the pressure relief valve begins to cycle. Because of the low total heat flux to the lading the pressure relief valve has more than enough capacity to maintain the tank pressure at the pressure relief valve set point.

Figure 3.8-40 presents the predicted tank wall temperatures for the case being considered. As can be seen from the figure, the predicted wall temperatures at the tank top dead centre rise very rapidly because of the intense heating by the flare at the location. Wall temperatures in other regions of the tank are of course significantly effected by the presence of the torch impingement. The heat flux drops rapidly as you move away from the stagnation point thus providing much slower rates of temperature increase and lower peak temperatures.

Figure 3.8-41 presents the predicted annulus liquid level for this torch impingement case. As can be seen from the figure, the annulus liquid level stays fairly stationary and then drops slowly due to action of the pressure relief valve.

Figure 3.8-42 presents the predicted liquid levels in the core and annulus regions within the tank. As can be seen from the figure, the liquid level in the annulus stays somewhat higher than the core level because of the effect of density variations between the annulus fluid and the core fluid.

Figure 3.8-43 presents the predictions for the tank wall stresses and the tank wall strength for the torch impingement simulation case. It should be noted that the tank wall strength and tank wall stresses are presented only for the top dead centre location of the tank wall. This is done because it is the top dead centre location (the torch stagnation point) that will experience the highest wall temperatures and therefore the most severe degradation in the tank wall material properties. As can be seen from the figure, the tank wall strength drops very rapidly because of the very rapid material strength drops below the predicted tank wall temperatures at 7 minutes into the test and this is an indication of probable tank failure.

The results of the simulation of a shell equipped tank exposed to torch fire impingement at the top dead centre indicate that the internal shell device is not capable of protecting the tank exposed to such fire conditions. If the torch is applied near the top of the tank where the tank wall is in contact with vapour the tank wall temperatures will rise very rapidly and the tank is likely to rupture due to degradation in the tank wall material properties. The internal shell device is not capable in this case of maintaining wall temperatures low enough to protect the tank from thermal rupture. The main problem is that the tank wall temperatures increase so rapidly that dangerous temperatures are reached before the pressure relief valve comes into action. The internal shell device can only provide the wall cooling effect when the pressure relief valve is in action. In such cases, some other means of thermal protection is required as a backup.

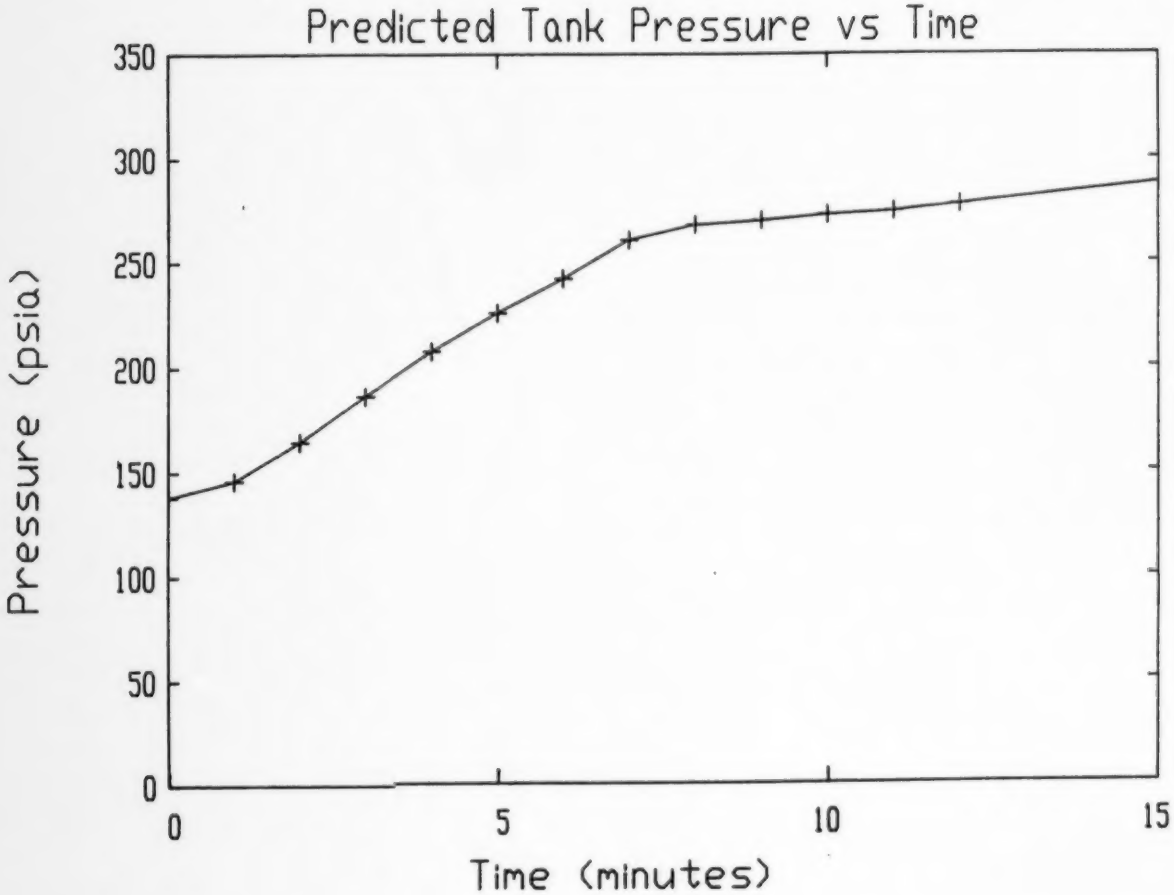

FIGURE 3.8-39 RUN CASE # 7

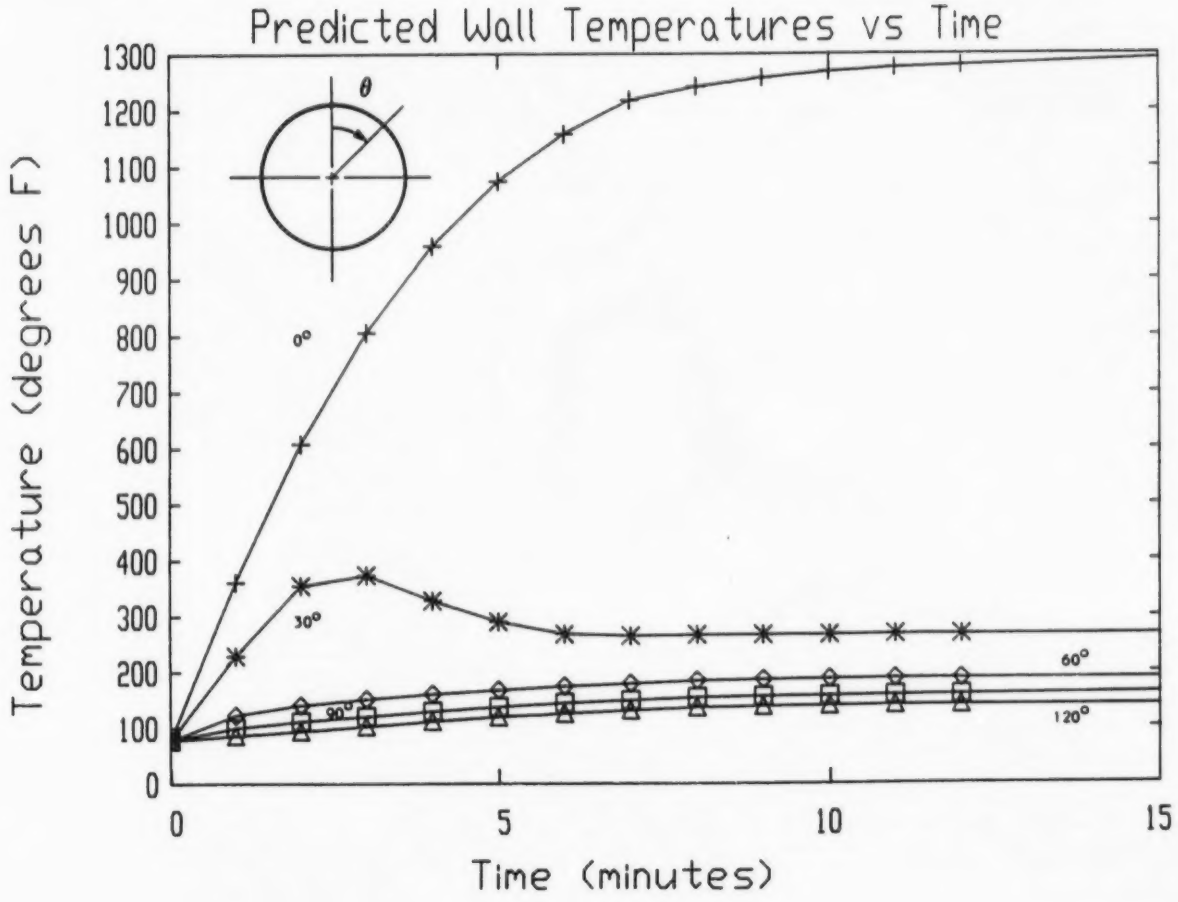

FIGURE 3.8-40 RUN CASE # 7

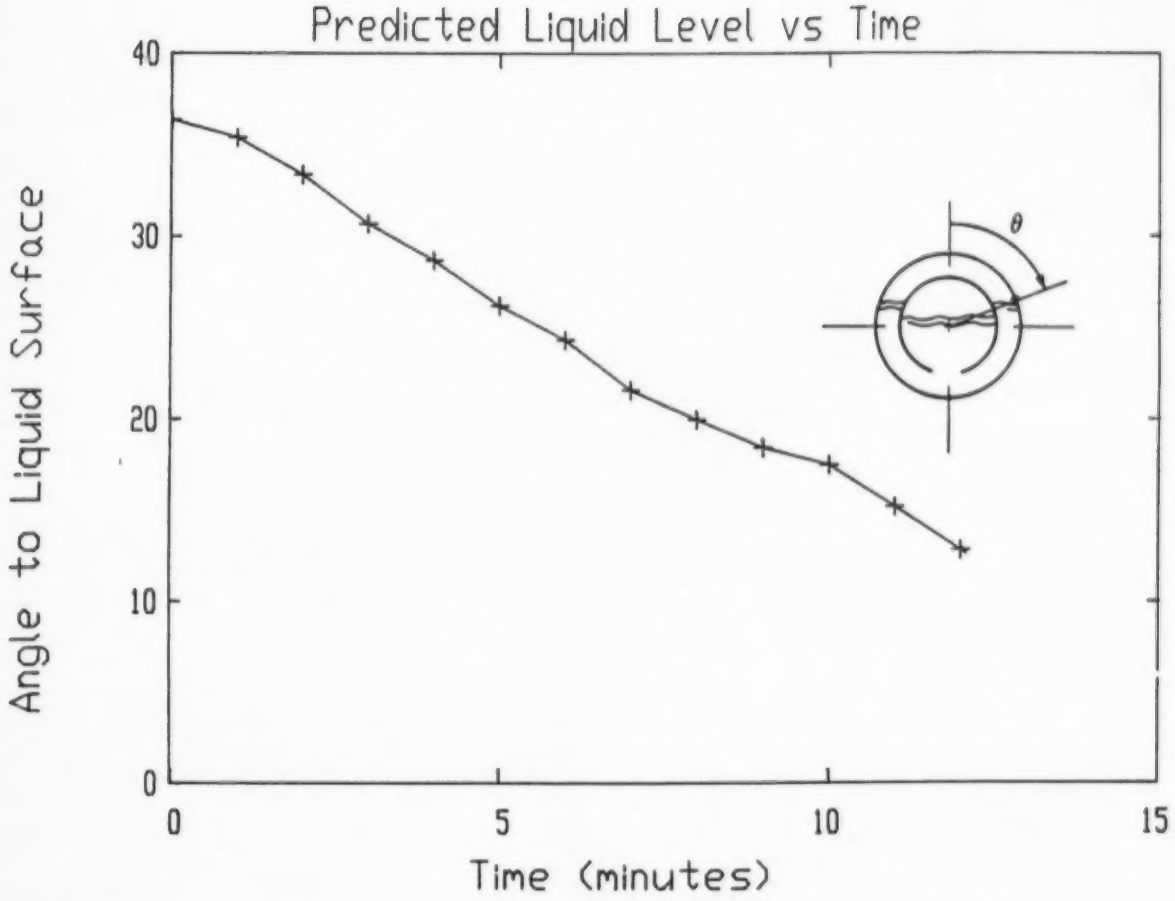

FIGURE 3.8-41 RUN CASE # 7

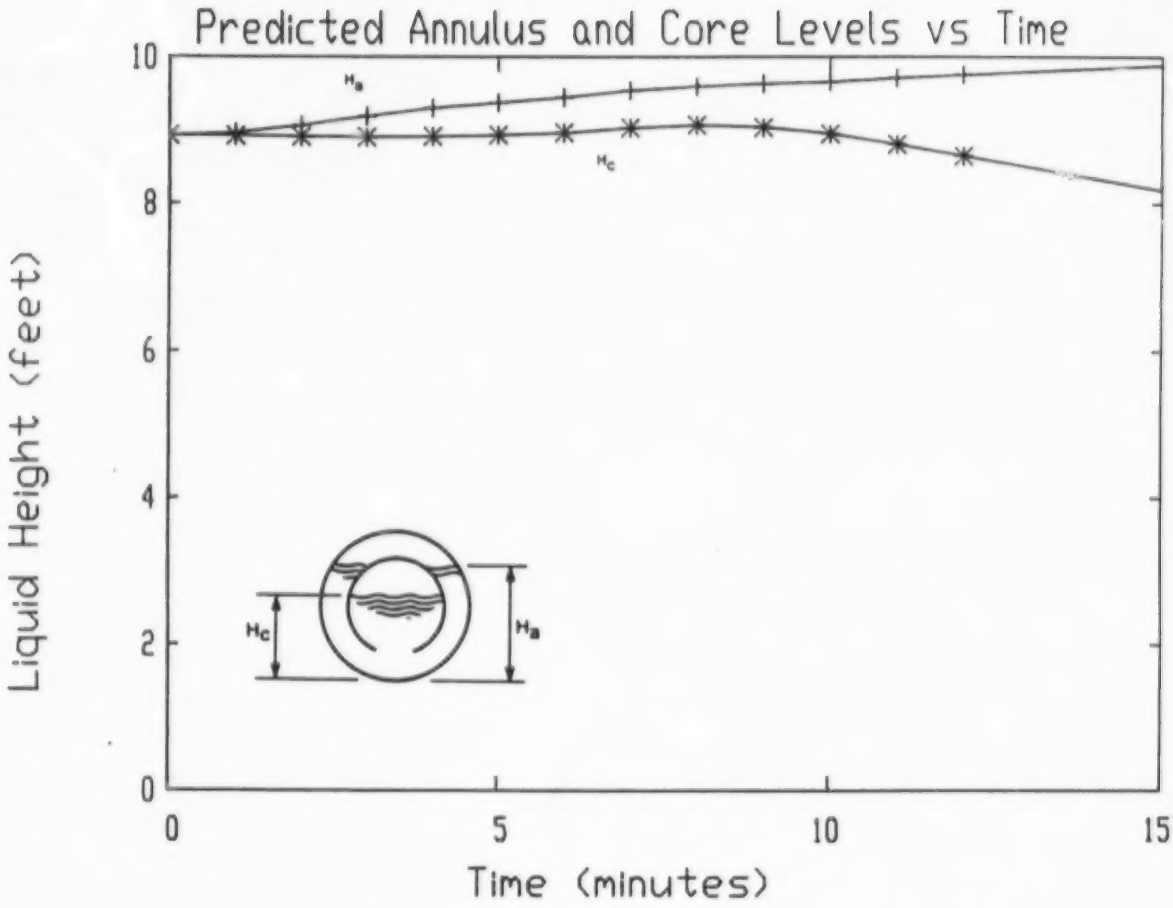

FIGURE 3.8-42 RUN CASE # 7

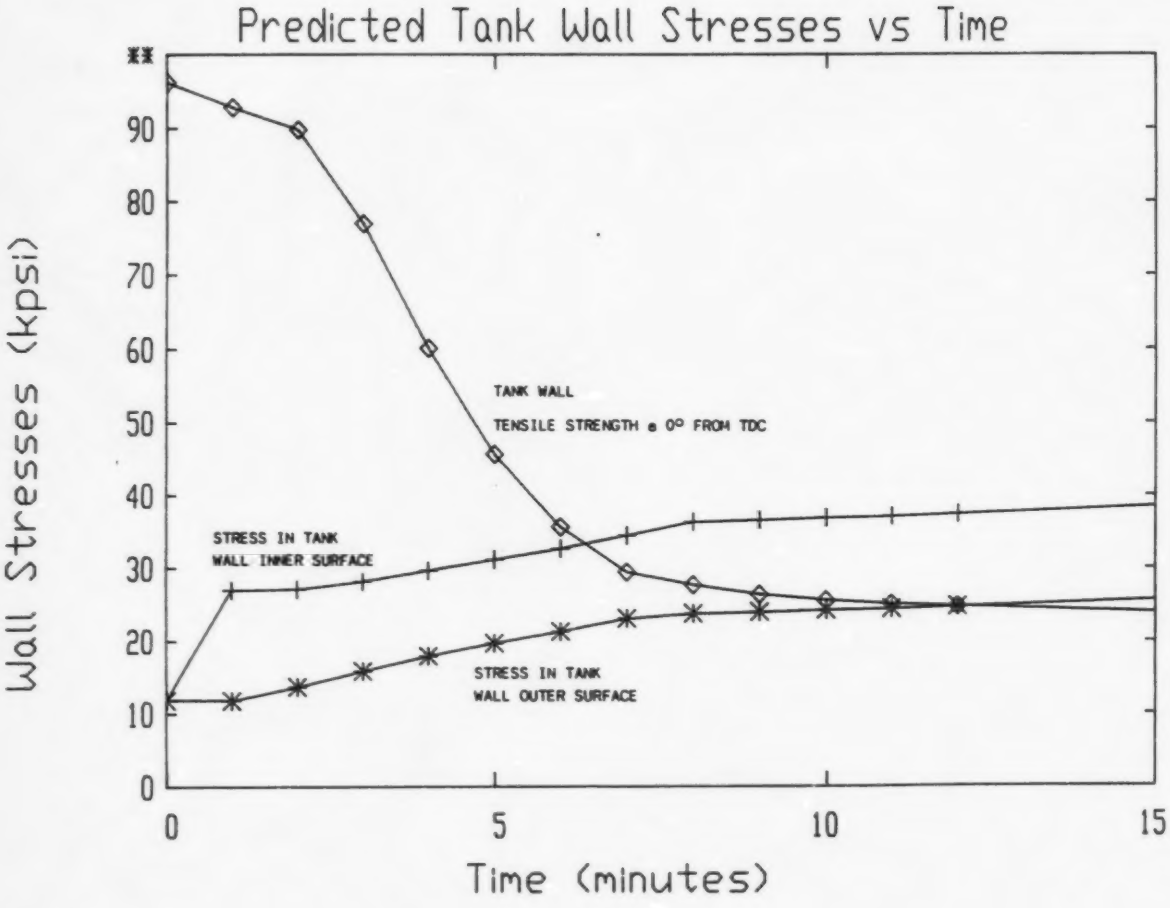

FIGURE 3.8-43 RUN CASE # 7

4.0 CONCLUSIONS AND RECOMMENDATIONS

Based on the results of the limited scope experimental tests conducted at the UNB test facility and the preliminary computer modelling conducted using the tank-car thermal model, the following conclusions have been made:

1. Based on the UNB tests it appears that the internal shell device does in fact direct two-phase fluid along the inside of the tank wall, thereby reducing the tank wall temperatures.

2. Based on the UNB tests, there was no significant pressure difference between the annulus and core regions caused by the actions of the pressure relief valve. However, one possible reason for this was the fact that the internal shell device was equipped with check vents and these check vents short-circuited the annulus to the core region. This short-circuit would, of course, eliminate any pressure differential that might be established.

3. Based on the results of the UNB tests internal shell device did not significantly reduce wall temperatures for the cases of rolled tanks.

4. Based on the UNB tests, the annular region was rapidly cleared of liquid in the cases involving rolled tanks where the pressure relief valve was initially below the liquid surface.

5. Based on the thermal modelling for the case of a full-scale upright tank equipped with an internal shell device it appears that an internal shell device if properly sized so that frothing would cover significant portions of the tank shell the tank would survive an engulfing fire accident.

6. Based on simulation results, the pressure relief valve size and the gap spacing could effect the margin of safety for an upright tank exposed to an engulfing fire.

7. Based on simulation results where it has been assumed that some forced convection will take place in the annulus. Tanks equipped with the internal shell device and rolled to one side could survive a fully engulfing fire situation.

However, this conclusion is not substantiated by any test data it is purely based on modelling considerations. If the calculation of the forced convected heat transfer for the annular flow is in error, then this simulation result would also be significantly in error.

8. Based on simulation results, the internal shell does not protect a tank from thermal rupture if the tank is exposed to a severe torch applied above the liquid level.

Based on the results of this study, it appears that the internal shell device does show potential for protecting upright tanks from thermal ruptures caused by engulfing fires. However, a great deal of experimental and analytical work is needed to establish optimum gap sizes to provide the adequate wall cooling necessary to prevent the tanks from thermal rupturing. The results of the mathematical modelling also show that it is possible that forced convection in the annulus could result in sufficient cooling of the tank wall to prevent a rolled tank equipped with an internal shell device from rupturing. This, however, is a totally unsubstantiated result and experimental work is necessary to establish whether or not the estimated convected heat transfer coefficients for this type of flow are correct.

Based on the results of the limited scope testing and computer modelling, the following recommendations are made:

1. The study should not proceed to the full thermal design phase before questions relating to the performance of the internal shell device in a rolled tank are answered.

2. Additional tests should be carried out to establish the convective heat transfer coefficients in the annulus of a rolled tank when vapour is passing through the annulus during venting.

REFERENCES

1. A.M. Birk, An Explosion Suppression System for Rail Tank-Cars and Other Containers Holding Pressurized Liquids, Unsolicited Proposal, Davis Engineering Ltd., April 1984.

2. J.E.S. Venart, Tank Car Thermal Response Analysis: Executive Summary: Volume 1, TP6809E, Transportation Development Center, Transport Canada.

3. A.M. Birk, User Documentation for the Rail Tank-Car Thermal Analysis Program (TANKCAR), Davis Engineering Report C83-29, Dec. 1983.

APPENDIX A

COMPUTER LANGUAGE LISTING OF INTERNAL SHELL RELATED MODELS

```
BUG
*****************************************************************

                        S H E L L

*****************************************************************

   This routine replaces HTBAL7 if an internal shell is
   present in the tank. SHELL carries out the thermodynamic
   heat balance for the annulus and core regions.

*****************************************************************

   SUBROUTINE SHELL

   REAL MVENT,MDOTV,MCV,MDOTCV,MAC,MDOTAC
   REAL MA1G,MA2G,MA1F,MA2F
   REAL MDOTC,MDOTFG,MG,M1G,M2G
   REAL MC1G,MC2G,MC1F,MC2F
   REAL MVLIQ,MVVAP,MDOT,MFC,MFS

   COMMON/SCALE/ISCALE,RINSIDE
   COMMON/HEAT/QFC,QFS,QG,QDOTF,QDOTG
   COMMON/RANGE/IRANGE,MDOTFG,MDOTC
   COMMON/RELIEF/MDOT,PSET,IPHASE,ROLL
   COMMON/MASS/MG,MFC,MFS
   COMMON/LIQUID/TFC,TFS,VFC,VFS,UFC,UFS,UFGS
   COMMON/VAPOR/TG,VG,HG,UG
   COMMON/TANK/RTANK(2),VTOT,TINIT,PTANK,THETA,THETA2,TLONG
   COMMON/STUFF/PI,ARC
   COMMON/STARL/AO,BO,CO,DO,EO,A,B,C,D,ALPHA,GAMMA,R,W
   COMMON/MATRIX/NX,NY,NXY
   COMMON/TSTEP/DELT,TIME
   COMMON/BLAYER/BLT(2),EFRAC(2)
   COMMON/TILTED/PITCH,ZPLANE,AWET,ADRY,A2PH,IFIRE,ANGLE,BINT
   COMMON/LAD/ILAD
   COMMON/FLO/PLGFLO,VALFLO

   COMMON/SHELL1/SHLGAP,THETAC,SLOT,QFRAC
   COMMON/SHELL2/MDOTCV,MDOTAC,HCV,HAC
   COMMON/SHELL3/MA2G,MA2F,MC2G,MC2F
   COMMON/SHELL4/TA2,TC2,PA2,PC2
   COMMON/SHELL5/HA,HC,HSLOT
   COMMON/SHELL6/VA,VC,VAF,VCF
   COMMON/SHELL7/HA2G,HC2G,HA2F,HC2F
   COMMON/SHELL8/MA1F,MA1G,MC1F,MC1G
   COMMON/SHELL9/APLUGS,AVALVE
   COMMON/SHEL10/VA2G,VA2F,VC2G,VC2F
   COMMON/SHEL11/ISHELL
   COMMON/SHEL12/UA2G,UA2F,UC2G,UC2F

    QFRAC = 0.80
    IF(TC2.GT.TA2) QFRAC = 1.0

.. ASSUME HEAT TRANSFERRED TO CORE IS PROPORTIONAL TO TA - TC

   QFRAC = 1. - (TA2 - TC2)/ 50.
   IF(QFRAC.LT.0.0) QFRAC = 0.0
   IF(QFRAC.GT.1.0) QFRAC = 1.0
```

```
... calculate vapour and liquid volumes

    THETAR = THETA * PI/180.
    THETCR = THETAC * PI/180.

    VCF = VC2F*MC2F
    VCG = VC - VCF
    IF(VCG.LT.0.0) VCG = 0.0
    VAF = VA2F*MA2F
    VAG = VA - VAF
    IF(VAG.LT.0.0) VAG = 0.0

... determine liquid level case

    CALL LEVELS(CASE)

... save properties from last time

    ICOUNT = 0
    TINC = 2.
    PA1 = PA2
    PC1 = PC2
    TA1 = TA2
    TC1 = TC2

    MA1G = MA2G
    MA1F = MA2F
    MC1G = MC2G
    MC1F = MC2F
    M1G = MA2G + MC2G

    UA1F = UA2F
    UA1G = UA2G
    UC1F = UC2F
    UC1G = UC2G
    U1G = ( MA2G*UA2G + MC2G*UC2G )/M1G

    HA1F = HA2F
    HA1G = HA2G
    HC1F = HC2F
    HC1G = HC2G
    H1G = ( MA2G*HA2G + MC2G*HC2G )/M1G

    VA1F = VA2F
    VA1G = VA2G
    VC1F = VC2F
    VC1G = VC2G
    V1G = ( MA2G*VA2G + MC2G*VC2G )/M1G

... choose appropriate thermodynamic model

    IF(CASE.EQ.1.) GO TO 100
    IF(CASE.EQ.2.) GO TO 200
    IF(CASE.EQ.3.) GO TO 300
    IF(CASE.EQ.4.) GO TO 400
    IF(CASE.EQ.5.) GO TO 500
    IF(CASE.EQ.6.) GO TO 600

... both liquids are below the slot in the shell and therefore
```

```
   the check valves are useless and the two vapour regions communicate
   freely through the slot opening. The core liquid is assumed to be
   subcooled and no mass transfers to or from it unless the annulus is
   free of liquid. The annulus liquid is saturated and in thermal
   equilibrium with the vapour in both the core and annulus.

0  CONTINUE
0  CONTINUE

.. heat transferred to regions

   QG = QDOTG * DELT
   QC = QDOTF * DELT * (1. - QFRAC)
   QA = QDOTF * DELT * QFRAC
   TA2 = TA2 - TINC

0  CONTINUE
   ICOUNT = ICOUNT + 1
   IF(ICOUNT.GT.50) GO TO 998
   TA2 = TA2 + TINC

   WRITE(*,1212) CASE,TA2,MA2F,MA2G,MC2F,MC2G
12 FORMAT( 5X,F4.1,5F12.2)

...determine properties at new T for annulus fluid

   CALL P(TA2,PA2)
   CALL VCAL(TA2,PA2,VA2F,VA2G)
   VC2G = VA2G
   V2G = VA2G
   CALL ENTHAL(VA2F,TA2,HA2F)
   CALL ENTHAL(VA2G,TA2,HA2G)
   HC2G = HA2G
   H2G = HA2G
   CALL EINT(PA2,VA2F,HA2F,UA2F)
   CALL EINT(PA2,VA2G,HA2G,UA2G)
   U2G = UA2G
   UC2G = UA2G

   CALL VENT(MDOTV,PA2,TA2,VA2G,TA2,VA2F)

   MDOT = MDOTV
   MVENT = MDOTV * DELT
   MCV = MDOTCV * DELT
   MAC = MDOTAC * DELT
   HAC = HAC
   HCV = HCV
   HVENT = HA1G

   IF(IPHASE.NE.3) GO TO 50
   HVENT = HA2G
   IF(MVENT.EQ.0.0) GO TO 50
   MVLIQ = MVENT * VALFLO / (VALFLO + PLGFLO)
   MVVAP = MVENT * PLGFLO / (VALFLO + PLGFLO)
   HVENT = MVLIQ/MVENT * HA2F + MVVAP/MVENT * HA2G

   CONTINUE
   IF(MA1F.LT.0.1) GO TO 55
   M2G = (M1G*U1G + MA1F*UA1F + QA + QG - MVENT*HVENT
  *     - (M1G + MA1F - MVENT) * UA2F) / (U2G - UA2F)
```

```
      MA2F = M1G + MA1F - MVENT - M2G

      MC2G = VCG/VC2G
      MA2G = M2G - MC2G

      MC2F = MC1F
      UC2F = (MC1F * UC1F + QC)/MC2F
      CALL TFROMU(UC2F,PA2,TC2,VC2F,0)
      GO TO 60

    5 CONTINUE

      M2G = (MC1F*UC1F + M1G*U1G + QA + QG - MVENT*HVENT
     *     - (M1G + MC1F - MVENT) * UC2F) / (U2G - UC2F)
      MC2G = VCG/VC2G
      MA2G = M2G - MC2G
      MA2F = 0.0
      MC2F = M1G + MC1F - MVENT - M2G

    6 CONTINUE
      V2 = M2G * V2G + MA2F * VA2F + MC2F * VC2F

      IF(ABS(VTOT-V2)/VTOT.LE.0.0015) GO TO 1000
      IF(VTOT-V2) 210,1000,220

  220 CONTINUE
      TA2 = TA2 - TINC
      TINC = TINC/5.
      GO TO 210

  900 CONTINUE
  900 CONTINUE
  900 CONTINUE
  900 CONTINUE

C.. the slot is below some liquid and therefore vapour can
C   not pass through it. The check valves may or may not be
C   operating depending on the conditions. The annulus fluid
C   is saturated. The core pressure is greater than or equal to
C   the annulus liquid.

C.. determine heat input

      QDOT = QDOTF + QDOTG
      QAF = QDOT * DELT * QFRAC
      QAG = 0.0
      QCF = QDOT * DELT * ( 1. - QFRAC)
      QCG = 0.0
      QA = QAF + QAG
      QC = QCG + QCF
      QG = QAG + QCG
      TA2 = TA2 - TINC

  210 CONTINUE
      ICOUNT = ICOUNT + 1
      IF(ICOUNT.GT.50) GO TO 998
      TA2 = TA2 + TINC

    WRITE(*,1212) CASE,TA2,MA2F,MA2G,VA,VA2
```

```
...determine properties at new T for annulus fluid

      CALL P(TA2,PA2)
      CALL VCAL(TA2,PA2,VA2F,VA2G)
      CALL VCAL(TC1,PA2,VC2F,VC2G)
      CALL ENTHAL(VA2F,TA2,HA2F)
      CALL ENTHAL(VA2G,TA2,HA2G)
      CALL EINT(PA2,VA2F,HA2F,UA2F)
      CALL EINT(PA2,VA2G,HA2G,UA2G)

      CALL VENT(MDOTV,PA2,TA2,VA2G,TA2,VA2F)

      MDOT = MDOTV
      MVENT = MDOTV * DELT
      MCV = MDOTCV * DELT
      MAC = MDOTAC * DELT
      HAC = HAC
      HCV = HCV
      HVENT = HA1G

      IF(IPHASE.NE.3) GO TO 350
      IF(MVENT.EQ.0.0) GO TO 350
      MVLIQ = MVENT * VALFLO / (VALFLO + PLGFLO)
      MVVAP = MVENT * PLGFLO / (VALFLO + PLGFLO)
      HVENT = MVLIQ/MVENT * HA2F + MVVAP/MVENT * HA2G

0     CONTINUE

...calculate new conditions in annulus

      WRITE(*,1111) MA1G,UA1G,MA1F,UA1F,MAC,HAC,MCV,HCV,MVENT,
     *QA,UA2G,UA2F,UA2G
11    FORMAT( 2X,6F10.2,/,7F10.2)

      MA2F = ( MA1G * UA1G + MA1F * UA1F + MAC * HAC - MCV * HCV
     &       - MVENT * HVENT + QA - (MA1G + MA1F - MVENT + MAC
     &       - MCV) * UA2G ) / (UA2F - UA2G)
      IF(MA2F.LT.0.0) MA2F = 0.0
      MA2G = MA1G + MA1F - MVENT + MAC - MCV - MA2F
      IF(MA2G.LT.0.0) MA2G = 0.0


      VA2 = MA2F * VA2F + MA2G * VA2G
      IF(ABS(VA-VA2)/VA.LE.0.0015) GO TO 900
      IF(VA-VA2) 310,900,320

0     CONTINUE

      CALL SHLFLO(CASE)

      TA2 = TA2 - TINC
      TINC = TINC/5.
      IF(TINC.GT.0.001) GO TO 310
      TA2 = TA2 - 10.
      TINC = 2.
      GO TO 310

...consider core region next

0     CONTINUE
```

```
      PC2 = PA2
      TINC = 2.
      TC2 = TC2 - TINC

 410  CONTINUE
      TC2 = TC2 + TINC
      WRITE(*,1212) CASE,TC2,MC2F,MC2G,VC,VC2

...determine properties at new temperature for the core fluid

      IF(CASE.EQ.5..OR.CASE.EQ.6.) CALL P(TC2,PC2)
      IF(PC2.LT.PA2) PC2 = PA2

      CALL VCAL(TC2,PC2,VC2F,VC2G)
      CALL VCAL(TC2,PC2,VC2F,CRAP)
      VC2G = VA2G
      CALL ENTHAL(VC2F,TC2,HC2F)
      CALL ENTHAL(VC2G,TC2,HC2G)
      HC2G = HA2G
      CALL EINT(PC2,VC2F,HC2F,UC2F)
      CALL EINT(PC2,VC2G,HC2G,UC2G)
      UC2G = UA2G

...calculate new conditions in core

      MC2F = ( MC1G * UC1G + MC1F * UC1F + MCV * HCV - MAC * HAC
     &        + QC - (MC1G + MC1F - MAC + MCV) * UC2G ) / (UC2F - UC2G)
      MC2G = MC1G + MC1F - MAC + MCV - MC2F
      IF(MC2G.LT.0.0) MC2G = 0.0
      VC2 = MC2G * VC2G + MC2F * VC2F

      IF(ABS(VC-VC2)/VC.LE.0.0015) GO TO 1000
      IF(VC-VC2) 410,1000,420

 420  CONTINUE
      TC2 = TC2 - TINC
      TINC = TINC/5.
      IF(TINC.GT.0.001) GO TO 410
      TC2 = TC2 - 10.
      TINC = 2.
      GO TO 410

 998  WRITE(2,999)
 999  FORMAT( 5X,//,'********** SHELL NOT CONVERGING **********',//)
1000  CONTINUE

      QFC = QC
      QFS = QA
      QG = QG
      MG = MA2G + MC2G
      MFC = MC2F
      MFS = MA2F
      TFC = TC2
      TFS = TA2
      VFC = VC2F
      VFS = VA2F
      UFC = UC2F
      UFS = UA2F
      UFGS = UA2F - UA2G
```

```
      TG = TA2
      VG = VA2G
      HG = HA2G
      UG = UA2G
      PTANK = PA2

      RETURN
      END
C*************************************************************************
C                              L E V E L S
C*************************************************************************
C
C     This routine is used to determine the mode (or case) of
C     operation of the internal shell system. The case or mode
C     is determined based on the relative position of the
C     liquid levels in the core and annulus.
C
C*************************************************************************
      SUBROUTINE LEVELS(CASE)

      REAL MDOT

      COMMON/SCALE/ISCALE,RINSIDE
      COMMON/RELIEF/MDOT,PSET,IPHASE,ROLL
      COMMON/TANK/RTANK(2),VTOT,TINIT,PTANK,THETA,THETA2,TLONG
      COMMON/STUFF/PI,ARC
      COMMON/SHELL1/SHLGAP,THETAC,SLOT,QFRAC
      COMMON/SHELL5/HA,HC,HSLOT

      ROLLR = ROLL * PI/180.
      THETCR = THETAC * PI/180.
      THETAR = THETA * PI/180.

      SLTANG = 2.*ASIN(SLOT/2./(RINSIDE-SHLGAP))
      THETS = PI - ROLLR + SLTANG/2.
      HSLOT = RINSIDE
     *      + (RINSIDE - SHLGAP)*COS(THETS)
      HC = RINSIDE + (RINSIDE - SHLGAP)*COS(THETCR)
      HA = RINSIDE * (1. + COS(THETAR))

      IF(HSLOT.GT.HA) GO TO 200

   0  CONTINUE
      IF(HSLOT.GE.HC) CASE = 4.
      IF(HSLOT.LE.HC.AND.HC.GE.HA) CASE = 5.
      IF(HSLOT.LE.HC.AND.HC.LE.HA) CASE = 6.
      GO TO 500

   0  CONTINUE
      IF(HSLOT.LE.HC) CASE = 3.
      IF(HSLOT.GE.HC.AND.HC.GE.HA) CASE = 1.
      IF(HSLOT.GE.HC.AND.HC.LE.HA) CASE = 2.

   0  CONTINUE
      RETURN
      END
```

```
*************************************************************************

                        S H L F L O

*************************************************************************

   SHLFLO is used to calculate the flow rates through the
   bottom slot and check vents. The flow rates depend on the
   mode of operation and if the relief valve is acting.

*************************************************************************

   SUBROUTINE SHLFLO(CASE)

   REAL MDOTV,MDOTCV,MDOTAC,MDOT
   REAL MA2G,MA2F,MA1G,MA1F,MAC
   REAL MC2G,MC2F,MC1G,MC1F
   REAL MDOTC,MDOTFG

   COMMON/SCALE/ISCALE,RINSIDE
   COMMON/RANGE/IRANGE,MDOTFG,MDOTC
   COMMON/RELIEF/MDOT,PSET,IPHASE,ROLL
   COMMON/TANK/RTANK(2),VTOT,TINIT,PTANK,THETA,THETA2,TLONG
   COMMON/STUFF/PI,ARC
   COMMON/TSTEP/DELT,TIME
   COMMON/FLO/PLGFLO,VALFLO
   COMMON/SHELL1/SHLGAP,THETAC,SLOT,QFRAC
   COMMON/SHELL2/MDOTCV,MDOTAC,HCV,HAC
   COMMON/SHELL3/MA2G,MA2F,MC2G,MC2F
   COMMON/SHELL4/TA2,TC2,PA2,PC2
   COMMON/SHELL5/HA,HC,HSLOT
   COMMON/SHELL6/VA,VC,VAF,VCF
   COMMON/SHELL7/HA2G,HC2G,HA2F,HC2F
   COMMON/SHELL8/MA1F,MA1G,MC1F,MC1G
   COMMON/SHELL9/APLUGS,AVALVE
   COMMON/SHEL10/VA2G,VA2F,VC2G,VC2F

   ROLLR = ROLL * PI/180.
   THETCR = THETAC * PI/180.
   THETAR = THETA * PI/180.
   THET2R = THETA2 * PI/180.

   SLTANG = 2.*ASIN(SLOT/2./(RINSIDE-SHLGAP))
   THETS2 = PI - ROLLR - SLTANG/2.
   HSLOT2 = RINSIDE + (RINSIDE - SHLGAP)* COS(THETS2)

.. calculate representative vapour velocity in gap

-------------------------------------------------------------------

   A1 = RINSIDE**2.*(THETAR - COS(THETAR)*SIN(THETAR))
   A2 = (RINSIDE*THETAR + (RINSIDE - SHLGAP)*THETCR) * SHLGAP
   FACTOR = .00070  * RINSIDE/SHLGAP
   FACTOR = 0.0


-------------------------------------------------------------------

   WRITE(*,*) AVALVE,APLUGS,MDOT,TLONG
```

```
      VVENT = VA2G
      AVENT = (AVALVE + APLUGS)/TLONG
      AVENT = A2
      IF(AVENT.EQ.0.0) AVENT = 0.00001
      UGAP = FACTOR * MDOT/3600. * VVENT / AVENT
      IF(IPHASE.NE.3) GO TO 20

      AVENT = APLUGS/TLONG
      AVENT = A2
      IF(AVENT.EQ.0.0) AVENT = 0.00001
      UGAP = FACTOR * PLGFLO/3600. * VVENT / AVENT

      CONTINUE

      IF(CASE.EQ.1.) GO TO 100
      IF(CASE.EQ.2.) GO TO 200
      IF(CASE.EQ.3.) GO TO 300
      IF(CASE.EQ.4.) GO TO 400
      IF(CASE.EQ.5.) GO TO 500
      IF(CASE.EQ.6.) GO TO 600

0     CONTINUE
0     CONTINUE

      MDOTCV = 0.0
      MDOTAC = 0.0
      HAC = 0.0
      HCV = 0.0
      GO TO 1000

0     CONTINUE

      AAC = SLOT
      IF(HC.LT.HSLOT2) AAC = HC - HSLOT
      HDRIVE = UGAP**2./2./VA2G*VC2F/32.2
     *       + (HC - HSLOT)
      UAC = SQRT(2. * HDRIVE * 32.2)
      VAC = VC2F

      MDOTAC = UAC * AAC /VAC

      IF(THETA.GT.2..AND.MDOT.GT.0.)
     *  MDOTAC = AMAX1(MDOT*VA2F/VC2F,MDOTAC)

      HAC = HC2F

      MDOTCV =  MDOTAC * VC2F/VA2G
      HCV = HA2G
      IF(PC2.GT.PA2) MDOTCV = 0.0
      IF(PC2.GT.PA2) HCV = 0.0

      GO TO 1000

0     CONTINUE

      AAC = SLOT
      IF(HA.LT.HSLOT2) AAC = HA - HSLOT
      HDRIVE =  UGAP**2./2./VA2G*VC2F/32.2
     *       - (HA - HSLOT)
```

```
      IF(HDRIVE.GE.0.0) UAC = 0.0
      IF(HDRIVE.LT.0.0) UAC = - SQRT(2. * ABS(HDRIVE) * 32.2)
      VAC = VA2F

      MDOTAC = UAC * AAC /VAC
      HAC = HA2F

      MDOTCV = 0.0
      HCV = 0.0

      GO TO 1000

   00 CONTINUE
   00 CONTINUE

      HAWANT =  UGAP**2./2./VA2G*VA2F/32.2  + HC*VA2F/VC2F
      HWANT = HAWANT - HC
      HHAVE = HA - HC
      HDRIVE = HWANT - HHAVE

      IF(HDRIVE.GT.0.0) UAC = SQRT(2. * 32.2 * HDRIVE)
      IF(HDRIVE.LE.0.0) UAC = - SQRT(2. * 32.2 * ABS(HDRIVE))
      VAC = VC2F
      IF(UAC.LT.0.0) VAC = VA2F
      AAC = SLOT
      IF(HA.LT.HSLOT2.AND.HC.LT.HSLOT2) AAC = ABS(HC-HA)

      MDOTAC = UAC * AAC /VAC

      IF(THETA.LE.2..AND.MDOT.GT.0.)
     *  MDOTAC = AMIN1(MDOT*VA2F/VC2F,MDOTAC)
      IF(THETA.GT.2..AND.MDOT.GT.0.)
     *  MDOTAC = AMAX1(MDOT*VA2F/VC2F,MDOTAC)
      IF(HA.LE.1.02*HSLOT.AND.MDOTAC.LT.0.0) MDOTAC = 0.0
      IF(THETAC.LE.2..AND.MDOTAC.LT.0.) MDOTAC = 0.0
      IF(HC.LE.1.02*HSLOT2.AND.MDOTAC.GT.0.0) MDOTAC = 0.0

      HAC = HC2F
      VAC = VC2F
      IF(UAC. LT.0.0) HAC = HA2F
      IF(UAC. LT.0.0) VAC = VA2F

      MAC = MDOTAC * DELT
      MDOTCV = 0.
      HCV = 0.

      GO TO 1000

   000 CONTINUE

      RETURN
      END
```

****

T H E T S H

****

THETSH is used to calculate the angle from the tank tdc to

```
  the liquid surface in the annulus and the core. These angles
  are used to calculate the liquid levels.

*********************************************************************

      SUBROUTINE THETSH

      REAL MA2G,MA2F,MC2G,MC2F,MDOT

      COMMON/SCALE/ISCALE,RINSIDE
      COMMON/TANK/RTANK(2),VTOT,TINIT,PTANK,THETA,THETA2,TLONG
      COMMON/RELIEF/MDOT,PSET,IPHASE,ROLL
      COMMON/STUFF/PI,ARC
      COMMON/SHELL1/SHLGAP,THETAC,SLOT,QFRAC
      COMMON/SHELL3/MA2G,MA2F,MC2G,MC2F
      COMMON/SHELL6/VA,VC,VAF,VCF
      COMMON/SHEL10/VA2G,VA2F,VC2G,VC2F

..    calculate angle for core region first

      ICOUNT = 0
      VRATIO = MC2F*VC2F/PI/(RINSIDE-SHLGAP)**2.
      IF(VRATIO.GT.1.0) VRATIO = 1.0
      DTHET = 10.
      THETAC = 0. - DTHET
      IF(VRATIO.LT..5) THETAC = 90. - DTHET

0     THETAC = THETAC + DTHET

      WRITE(*,2323) ICOUNT,THETAC,THETC2,DTHET
23    FORMAT( 5X,I5,3F10.4)

      ICOUNT = ICOUNT + 1
      IF(ICOUNT.GT.50) GO TO 299
      RATIO = SIN(2.*PI*THETAC/180.)/2./PI
      THETC2 = 180.*(1.-VRATIO+RATIO)
      IF(THETC2.EQ.0.0) THETC2 = .00001
      IF(ABS(THETAC-THETC2)/THETC2.LT..0001) GO TO 300
      IF(THETAC - THETC2) 100,300,200

0     CONTINUE
      THETAC = THETAC - DTHET
      DTHET = DTHET/10.
      GO TO 100

...   calculate angles for annulus region

0     CONTINUE
      VAF = MA2F * VA2F
      IF(VAF.GT.VA) VAF = VA
      IF(VAF.EQ.0.0) VAF = .0000001
      RATIO = VAF/VA
      ICOUNT = 0

      R = RINSIDE
      RS = R - SHLGAP
      DH = 0.02 * R
      VAFTRY = 0.0
      VAFSAV = 0.0
      Y = 0. - DH
```

```
      IF(RATIO.GT.0.5) DH = - R * .02
      IF(RATIO.GT.0.5) VAFTRY = VA
      IF(RATIO.GT.0.5) VAFSAV = VA
      IF(RATIO.GT.0.5) Y = 2. * R - DH
      W = 0.0
      WSAVE = 0.0
      WC = 0.0
      WCSAVE = 0.0

   0  CONTINUE
      Y = Y + DH

      WRITE(*,2323) ICOUNT,Y,VAFTRY-VAF,DH

      ICOUNT = ICOUNT + 1
      IF(ICOUNT.GT.200) GO TO 299
      YLESSR = ABS(Y - R)
      ZZZ = R**2. - YLESSR**2.
      WSAVE = W
      W = 0.0
      IF(ZZZ.GT.0.0) W = SQRT(ZZZ)
      WCSAVE = WC
      WC = 0.0
      ZZZ = 0.0
      IF(ABS(Y-R).LT.RS) ZZZ = RS**2. - YLESSR**2.
      IF(ZZZ.GT.0.0) WC = SQRT(ZZZ)
      VAFSAV = VAFTRY

      WRITE(*,11) VAF,VAFTRY,Y
   1  FORMAT( 5X,I6,5F12.4)

      VAFTRY = VAFTRY + (W + WSAVE - WC - WCSAVE) * DH

      VAFTST = (VAFTRY - VAF)/VAF
      IF(VAFTST.LT.0.0) VAFTST = - VAFTST

      WRITE(*,11) ICOUNT,Y,DH,VAFTRY,VAF,VAFTST

      IF(VAFTST.LT..001) GO TO 330
      IF(RATIO.GT.0.5) GO TO 315
      IF(VAFTRY - VAF) 310,330,320
   5  CONTINUE
      IF(VAFTRY - VAF) 320,330,310
      GO TO 310

   0  CONTINUE
      Y = Y - DH
      VAFTRY = VAFSAV
      DH = DH/2.
      IF(ABS(DH).LT.0.00001) GO TO 299
      GO TO 310

   0  CONTINUE

      GO TO 400

   9  WRITE(2,298)
   8  FORMAT(5X,//,' **** SUBROUTINE THETSH NOT CONVERGING **** ',//)

   0  CONTINUE
```

```
      ARG = (Y - R)/R
      SIGN = 1.
      IF(ARG.LT.0.) SIGN = -1.
      IF(ABS(ARG).GT.1.0) ARG = SIGN
      THETA = ACOS(ARG)*180./PI

      WRITE(*,1212) MDOT,H2PHAS
12    FORMAT( 2F12.2)

      CALL FROTHS(H2PHAS)

      WRITE(*,1212) MDOT,H2PHAS

      THETAR = THETA*PI/180.
      X = R*COS(THETAR)
      XX = X + H2PHAS
      THET2R = 0.0
      IF(XX.LT.R) THET2R = ACOS(XX/R)
      THETA2 = THET2R *180./PI

      RETURN
      END
```

****

S H E L H T

****

SHELHT is used to calculate the heat transfer coefficients on the inner surface of the tank when an internal shell is present. SHELHT replaces HTSURF when an internal shell is present.

****

```
      SUBROUTINE SHELHT(T)

      REAL T(36,14,2)
      REAL LFREE,LFORCE,NUFREE,NUFOR,KEXPC,KEXPR,MG,MDOT
      REAL HBOIL(4)
      REAL MA2F,MA2G,MC2F,MC2G,MDOTAC,MDOTCV

      COMMON/SCALE/ISCALE,RINSIDE
      COMMON/TANK/RTANK(2),VTOT,TINIT,PTANK,THETA,THETA2,TLONG
      COMMON/STUFF/PI,ARC
      COMMON/EXPLOS/NYEXP,WEXP,KEXPC,KEXPR,CEXP,AEXP,RHOEXP
      COMMON/VAPOR/TG,VG,HG,UG
      COMMON/RELIEF/MDOT,PSET,IPHASE,ROLL
      COMMON/HCOEFF/HWALIQ,HWAGAS,HWA2PH,HEXLIQ,HEXGAS,HEX2PH
      COMMON/TILTED/PITCH,ZPLANE,AWET,ADRY,A2PH,IFIRE,ANGLE,BINT
      COMMON/LAD/ILAD
      COMMON/FLO/PLGFLO,VALFLO
      COMMON/SHELL1/SHLGAP,THETAC,SLOT,QFRAC
      COMMON/SHELL2/MDOTCV,MDOTAC,HCV,HAC
      COMMON/SHELL3/MA2G,MA2F,MC2G,MC2F
      COMMON/SHELL4/TA2,TC2,PA2,PC2
      COMMON/SHELL5/HA,HC,HSLOT
      COMMON/SHEL10/VA2G,VA2F,VC2G,VC2F
```

```
      DATA EWALL,EEXP/0.90,0.20/
      DATA CFAC/0.20/
      DATA X/0.99/

      **** PROBLEM ****    need boiling data for new ladings

      DATA HBOIL/2300.,2300.,2300.,2300./

..    calculate heat transfer coefficients for the interior surfaces

      LFREE = SHLGAP
      LFORCE = TLONG/2.
      TGAV = (TA2 + T(1,NYEXP+1,2))/2.

      CALL VISCOS(TGAV,VISC)
      CALL THCOND(TGAV,COND)
      CALL VOLEXP(TGAV,BETA)

..    calculate vapour specific heat by considering two vapour temperatures

      TGPLUS = TGAV + 5.
      CALL VCAL(TGAV,PTANK,VJUNK,VGAV)
      CALL ENTHAL(VGAV,TGAV,HGAV)
      CALL VCAL(TGPLUS,PTANK,VJUNK,VGPLUS)
      CALL ENTHAL(VGPLUS,TGPLUS,HGPLUS)
      CP = (HGPLUS-HGAV)/(TGPLUS-TGAV)

      PR = 3600.*CP*VISC/COND
      GR = 32.2*BETA*LFREE**3.0*
     & (T(1,NYEXP+1,2) - TG)/VG**2/VISC**2
      IF(GR.LE.0.) GR = 0.

..    estimate mean forced flow velocity

      VG = VA2G
      Q = MDOT*VG*TLONG/3600.
      IF(IPHASE.EQ.3.AND.MDOT.NE.0.0)
     & Q = Q * PLGFLO/(PLGFLO + VALFLO)

..    vapour flow passage area

      APASS = VA2F*MA2F

..    mean flow velocity

      VEL = 0.
      IF(APASS.LE.0.) GO TO 40
      VEL = Q/2./APASS

..    mean flow Reynolds number

      RE = LFORCE*VEL/VISC/VGAV
      IF(RE.LT.0.0) RE = 0.0

...turbulent forced convection in annulus (approximately)

      NUFOR = .664*PR**.333*RE**.5

...free convection from horizontal surface.
```

```
      NUFREE = .58*(GR*PR)**.20

C     calculate convective heat transfer coefficients

      HFREE = 0.
      IF(LFREE.LE.0.) GO TO 20
      HFREE = NUFREE*COND/LFREE
      HFORC = NUFOR*COND/LFORCE

   20 CONTINUE

C     boiling heat transfer coefficients

      HWALIQ = HBOIL(ILAD)

C     if torch fire then reduce boiling coefficient by 80 %
      (this is a guess)

      IF(IFIRE.EQ.2) HWALIQ = 0.20 * HBOIL(ILAD)

C     assign heat transfer coefficients for case with no Explosafe

      HRAD = 0.0
      HWAGAS = HRAD + HFREE + HFORC
      HWA2PH = (1.-X)*HWALIQ + X*HWAGAS
      HEXLIQ = 0.0
      HEXGAS = 0.0
      HEX2PH = 0.0

      WRITE(3,200) HWALIQ,HWAGAS,HWA2PH
  200 FORMAT( 10X,3F12.2,/)

C     if 'Explosafe' is present the coefficients are different

      IF(NYEXP.EQ.0) GO TO 300
      HFREE = CFAC * HFREE
      HFORC = CFAC * HFORC
      HRAD = 0.
      HWAGAS = HFORC + HFREE + HRAD

C     boiling heat transfer coefficients

      HEXLIQ = CFAC*HBOIL(ILAD)

C     if torch fire then reduce boiling coefficient by 80 %
      (this is a guess)

      IF(IFIRE.EQ.2) HEXLIQ = 0.20 * HEXLIQ

C     neglect thermal radiation from Explosafe

      HRADEX = 0.

  300 CONTINUE
      HEXGAS = HFREE + HFORC + HRADEX
      HEX2PH = (1.-X)*HEXLIQ + X*HEXGAS

  400 RETURN
      END
```

```
*************************************************************************

                        F R O T H S

*************************************************************************

... subroutine FROTHS calculates the thickness of the 2-phase frothing
    region which exists above the liquid level in the annulus when a
    internal shell is present.

*************************************************************************

    SUBROUTINE FROTHS(H2PHAS)
    REAL MDOT,MDOTCV,MDOTAC

    COMMON/RELIEF/MDOT,PSET,IPHASE,ROLL
    COMMON/SCALE/ISCALE,RINSIDE
    COMMON/TANK/RTANK(2),VTOT,TINIT,PTANK,THETA,THETA2,TLONG

    COMMON/SHELL1/SHLGAP,THETAC,SLOT,QFRAC
    COMMON/SHELL2/MDOTCV,MDOTAC,HCV,HAC
    COMMON/SHELL5/HA,HC,HSLOT
    COMMON/SHELL9/APLUGS,AVALVE
    COMMON/SHEL11/ISHELL

    WRITE(*,1212) MDOT,H2PHAS
212 FORMAT( 2F12.2)
    H2PHAS = 0.0

... if venting is taking place then the height of the frothing zone
    is assumed to be a function of the relief flow rate and the annular
    gap size.

********************************************* GUESSED FOR TEST ********
    FACTOR IS FUNCTION OF GAP AND ANNULUS VELOCITY ETC.

    FACTOR = .333 * 0.5/SHLGAP
    IF(MDOT.GT.0.01) H2PHAS = 2.* RINSIDE*FACTOR
    IF(IPHASE.EQ.3) H2PHAS = 0.
*********************************************GUESSED FOR TEST **********

    WRITE(*,1212) MDOT,H2PHAS
    RETURN

    END
```